INVESTIGATIONS OF THE MECHANISMS OF ANTITUMOUR ACTIVITY OF PK1, THE FIRST MACROMOLECULAR PRODRUG TO REACH CLINICAL TRIALS.

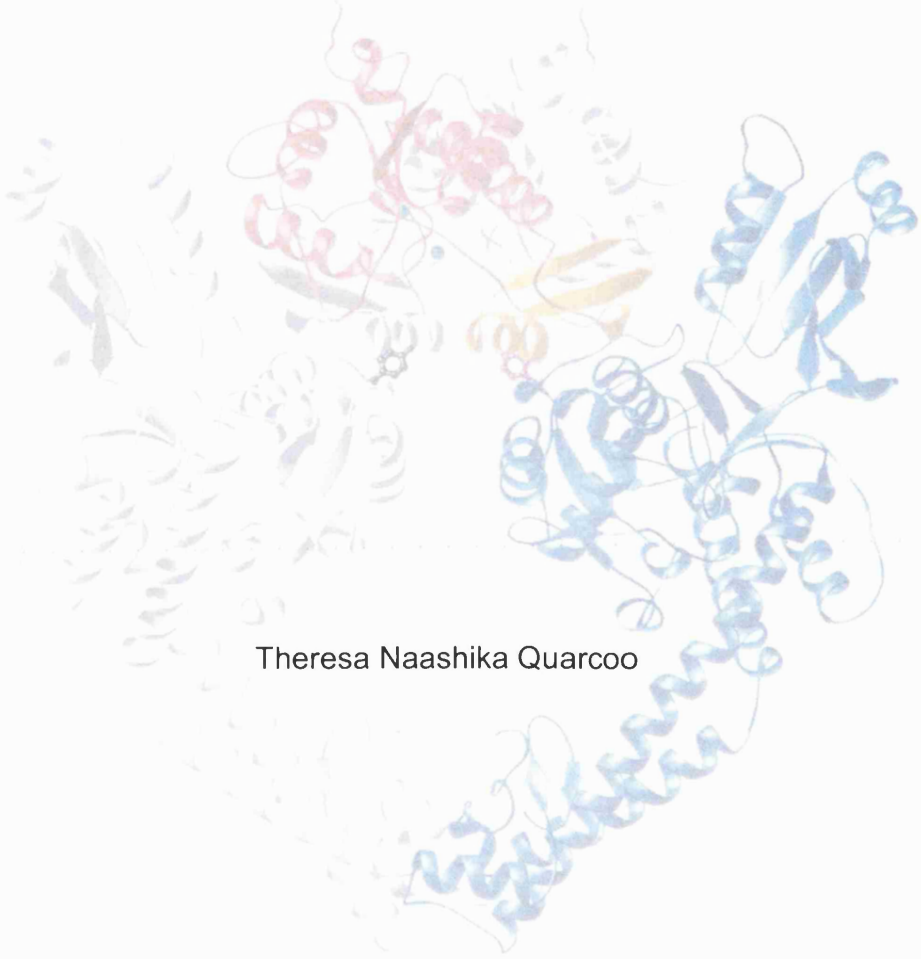

Theresa Naashika Quarcoo

Submitted for the degree of Doctor of Philosophy
The School of Pharmacy, University of London
October 2002

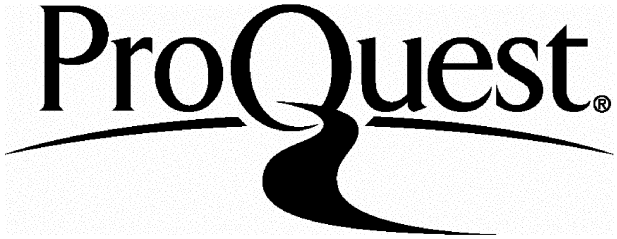

To my father

'In questions of science the authority of a thousand is not worth the humble reasoning of a single individual.'

- GALILEO GALILEI

ABSTRACT

Twenty seven years ago the use of water soluble synthetic polymers as targetable carriers to provide better and more effective treatment for cancer was proposed. To date, the most exploited carrier, HPMA [*N*-(2-Hydroxypropyl)methacrylamide], has been successfully used to specifically target tumours by taking advantage of the increased vascular permeability and the lack of effective tumour lymphatic drainage. In 1999, a phase 1 clinical trial result of the first drug-polymer conjugate, PK1, was published. PK1 comprises of doxorubicin covalently bound to HPMA via a tetrapeptide spacer, which is susceptible to cleavage by cathepsin B, a lysosomal protease found to be upregulated in most human cancers.

Given the progression of PK1 into phase II testing, its mode of action and toxicological profile are poorly understood. This study set out to investigate the mechanism of antitumour activity *in vitro* and *in vivo*.

PK1 was found to be toxic against a panel of tumour cell lines with varying levels of cathepsin B activity. However, cytotoxicity could always be attributed to the 0.02% free doxorubicin present in the polymer preparation. Following confirmation of PK1 internalisation by all cell lines with fluorescence microscopy, the ability of PK1 to induce DNA damage at the single cell level with the Comet assay was investigated. Induction of DNA damage was observed in the B16F10 murine melanoma model, but not *in vitro*. Furthermore, DNA damage to bone marrow cells paralleled that of PK1 and the parent drug, doxorubicin observed in tumour cells.

In light of our results, we propose that the mechanism for the antitumour activity of PK1 may be due cleavage of the conjugate by cathepsin B at the tumour periphery and not within lysosomes as initially proposed. However, further experiments are needed to confirm our hypothesis.

ACKNOWLEDGEMENTS

Firstly, I would like to thank the Almighty God for the abundant blessings and for giving me wisdom and knowledge throughout the work for this thesis.

Many thanks to my supervisors Andreas Kortenkamp and Montserrat Casadevall-Callis. Andreas, thanks for your impeccable supervision, patience and for that final push that I so much needed. Montse, thanks for all your help, the encouragement, friendship and those brainstorming sessions that we used to have.

Also, I would like to thank The School of Pharmacy for the funding and my friends and colleagues Nissanka and Elisabete, thanks for everything and for making Toxicology a pleasant working environment. A lot of this work would have been more difficult without the help and guidance from Dr Ian Trayner, Dave McCarthy, Adrian Rogers, and Steve Coppard.

Thanks also go to our collaborators, Ruth Musila now 'Dr' and Professor Ruth Duncan (Welsh School of Pharmacy, Cardiff, Wales) for providing PK1, HepG2 and B16F10 cell lines. Ruthie, the *in vivo* work would have been impossible without you, especially the long nights in the Lab and those i.v. injections – many thanks.

I am very grateful to my Mother for believing in me, my sisters Lizzy, Mavis and Meyer for their patience and tolerance, and all my friends and MCA colleagues for the encouragement.

Last but not least, a special thanks to JB for the immense sacrifice and for the emotional and financial support, you are very special – I am truly grateful.

TABLE OF CONTENTS

LIST OF FIGURES AND TABLES

LIST OF ABBREVIATIONS

5-Fura	5-Fluorouracil
APS	Ammonium persulphate
AUC	Area under the curve
BSA	Bovine serum albumin
CFA	Colony forming assay
DAB	3,3'-diaminobenzidine
dH_2O	De-ionised water
DMF	Dimethylformamide
DMSO	Dimethyl sulphoxide
Dox	Doxorubicin
DSB	Double strand breaks
ECL	Enhanced chemi-luminescence
EDTA	Ethylenediaminetetraacetic acid
GFLG	Glycyl-phenyl-leucyl-glycyl
H&E	Haematoxylin and eosin
HBSS	Hank's balanced salt solution
HPMA	N-2-(Hydroxypropyl)methacylamide
HRP	Horse radish peroxidase
IC_{50}	Concentration required for 50% cell kill
IHC	Immunohistochemistry
LSB	Laemli sample buffer
MTD	Maximum tolerated dose
OD	Optical density
PAB	Pericellular assay buffer
PBS	Phosphate buffered saline
PK1	N-2-(Hydroxypropyl)methacylamide copolymer dox
PMSF	Phenylmethylsulfonyl fluoride
RFU	Relative fluorescence units
SDS	Lauryl sulphate, sodium salt
SSB	Single strand breaks
TCA	Trichloroacetic acid
Temed	N, N, N', N-tetramethylethylenediamine

CHAPTER 1 – INTRODUCTION

Cancer is predominantly a disease of old age with the exceptions of neuroblastomas, retinoblastomas, and some childhood leukaemias. The transformation of a normal cell to a tumour cell depends on mutations in genes that control both cell proliferation and survival. Functional or physical inactivation of the genes that guard the genome leads towards the advancement of cancer. Cancer is thus the result of genomic instability, often initiated by the accumulation of mutations in genes that control cell proliferation and programmed cell death. There are four major types of genetic alterations characteristic of tumour cells that are rarely found in normal cells. These include, 1) subtle sequence changes such as base substitutions, deletions or insertions of a few nucleotides, 2) alteration in the number of chromosomes – loss or gain of whole chromosomes, 3) chromosomal translocations, and 4) gene amplifications. Consequently, most solid tumours are genetically unstable giving rise to both tumour progression and tumour heterogeneity, ensuring that no two tumours are exactly the same and that a tumour is often composed of cells with non-identical genetic makeup [Brown and Giaccia, 1998].

1.1 The unique pathophysiology of solid tumours: a barrier to drug delivery

As a disease that affects millions of people in the western world, cancer can arise in any organ with the most common sites being lung, breast and prostate. Most solid cancers can be cured by surgical removal if confined to the primary site or organ. Unfortunately, sometimes cancer cells migrate via the lymphatic system and form secondary tumours in other sites of the body, which is often the cause of death in patients. In the past 40 years, therapy of non-operable tumours has mainly been dominated by the use of cytotoxic chemotherapeutic drugs and radiation. These approaches are mainly designed to attack tumour cells directly by interfering with cell growth signals of cancer cells. To an extent they also interfere with growth signals of normal healthy cells. Apart from the associated systemic toxicity, the

limited successes of most current cancer treatment regimes are due to barriers posed by tumour physiology.

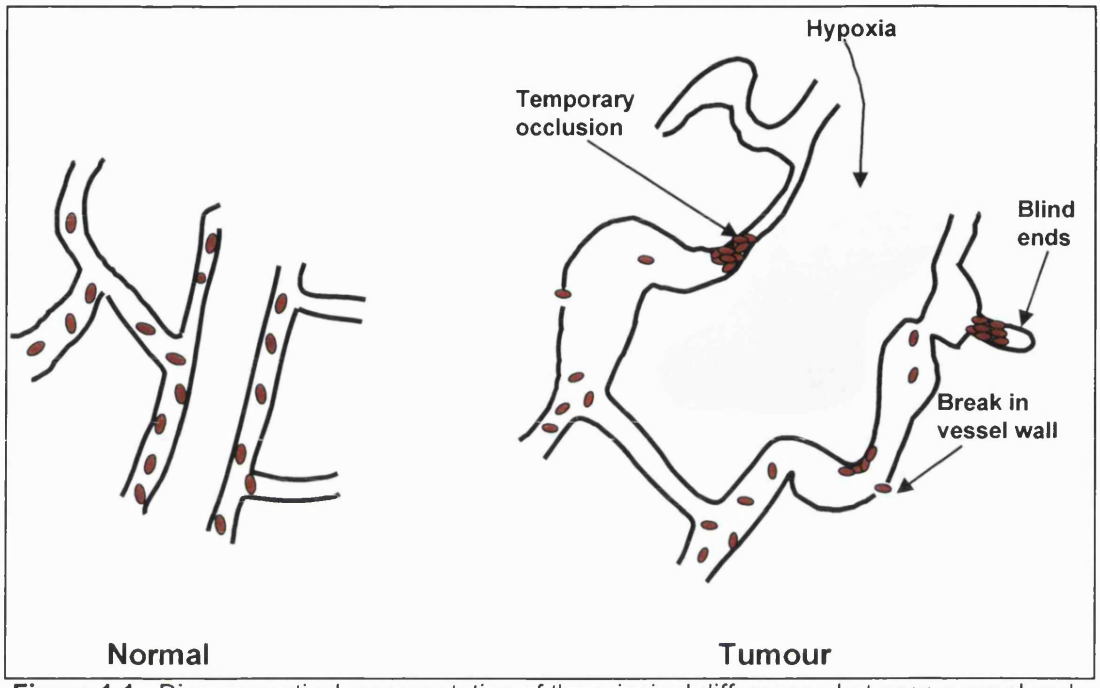

Figure 1.1 - Diagrammatical representation of the principal differences between normal and tumour vasculature. Normal tissue vasculature is well organised and relatively uniform. In contrast, tumour vasculature is irregular in shape with incomplete vessel walls, slow and irregular blood flow with hypoxic regions between vessels. *Adapted from Brown and Giaccia, 1998.*

1.1.1 Tumour vasculature and angiogenesis

Normal vascular endothelium consists of thin squamous endothelial cells that line blood vessels, and plays an important role in the distribution of many substances to tissues by selective permeability. Being multi-functional, endothelial cells also participate in vascular remodelling via the production of growth promoting and inhibitory factors. Typically, cancer cells occupy less than half the volume of a solid tumour. 1-10% of tumour volume are occupied by blood vessels weaving through the tumour mass. In addition, there is an abundant collagen matrix, which fills the interstitium, separating cancer cells from the vasculature. For an antitumour drug to reach cancer cells, it has to travel through blood vessels of the tumour and through the vessel wall into the interstitium. Once in the vessel wall, the drug then has to exit

and migrate through the matrix and disperse throughout the tumour in high enough concentrations to kill every cancer cell [Rakesh Jain et al].

For a tumour to grow beyond 1-2 mm in diameter, it requires an increased blood supply dedicated to that tumour alone. Thus, further tumour growth is dependent on the formation of new blood vessels, a process known as angiogenesis [Folkman, 2002]. Tumours initially obtain blood from the existing neighbouring vasculature. However, as they grow out and away from the vessels that supply them with nutrients, the need for new blood vessels arises and as a result, tumours trigger angiogenesis from outside the growing tumour mass. The precise mechanism by which the process of angiogenesis is triggered by tumours is still currently being investigated. Angiogenesis results from an intricate interplay between cells, soluble factors and extracellular matrix components. Endothelial cells have the multi-factorial role of degrading basement membrane, migrating and proliferating to form new capillary tubes. This process is thought to be mediated by the secretion of vascular endothelial growth factor (VEGF) by tumours. Once secreted, VEGF mediates the generation of endothelial cells, blood vessels, and directs vascular growth by sprouting of endothelial cells from pre-existing vessels [Molema et al, 1997].

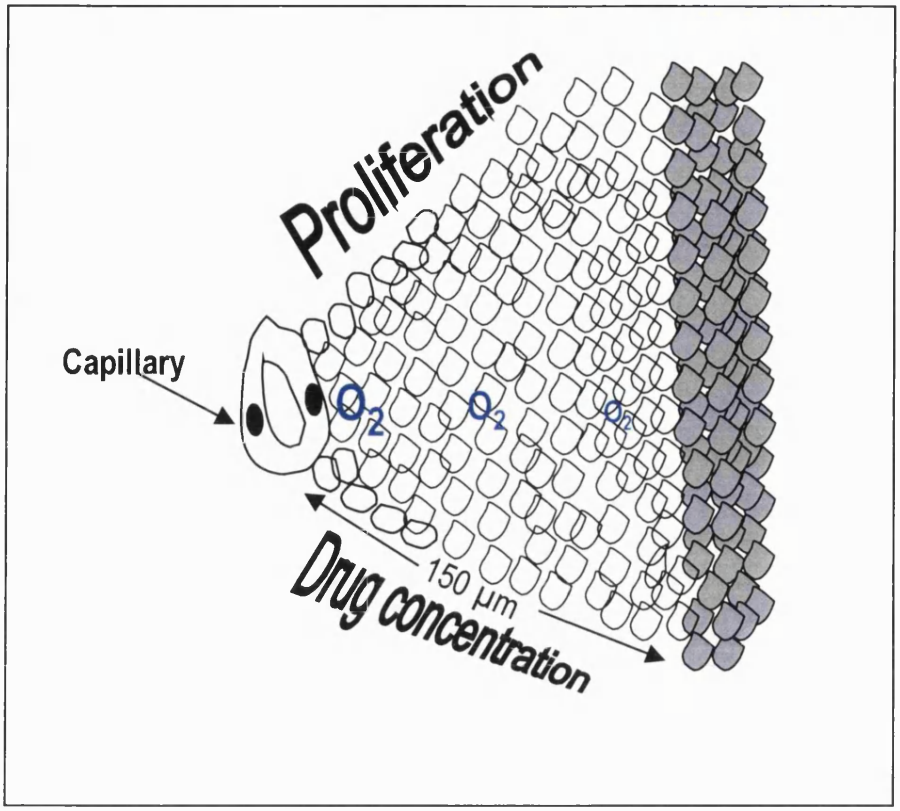

Figure 1.2 - Diagrammatical representation of well oxygenated (○) and hypoxic (◍) tumour cells surrounding a capillary. Both oxygen concentration and tumour cell proliferation decreases as a function of distance from the capillary.

Interestingly, tumour vasculature is severely disorganised. Normal blood vessels are laid out to provide a continuous supply of blood to all areas in a tissue, delivering oxygen, fluid and nutrients into the surrounding matrix and cells. Tumour blood vessels on the other hand, are not uniform, vessels branch extensively and twist into tortuous shapes with incomplete vessel walls, which results in sluggish and irregular blood flow, and much leakier vessels compared to that of normal tissues (Figure 1.1). Consequently, while some areas in the tumour are well vascularised, others have little or no blood supply. The non-uniform and relatively slow flow of blood flow in tumours hinders dispersion of chemotherapeutic agents, and is therefore a major obstacle in cancer chemotherapy [Jain, 2001and 1994].

1.1.2 Tumour hypoxia and interstitial pressure

The partial pressure of oxygen is often lower in tumours compared with normal tissues. These less than normal amounts of oxygen in tissues or tumour, hypoxia, poses another barrier to the delivery of anticancer agents. With the formation of new blood vessels on the outward surface of growing tumours, the distance between blood vessels and cells within the core of the tumour increases, and consequently the diffusion of oxygen to these cells is severely compromised (Figure1.2, Table 1.1). A tumour larger than 150 μm in diameter has a low partial oxygen pressure of <5 mm Hg, in comparison to 24-66 mm Hg for normal tissues [Jain, 1984]. Cells within the hypoxic environment become growth retarded and therefore unresponsive to radiation therapy and to chemotherapeutic agents that rely on cell proliferation for toxicity.

Table 1.1 Microenvironmental differences between normal and tumour tissue

Characteristics	Normal tissue	Tumour	Detrimental aspects for therapy
Microvasculature	Developed with regulated blood flow	Constant growth of new vessels; tortuous and leaky vessels, often sluggish and irregular blood flow	Poor delivery of some therapeutic agents due to irregular flow and high interstitial pressure
Oxygenation	Heterogenous, but rarely hypoxic regions	Highly heterogenous with hypoxic regions common	Reduces tumour sensitivity to radiation and anticancer drugs; predisposes to increased malignancy
Necrosis	Not present	Present	Not known if any

Taken from Brown and Giaccia

Furthermore, the extracellular pH of tumours is relatively acidic. One possible contributing factor is the secretion of lactic acid which can interfere with the effectiveness of treatment with certain anticancer drugs. For example, the use of a weak basic and or an acidic drug such as doxorubicin and chlorambucil will not be effective due to inadequate accumulation within tumours.

Another barrier to delivery of agents to cancer cells is lack of drainage by lymphatic tissue and elevated interstitial pressure associated with large tumours (>0.5

cm). Increased pressure is known to affect the transport of molecules by convection, whereas molecules that leave vessels are unaffected. This elevated tumour interstitial pressure is thought to be due to the compression of blood vessels by proliferating tumour cells and the irregularity of tumour vasculature [Jain, 2001].

Due to the lack of selective targeting with existing chemotherapeutic agents, there is an urgent need for the development of drugs that can target tumour cells with selective toxicity. One of the aims of this thesis is set out to investigate one such drug, PK1, which is currently in phase II clinical testing, organised by the British Cancer Research Campaign [Vasey et al., 1999]. Before discussing PK1 specifically it is important and relevant to make general points about problems associated with existing chemotherapeutic drugs focusing on the mechanism of antitumour activity, toxicity and drug resistance of the anthracycline antibiotic doxorubicin, the active component of PK1.

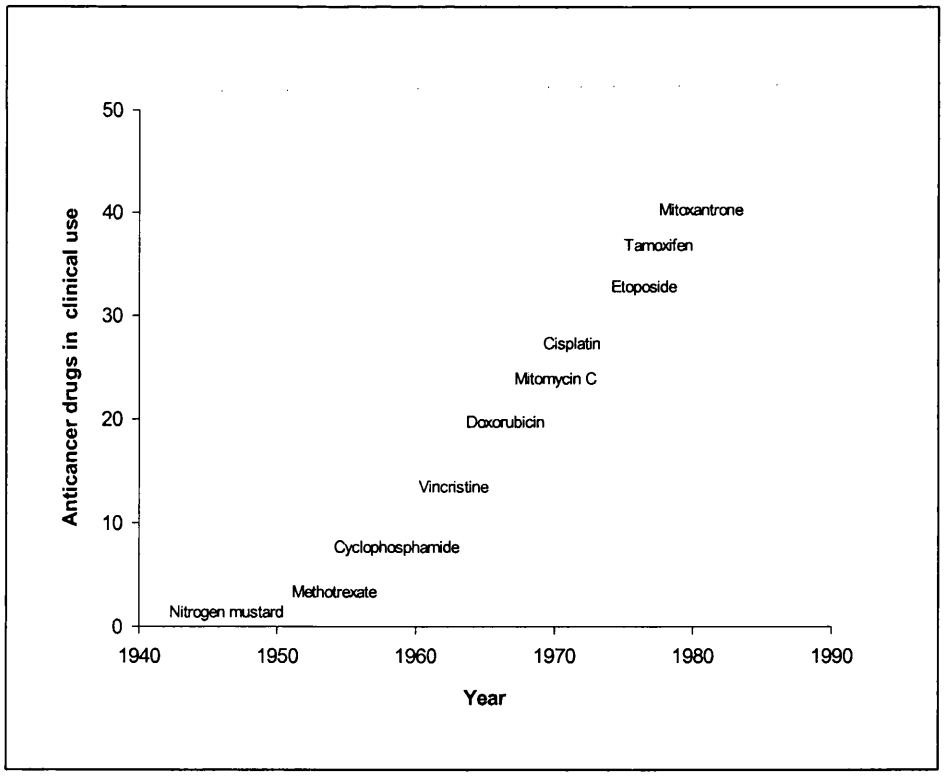

Figure 1.3 – Some anticancer drugs approved for clinical use over the past decades.

1.1.3 Problems associated with conventional cancer chemotherapy

Over the past four decades the development of chemotherapeutic agents and their introduction into the clinic has been rising steadily (Figure 1.3). Since the introduction of nitrogen mustards in the 1940's, the battle against cancer is still ongoing 60 years later. Apart from the barriers posed by the physiology of tumours, drug toxicity to normal healthy cells is a major problem associated with many chemotherapeutic agents, with toxicity affecting almost every organ and tissue in the body. There is no doubt that extensive progress has been made both in the understanding of the disease and treatment over the past - decades.

The anthracycline antibiotics are amongst the most widely used anticancer agents in the treatment of most solid tumours and soft tissue sarcomas. Likewise, with most chemotherapeutic agents, the therapeutic index of anthracyclines is limited, with a toxicity profile ranging from dose dependent cardiotoxicity, bone marrow suppression, severe extravasation, alopecia and development of secondary tumours.

1.2 Proposed mechanisms for the efficacy of anthracycline antibiotics

The reign of anthracyclines in cancer chemotherapy began as early as 1963 with the isolation of daunorubicin from *Streptomyces peucetius* [DuBost et al 1963], followed by the isolation of doxorubicin from a related strain 6 years later [Arcamone et al., 1969]. Since then, several analogues of anthracyclines have been made either by partial or total synthesis (Figure 1.4). However, doxorubicin is by far the best known and most widely used anthracycline antibiotic due to its efficacy against many human solid tumours including those of the lung, breast, ovary, head and neck, endometrium, prostate, and bladder. And it is also the most effective single agent against soft tissue sarcomas in adults.

To date, several mechanisms have been postulated for the efficacy of doxorubicin. These include interference with topoisomerase II, production of free radicals, interference with the cell cycle, and induction of apoptosis.

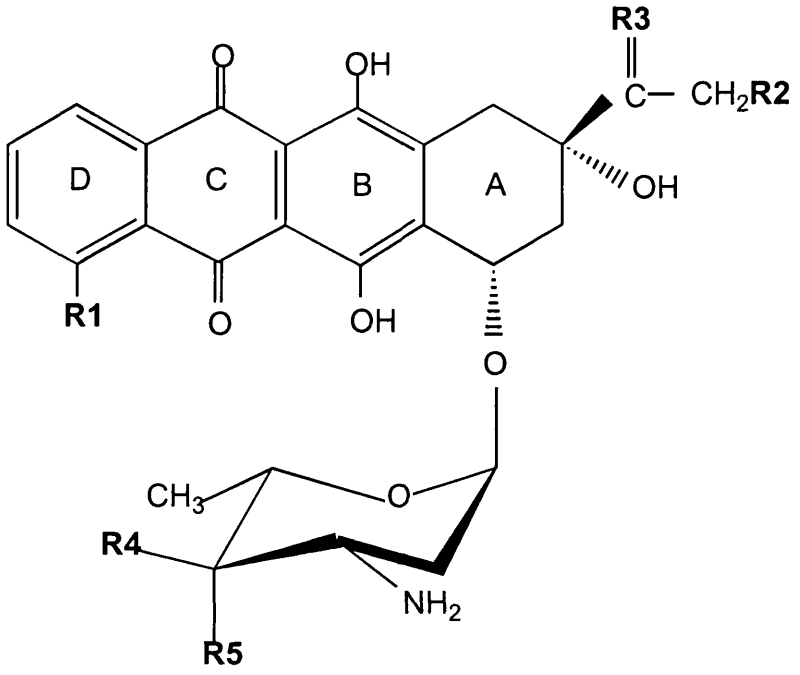

Anthracycline	R1	R2	R3	R4	R5
Doxorubicin	OCH_3	OH	O	H	OH
Daunorubicin	OCH_3	H	O	H	OH
Epirubicin	OCH_3	OH	O	OH	H
Idarubicin	H	H	O	H	OH
Pirarubicin	OCH_3	OH	O	H	OC_5H_9O
Zorubicin	OCH_3	H	$NNHCOC_6H_5$	H	OH
Carminomycin	OH	H	O	H	OH
Esorubicin	OCH_3	OH	O	H	H
Iododoxorubicin	OCH_3	OH	O	H	I

Figure 1.4 - Chemical structure of doxorubicin and other anthracycline antibiotics that are in clinical use or have been clinically evaluated.

1.2.1 Topoisomerase II-dependent mechanism of action and DNA breakage

Like all DNA, doxorubicin stabilises the break produced by topoisomerase II (Topo II). This action is thought to be the primary mechanism of doxorubicin induced cytotoxicity. Studies by Tewey et al.[1984a and 1984b] and others in the early 1980's demonstrated that topoisomerase II may be a primary target for doxorubicin antitumour activity. Topo II functions as a homodimer, consisting of two polypeptides of which two isoforms exist; α and β, coded for by two different genes. Topo IIα is expressed and regulated in a cell cycle dependent manner, whilst Topo IIβ is mainly localised in the nucleolus of cells during interphase of the cell cycle. The level of Topo IIβ remains more or less constant during the cell cycle and accounts for approximately 30% of the total Topo II activity in proliferating cells. Proliferating cells are said to have between 10^5 to 10^6 Topo IIα monomers per cell [Larsen et al., 1996].

Topo II controls DNA topology by relaxing supercoiled DNA or introducing supercoils via induction of double strand breaks. This involves the covalent binding of Topo II at the 5' end of both double and single strands via the phosphate backbone through the formation of a tyrosine phosphate bridge. This results in the initiation of a transient double strand break enabling the passage of a separate double helical strand [Kohn, 1996]. The stabilisation of the Topo II-DNA complex inhibits strand passage or reannealing of the break.

Chemically, doxorubicin and all anthracyclines consist of an aglycone tetracycline ring coupled to an amino sugar. There is extensive evidence to suggest that the pharmacological activity of doxorubicin is due to its ability to intercalate with DNA with base specificity as shown in Figure 1.7. An X-ray diffraction study suggests that the intercalation of doxorubicin involves the amino sugar moiety of the molecule, which lies in the major groove of DNA with the hydrophobic faces of the DNA base pairs and the drug overlapping. The outcome of intercalation is uncoiling of the double helix, and stabilisation of the covalent Topo II-DNA complex.

The function of Topo II is to control the unwinding of DNA supercoiled twisting prior to DNA replication. This involves the formation of double strand breaks and the covalent binding of Topo II at the 5' end of both double and single

strand breaks via the phosphate backbone through the formation of a tyrosine phosphate bridge.

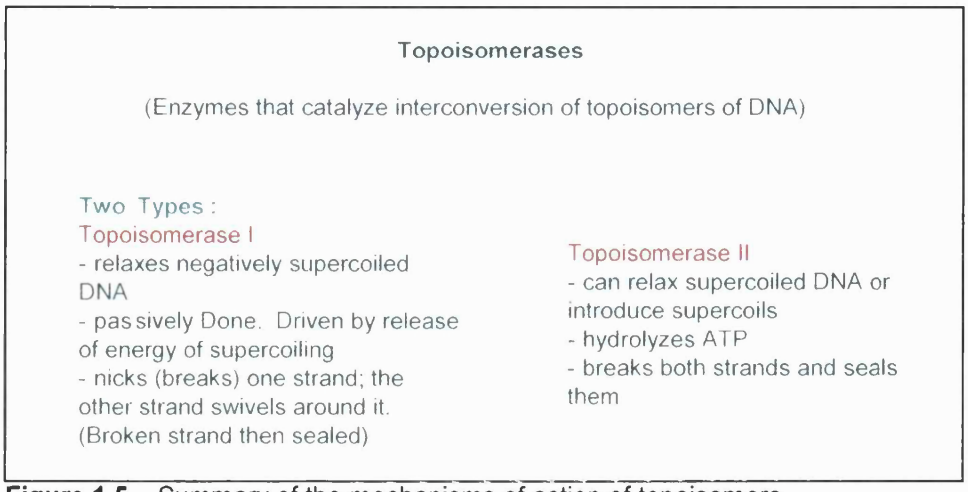

Figure 1.5 – Summary of the mechanisms of action of topoisomers.

This results in the initiation of a transient double strand break enabling the passage of a separate double helical strand [Kohn, 1996]. The stabilisation of the Topo II-DNA complex by for example doxorubicin would inhibit strand passage or reannealing of the break, thus resulting in DNA damage.

Studies by Tewey et al. in the early 1980's demonstrated that topoisomerase II may be a primary target for doxorubicin antitumour activity.

There is also evidence to suggest that doxorubicin inhibits activity of topoisomerase I in a dose dependent manner [Foglesong et al., 1992]. In addition, helicases, involved in the separation of double strand DNA, replication and transcription are also inhibited by the doxorubicin [Gewirtz, 1999].

1.2.2 Free radical-dependent mechanism of antitumour activity

The formation of free radicals during the metabolic activation of doxorubicin is due to its quinone structure. This enables doxorubicin to undergo reversible oxidation and reduction by accepting electrons, and is believed to contribute to its pharmacological activity [Sinha et al., 1987 and 1989]. Redox cycling of doxorubicin as shown in Figure 1.6, can occur in the cytoplasm, mitochondria, endoplasmic reticulum and in the nucleus, where doxorubicin selectively binds to DNA

[Doroshow and Davies, 1986 and Davies and Doroshow 1986]. Enzymes shown to be involved in the one-electron reduction of doxorubicin include, cytochrome P-450 reductase, NADH dehydrogenase, cytochrome b5 reductase, and xanthine oxidase [Sinha et al., 1987, 1984, and reviewed in Keizer et al., 1990].

During the one electron reduction of doxorubicin, cellular enzymes as shown in FIG 1.5 reduce the quinone (ring c) to form the semiquinone free radical. The semiquinone radical then reacts with oxygen with a bimolecular rate constant of 10^8 M^{-1} s^{-1} to form superoxide anion radical, ($O2^{\cdot-}$), hydrogen peroxide (H_2O_2), and the hydroxyl radical ($OH^{\cdot}$) [Sinha and Politi, 1990]. Under hypoxic conditions, the semiquinone becomes unstable, loses its daunosamine sugar moiety followed by its oxidation to the C_7 aglycone intermediate metabolite. The C_7 intermediate can either bind covalently to macromolecules or is further reduced to the more stable C_7 aglycone. The C_7 aglycone metabolite is pharmacologically inactive, however, its C_7 quinone methide tautomer is a potent DNA alkylating species.

The redox cycling of doxorubicin, as would be expected, is slow under hypoxic conditions where the semiquinone radical accumulates. However, it is possible that different mechanisms of toxicity may be evident under these conditions, depending on the partial pressure of oxygen. In addition to the above chemical reactions, doxorubicin has also been demonstrated to have high affinity for metals such as intracellular ferric ion (Fe^{3+}) and copper (Cu^{2+}).

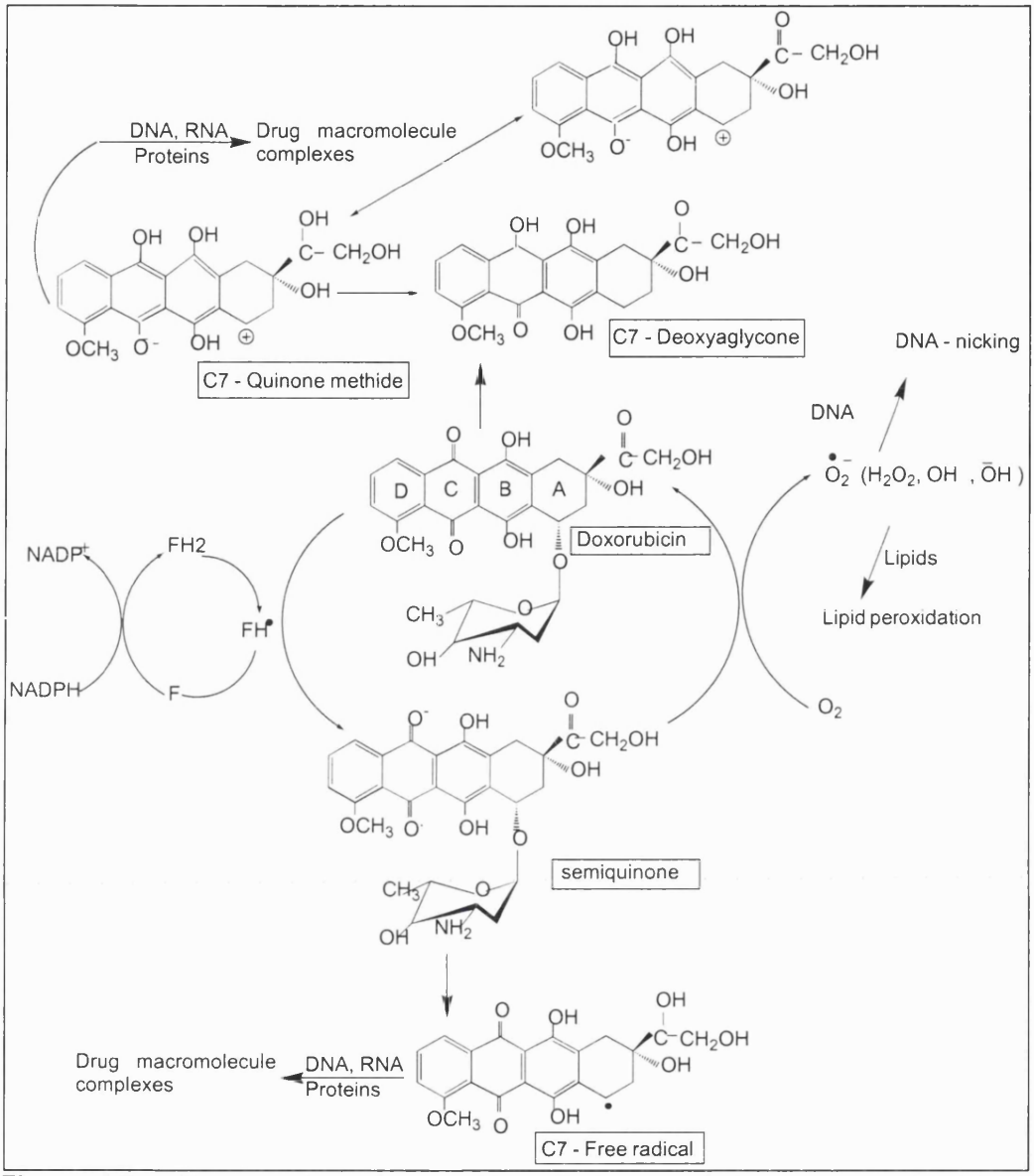

Figure 1.6 – Redox-cycling of doxorubicin. Reduction of doxorubicin and related anthracyclines by flavoproteins results in the formation of a semiquinone. The semiquinone can be oxidised back to the parental structure in the presence of oxygen, thereby producing superoxide radicals. During anaerobic metabolic reduction of doxorubicin, the semiquinone becomes unstable and loses its daunosamine sugar to form a C7 free radical intermediate. This doubly reduced doxorubicin molecule covalently binds cellular macromolecules.

Formation of an iron–doxorubicin complex has been observed which acts as a catalyst for the subsequent formation of the hydroxyl radical and hydrogen peroxide. Furthermore, evidence suggests that the iron–doxorubicin complex binds DNA and membranes with detrimental effects on mammalian cells of both tumour and normal origin [Minotti et al., 1999].

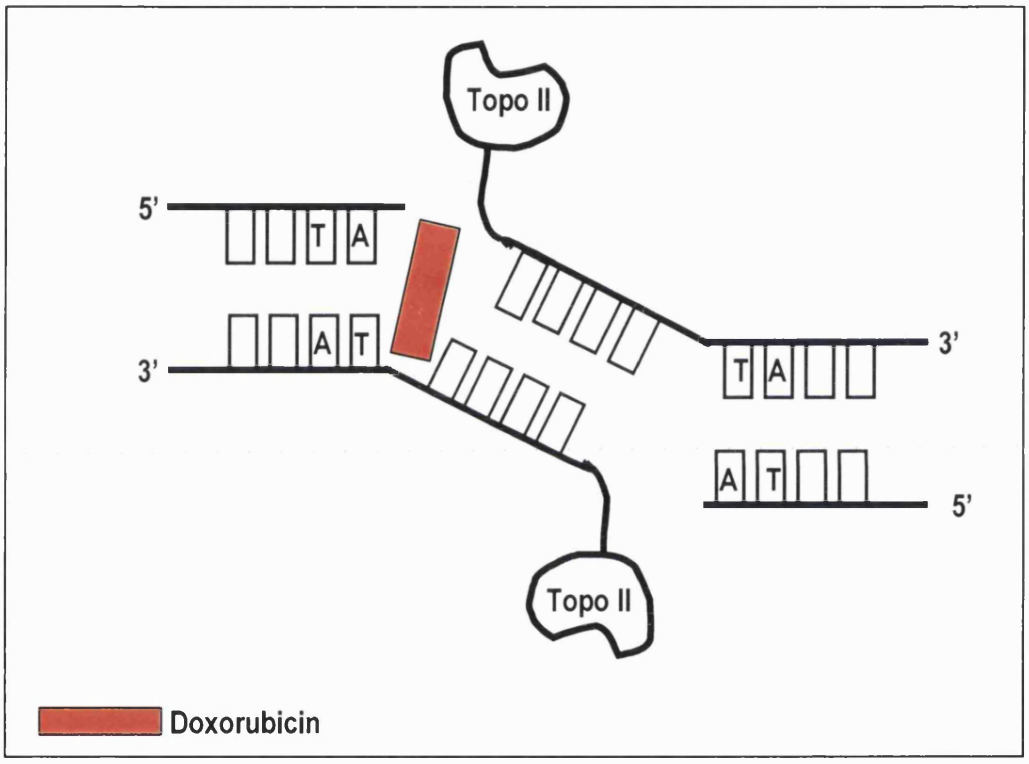

Figure 1.7 - Model representation of doxorubicin-stabilised Topo II-DNA complex with a strong base preference for an adenine (A) upstream of the DNA strand break. *Adapted from Kohn, 1996.*

Since the formation of free radicals is a normal event in cell metabolism, there are detoxifying enzymes in place, which scavenge these toxic radicals. These include superoxide dismutase (SOD) and glutathione peroxidase. SOD converts superoxide to hydrogen peroxide, which is then broken down to water and oxygen by catalase or glutathione peroxidase depending on the concentration of peroxide produced. Hence, the production of free radicals, with subsequent damage to macromolecules that is mediated by doxorubicin, can be counteracted by these detoxifying enzymes. However, the formation of these radicals following the reduction of doxorubicin is

still able to induce significant damage to cellular DNA and hence, enhance drug efficacy due to its ability to deplete glutathione levels.

1.2.3 Lipid peroxidation and cell membrane interactions

Under both hypoxic and normoxic conditions, peroxidation of unsaturated fatty acid is observed during redox cycling of doxorubicin. Lipid peroxidation can occur following metabolic activation of doxorubicin by the heart, liver, kidney microsomes, mitochondria or nucleus [Gewirtz, 1999]. Unsaturated fatty acids are peroxidised when exposed to hydroxyl radical in the presence of a metal catalyst such as iron. The consequence of lipid peroxidation is damage to cellular membranes, which can lead to cytotoxicity. Analogous to DNA damage, peroxidation of lipids can occur under low oxygen conditions but in the presence of hydrogen peroxide produced during the oxidation of doxorubicin semiquinone radical [Winterbourn et al., 1985]. Peroxidation of lipids can also be inhibited by SOD, catalase, glutathione, iron chelaters and scavengers of hydroxyl radicals [Mimnaugh et al., 1989]. However, it is not known to what extent lipid peroxidation contributes to the antitumour activity of doxorubicin since the majority of published reports were prepared using data from a cell free system, non-physiological conditions and very high concentrations of the drug.

Other mechanisms thought to contribute to the activity of doxorubicin are interactions with cell membranes that trigger signal transduction pathways leading to cell death. Studies performed by Triton and Yee [1983] using L1210 leukaemic cells, observed that doxorubicin was more toxic to cells than free drug when coupled to insoluble agarose beads, which are unable to traverse the cell membrane. In a subsequent series of experiments, Vichi and Tritton [1992] used calf thymus DNA in the incubation medium which abrogated drug toxicity of the drug due to the binding of the DNA to doxorubicin at the cell surface. However, the contribution of intracellular targets to doxorubicin induced toxicity cannot be ruled out since the intracellular concentration of doxorubicin in these experiment were not taken into consideration.

1.2.4 Cell cycle mediated effects and induction of apoptosis

The cell cycle is a well organised sequence of events resulting in the formation of two daughter cells from a single parental cell. The cycle proceeds through multiple checkpoints to ensure that previous events of the cycle are complete before the next phase is initiated. For example, the G1/S and G2/M phases are constantly surveyed by checkpoint gene products for protection against DNA damaging agents, and endogenous agents such as reactive oxygen radicals. Aside from the gene product ATM (mutated in ataxia-telangiectasia), another important regulator of the cell cycle is the p53 tumour suppressor gene, also known as the "guardian of the genome" due to its role in orchestrating cell death to ensure genomic stability. Consequently, lack of p53 protein expression, or mutations in the gene, are major steps towards carcinogenesis. Mutations in p53 have been found in 60-70% of human cancers resulting in inappropriate survival of genetically damaged cells [Wani et al, 1999 and Agarwal et al, 1998]. Non-cancerous or normal cells usually have low levels of p53 protein with a half-life of 20 minutes. P53 is thought to be phosphorylated by the DNA damage sensitive protein (ATM). This induces a change in P53 conformation upon which it cannot be targeted for destruction by MDM-2. Phosphorylated p53 is also a transcription factor that activates pro-apoptotic genes [Agarwall et al., 1998, Bennet, 1999, and Bellamy, 1996].

Mechanisms by which p53 dependent cell death occurs include upregulation of pro-apoptotic genes such as Bax, and suppression of anti-apoptotic genes such as bcl-2 (Tsujimoto and Shimizu, 2000), and translocation of intracellular Fas from the Golgi complex to the cell surface (Muller et al., 1997). P53-dependent G1 cell cycle arrest is thought to be mediated via the induction of WAF-1 with subsequent inhibition of cyclin dependent kinases, which represses the phosphorylation of the retinoblastoma protein (pRB) resulting in the release of E2F-1, thus preventing G1-S phase transition (Hartwell and Kastan, 1994, and Bartek et el., 1997).

The effect of doxorubicin on the cell cycle machinery has mainly been investigated by flow cytometric analysis of DNA content in cultured mammalian cells. The effect of doxorubicin on the cycle is dose- and time-dependent, where cells have been observed to arrest in early S phase using high concentrations, whereas lower concentrations arrest cells mainly in the G2 phase, via the disruption of cyclin dependent kinase, p34cdc2 [Ling et al., 1993]. Other studies provide evidence of a

G1 growth arrest following restoration of p16ink4A, a cyclin dependent kinase inhibitory protein (Shapiro et al., 1998). In addition, synchronised cells treated with doxorubicin show a cell cycle dependent toxicity with a gradual increase in toxicity from G1 to G2M (Minderman et al. 1993).

Apoptosis or programmed cell death, as the name suggests, is a form of cell suicide triggered by a variety of stimuli. It is initiated by a cascade involving several enzymes and proteins including caspases. Caspases are normally present in the cell as proenzymes that limited proteolysis for activation of enzymatic activity. Figure 1.8 shows the proposed steps of apoptosis induced by cell surface receptors like the FAS ligand.

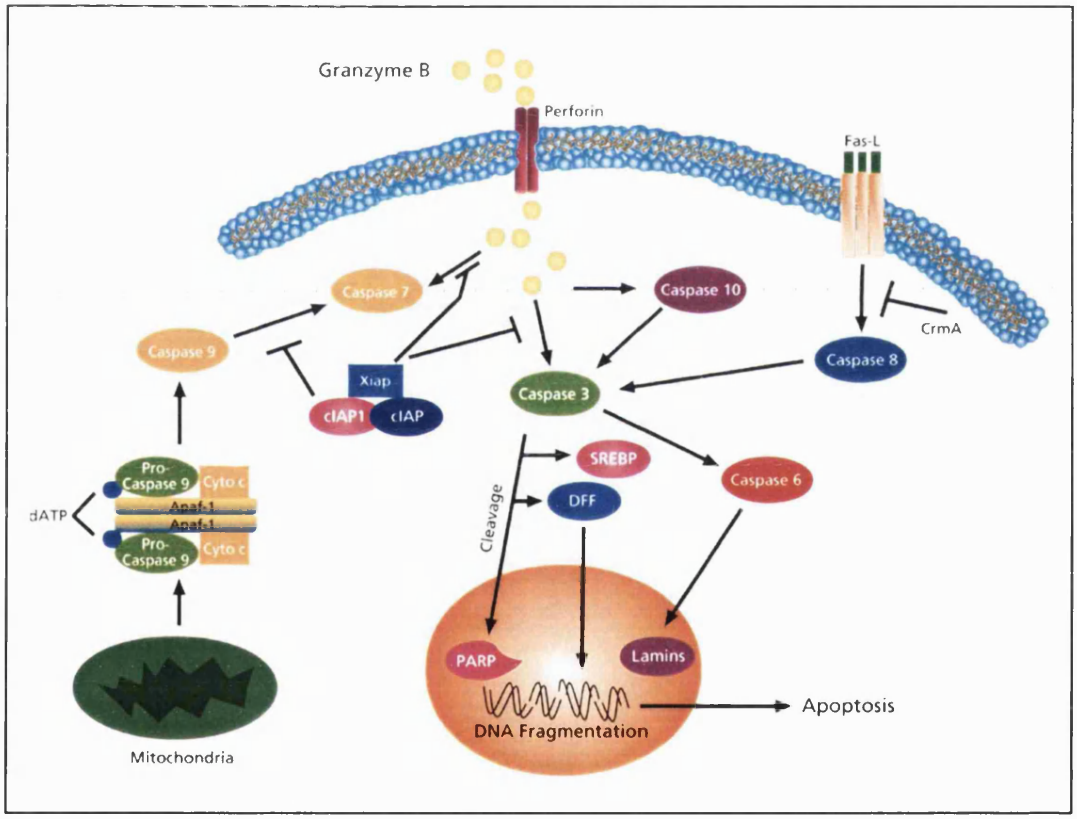

Figure 1.8 – Proposed steps of apoptosis involving caspases. Enzymatic activation of initiator caspases leads to proteolytic activation of effector (downsteam) caspases and cleavage of vital proteins. Activated caspases 8 activates caspases via two pathways; the first is cleavage of Bcl-2 interacting protein (Bid) which triggers cytochrome c release from the mitochondria. The released cytochrome c binds apoplectic protease activating factor-1 (APAF-1) together with dATP causing self-cleavage and activation of caspase 9. The second pathway involves direct cleavage and activation of procaspase 3. Caspase 3, 6 and 7 are effector caspases that act to cleave various cellular targets. Granzyme B and perforin are released by cytotoxic T cells and induce apoptosis by forming transmembrane pores. Diagram was taken from Sigma-Aldrich website.

There are usually three microscopically visible, distinct phases displayed by cells undergoing apoptosis; the first involves condensation of chromatin, disintegration of nucleoli, reduction in nuclear size, shrinkage of total cell volume, increase in cell density, compaction of some cytoplasmic organelles and dilation of the endoplasmic reticulum. The second phase of apoptosis involves blebbing and constriction of both the nucleus and cytoplasm into small membrane bound bodies. The third and final stage of apoptosis is associated with progressive degeneration of residual nuclear and cytoplasmic structures [Allen et al., 1997, Hickman and Boyle, 1997]. Two important biochemical markers for the detection of apoptosis are the production of 180-200 bp internucleosomal DNA fragments and early endonucleolytic cleavage of DNA to produce fragments of 50 or 300 kb [Skladanowski and Konopa, 1994a and 1994b].

Both doxorubicin and its derivative annamycin have been shown to produce internucleosomal DNA fragmentation in the cervical cancer cell line, HeLa, [Skladanowski and Konopa, 1993], and in murine thymocytes [Zaleskis et al., 1994]. There is also evidence suggesting that doxorubicin-induced apoptosis is dose dependent, whereby apoptosis was not observed at supraclinical concentration of 5 μM and above [Zaleskis et al., 1994]. At present, research on anthracycline antibiotics is very much focused on how these compounds trigger the apoptotic pathway.

1.3 Multi-drug resistance

Like many anticancer agents, doxorubicin is not selective for tumour cells, and, being a small amphipathic molecule with high affinity for DNA, it is able to traverse the cell membrane readily with intercalation into DNA of both normal and cancerous cells. As a consequence, its clinical use is limited due to toxicities ranging from bone marrow suppression, oral ulceration, alopecia, gastrointestinal mucosities, neutropenia and dose dependent cardiomyopathy. Usually administered to patients at a dose of 60-75 mg/m^2 every 21 days, with a maximum accumulated tolerated dose of 550 mg/m^2 [Bates et al., 1996], repeated administration of doxorubicin and other anthracyclines often results in multi-drug resistance (MDR).

1.3.1 Mechanisms of drug resistance

Several haematological and solid tumours have been shown to acquire resistance to anthracyclines. In 1979, an active outward transport mechanism for anthracyclines in the murine P-388 human leukaemic cell line was reported [Gewirtz, 1996]. The gene found to be responsible for this action, MDR1, encodes a 170 KD protein, p-glycoprotein (pgp), the cDNA of which was isolated from Chinese hamster ovarian cells and at a later date from tumour cells known to be resistant to drug treatment. Pgp mediates the ATP dependent export of many anticancer drugs from the cell, thereby preventing their intracellular accumulation and thus efficacy. Studies have since shown that the level of pgp expression correlates well with the degree of drug resistance [Sinha et al., 1989]. In humans, the MDR1 gene is localised on chromosome 7 and the protein functions as a transmembrane ATP dependent drug efflux pump, transporting anthracyclines and other cytostatic agents out of the cell [Hortobagyi, 1997]. Furthermore, a doxorubicin resistant HL-60 myeloid leukaemia cell line was found not to express the 170 KD protein but rather a 190 KD protein not expressed by the parental cell line. The product, MRP, was localised to chromosome 16, which encodes several ATP binding transmembrane trasporters.

Apart from the expression of either MRP and or MDR1, other mechanisms that play a role in anthracycline resistance have been described. These include decreased levels of topoisomerase II activity, increased levels of glutathione and other detoxifying enzymes, downregulation of pro-apoptotic genes Fas/Apo-1 and bax, and upregulation of anti-apoptotic genes such as bcl_2 and bcl_{xl} [Muller et al., 1998a and 1998b].

1.4 Drug delivery systems

In spite of being one of the most potent anticancer drugs, the main limitation of anthracycline antibiotics as mentioned previously is a myriad of toxic effects. Foremost amongst these is the dose-related cardiotoxicity. In contrast to heart mitochondria, liver lacks the NADH reduction pathway of the respiratory chain from the cytosol, and therefore it is unable to initiate the production of free radicals from redox cycling of doxorubicin as shown in Figure1.5 Whereas NADH dehydrogenase

is present in heart mitochondria for ATP production, in the presence of doxorubicin, electrons are transferred from NADH to the quinone instead of the respiratory chain. This results in concomitant damage to cardiac myocytes through free radical dependent mechanisms including stimulation of lipid peroxidation. Thus, the presence of NADH dehydrogenase in the heart is a major contributing factor for the dose dependent cardiotoxicity often observed in patients undergoing treatment with anthracyclines. Since cardiotoxicity is directly related to the cumulative dose of doxorubicin, a reduction or prevention of this undesired effect would enable administration of higher doses thereby enhancing the therapeutic index of the drug and in addition increase the quality and extent of life of patients.

1.4.1 Polymeric macromolecules as delivery systems for low molecular weight agents

Over the past few decades, our understanding of the molecular basis of cancer has considerably advanced and has opened new avenues for improving drug therapy to solid tumours. As shown in Figure 1.1 there has been an increase in the synthesis of new anticancer agents for clinical use. However, most of these agents also elicit nonspecific toxicity, thereby compromising their efficacy. In conjunction with these limitations is the development of tumour cell resistance. To circumvent these problems, a number of drug delivery systems for anthracyclines have been developed with the aim of improving therapeutic response, but most importantly a reduction in drug toxicity to normal tissues. Amongst the systems explored for the efficient delivery of existing anticancer agents to target sites are 1) low-molecular weight prodrugs, 2) macromolecular carriers, 3) synthetic polymers, 4) natural polymers, 5) nanoparticles, and 6) liposomes.

Helmut Ringsdorf (Batz et al., 1972] proposed the rationale for the development of prodrugs in the early 1970's, the idea being that an inert or a non-reactive degradable carrier can be used to attach a drug via spacer moieties (Figure 1.9). According to this proposal, the conjugate has to be stable in the bloodstream but cleaved intracellularly at the target site. Therefore the drug carrier has to be 1) water soluble, 2) amenable to covalent conjugation 3) a candidate for pinocytic capture 4) biocompatible and 5) amenable to degradation or excretion from the body following drug release. These criteria would ensure that the conjugate could be easily

administered. In addition, the conjugate must be non-immunogenic, non-carcinogenic and pharmacologically inert following cleavage of the spacer moiety.

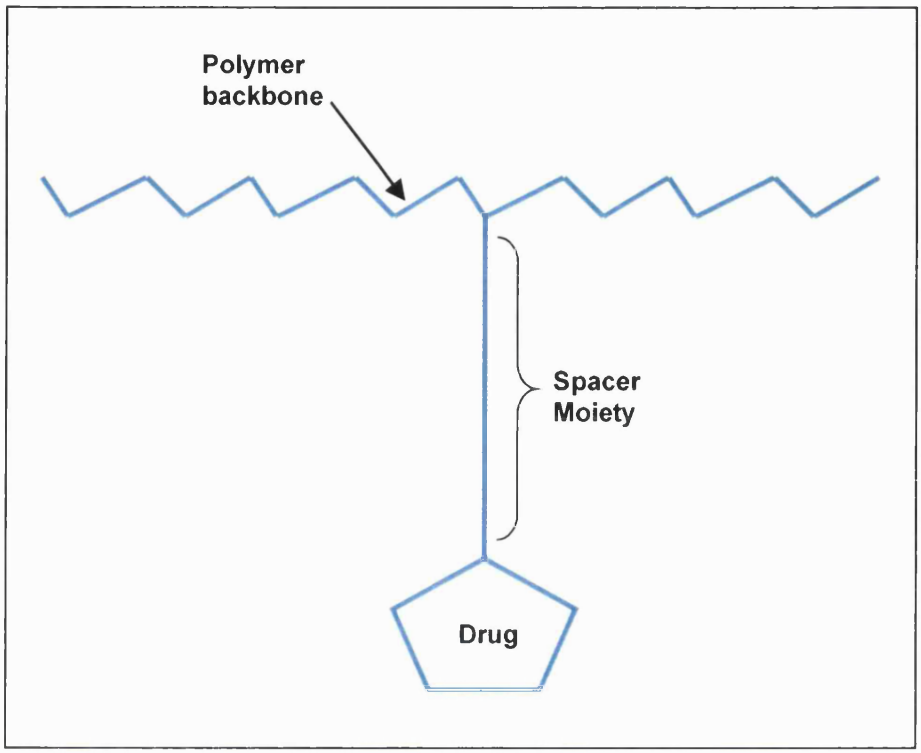

Figure 1.9 - Proposed model for the development of a macromolecular prodrug

Polymers or polymeric controlled drug delivery systems have been utilised with the aim of targeting tumours specifically, and for the delivery of an anticancer agent in a controlled manner over an extended period of time, thereby increasing drug accumulation at the target site. The use of delivery systems to target drugs to tumours would be particularly beneficial for existing anticancer agents that are rapidly metabolised and eliminated from the body (e.g. doxorubicin) following administration.

At present, polymer based drug delivery systems for controlled release have become the focus of attempts to improve cancer chemotherapy. To date, there are 4 major types of polymers for controlled release, these are, 1) diffusion control systems, 2) solvent activated systems, 3) magnetically controlled systems and 4) chemically controlled systems [Ranade, 1990]. Diffusion controlled systems may take the form of a reservoir or a matrix. A reservoir is a physical structure which comes in different shapes; spherical, cylindrical or slab-like, with the core consisting

of the drug in a powdered or liquid form surrounded by a layer of nonbiodegradable polymer for controlled drug release. In a matrix system, the drug is distributed in a non-uniform manner within the polymer, subsequently a non-uniform release of the drug from the matrix is observed.

Solvent activated systems also include two forms; an osmotic and a swelling controlled system. In the osmotically controlled system, a combination of an external fluid with low drug concentration moves across a semipermeable membrane to an area in the device containing high concentrations of the drug. This movement of fluid by osmotic pressure forces the drug out through a tiny pore created in the device. The swelling controlled system on the other hand, consists of hydrophilic macromolecules cross-linked to form a three-dimensional structure; the polymer is then able to hold a large quantity of water without dissolving itself.

Magnetically controlled systems are composed of albumin and magnetic microspheres. These systems are used for selective targeting because of their magnetic characteristics. Aside from area specific localisation, magnetic controlled systems can accommodate a variety of drugs [Ranade 1990].

Chemically controlled systems comprise of pendent chain and biodegradable systems. Pendent chain systems involve chemical linkage of the drug to the backbone of a polymer directly or via a spacer moiety. Once at the target site, chemical hydrolysis or enzymatic cleavage occurs with concomitant intracellular release of the drug at a controlled rate. With biodegradable systems, the controlled release of the drug is mediated via the gradual decomposition of the polymer.

1.4.2 PK1

Over the past decade, 4 polymer drug conjugates have entered clinical trials. The first of these is PK1 (FCE28068) as shown in Figure 1.10. This is an [N-(2-hydroxypropyl)methacrylamide] (HPMA) copolymer covalently linked to doxorubicin via a peptidyl spacer group, glycylphyenylalanylleucylglycine (Gly-Phe-Leu-Gly = GFLG). HPMA homopolymer was initially developed for use as a plasma expander in 1973. Plasma expanders are used to expanding intra-vascular plasma and total blood volume concentrated within muscle tissue. The covalent conjugation of doxorubicin to this hydrophilic, non-immunogenic and chemically inert polymer has led to improved tumour targeting, enhanced drug accumulation within the tumour

(bioavailability) and increased plasma half-life (15 times longer than doxorubicin), decreased cardiotoxicity, hence, improved drug efficacy.

PK1 has been designed specifically to achieve increased tumour selectivity and for

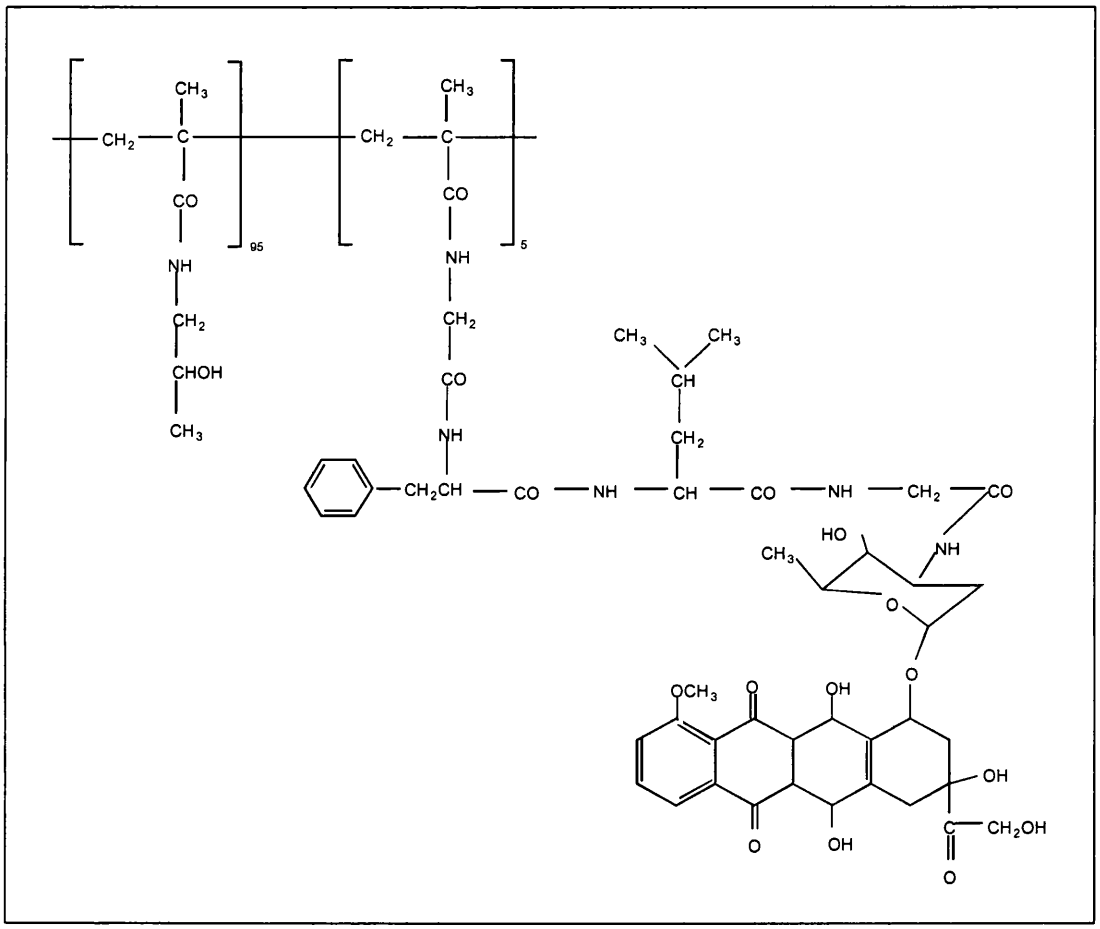

Figure 1.10 - Chemical structure of HPMA copolymer-doxorubicin (PK1, FCE 28068) linked via a GFLG tetrapeptide spacer to the sugar amine by a peptide bond.

the intracellular controlled release of doxorubicin within the tumour. The conjugate is stable in blood and serum, and unlike the parent drug (doxorubicin), too large to diffuse across the membrane of cells of both normal and tumour tissues. Its mechanism of cell entry is thought to be limited to fluid phase pinocytic capture with subsequent release of doxorubicin from the lysosomal compartment, accompanied by intercalation into DNA prior to degradation of the GFLG linker by lysosomal cathepsin B [Duncan et al., 1982, Duncan, 1986, Subr et al., 1988 Kopecek et al, 2000]. Cathepsin B levels have been found elevated in many human tumours and this correlates with poor prognosis [Berquin and Sloane, 1996, Yan et al., 1998, Campo et al.,1994 and Sloane et al., 1981].

1.4.3 Fluid phase pinocytosis; trafficking of PK1 to lysosomes

Fluid phase pinocytosis is a form of endocytosis, a mechanism used by cells to sample extracellular fluid, clear membrane proteins, lipids and receptor bound ligands from the cell surface. Phagocytosis, another form of endocytosis, involves engulfment of particulate matter such as bacteria, erythrocytes, latex beads and liposomes. Depending on the structure of the macromolecule to be internalised, three types of pinocytosis can occur; receptor mediated, adsorptive or fluid phase. PK1 is unable to traverse the plasma membrane, and, being electrically uncharged, does not have affinity for plasma membranes. Internalisation is thought to occur via fluid phase pinocytic capture.

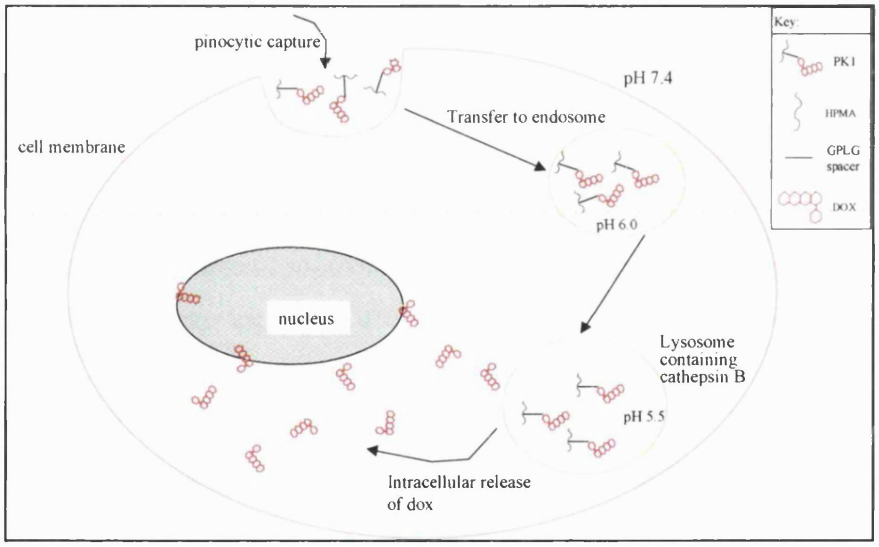

Figure 1.11 – Proposed mechanism for internalisation of PK1 and other polymeric drug conjugates. (modified from Duncan, 1992).

Fluid phase pinocytosis or "cell drinking" is a constitutively active process, and the prodrug is thought to be captured as a solute in the extracellular fluid by membrane invagination, and the formation of membrane bound vesicles. These vesicles then pinch off from the plasma membrane to form endosomes, which migrate through the cytoplasm to fuse with primary lysosomes, to form secondary lysosomes. Present in the lysosomes are numerous proteases that degrade intracellular and extracellular proteins and therefore play a major role in protein turnover. One of these proteases is the thiol-dependent protease cathepsin B, which will hydrolyse the GFLG spacer in

PK1 with the release of doxorubicin, (Figure 1.10). Following hydrolysis of the spacer with the subsequent release of doxorubicin, it is thought that the lysosome membrane allows passage of low molecular weight substances such as doxorubicin into the cytoplasm [Subr et al., 1992], while preventing entry of undigested macromolecules and lysosomal enzymes. Being a lysosomotropic agent, the rate of pinocytic capture of PK1 is relatively slow and directly proportional to its concentration in the extracellular fluid [Duncan et al., 1981].

1.4.4 Cathepsin B

Cathepsin B is a lysosomal thiol protease initially defined as an enzyme that will deamidate benzyoyl-L-arginine (Bz-Arg-NH_2), in the presence of a reducing sugar. Its functional role is in the degradation of proteins that enter the lysosomes from the cell exterior or from other compartments within the cell. The cathepsin B gene consist of 13 exons, and cathepsin B initially translated as a preproenzyme of 339 amino acid polypeptide chain, which is processed to the mature form of 254 amino acid residues through several proteolytic cleavages (Figure 1.12). Protein products of a 30 KDa single chain, and a 26/25 KDa glycosylated and unglycosylated heavy chain of double chain cathepsin B are usually present in cells. Cathepsin B has been isolated from different species including rat, rabbit, bovine and human, and found localised in liver, spleen, brain and in human leukocytes with varying concentrations in different tissues [Keppler, Sloane, 1996, Moin et al., 1992.]

Analogous to other cathepsins, cathepsin B possesses endopeptidase and exopeptidase activity, cleaving internal peptide bonds, and dipeptides sequentially from the C-terminus respectively. Being thiol-dependent, cathepsin B requires the intactness of its lone thiol group for biological activity over a pH range of 4.0-8.5 if properly stabilised. Most low molecular weight synthetic substrates for cathepsin B have arginine in the P1 position and are efficiently hydrolysed, however, according to Kirschke and Barret [1985], the most important amino acids that determine efficient cleavage are residues in the P2 and P3 positions, the presence of phenylalanine or leucine in the P2 position also provides an excellent substrate for cathepsin B.

Several investigations have implicated cathepsin B in the progression of human tumours. Certain cells of cancer origin secrete procathepsin B constitutively. In non-transformed cells, cathepsin B is secreted to perform specific functions. For example, osteoclasts secrete cathepsin B during bone remodelling and resorption [Rifkin et al., 1991], and macrophages secrete cathepsin B during inflammation [Reddy et al., 1995]. Studies on human prostate cancer demonstrated high levels of cathepsin B mRNA in cells at invading margins. Degradation of basement membrane constituents has been shown to be related to invasion and metastasis of tumours, and cathepsin B has therefore been implicated in the facilitation of tumour metastasis [Sloane et al, 1984]. It is known that at physiological pH, cathepsin B degrades type IV collagen, fibronectin and laminim *in vitro*, all of which are major constituents of basement membranes [Buck et al., 1992].

As well as being implicated in tumour invasion and metastasis, cathepsin B has also been implicated in tumour angiogenesis. As previously mentioned, tumours cannot grow beyond 2 mm in diameter without their own blood supply. It is thought that cathepsin B may initiate the stimulation of endothelial cells in vessels neighbouring the tumour for the degradation of basement membrane, migration into perivascular stroma and sprouting of new capillaries. Endothelial cells in neovessels at the infiltrating margins of prostate cancer showed increased immunostaining for cathepsin B [Sinha et al., 1995]. In addition, cathepsin B protein and enzymatic activity have been found to be elevated in tumours of the breast, cervix and ovary, colon, stomach, glioma, lung and thyroid [Berquin and Sloane, 1996]. Furthermore, increased levels of this protease have been found in the serum and fluids surrounding tumours in patients [Poole et al., 1978].

Because of the association of increased cathepsin B expression with cancers and the possible implication of cathepsin B in invasiveness, doxorubicin has been conjugated to HPMA via a spacer moiety susceptible to cleavage by cathepsin B for selective targeting to tumour cells. Moreover, the GFLG linker in PK1 was also found to be a better substrate for cathepsin B in relation to other oligopeptide spacers [Subr et al., 1988], with significant antitumour activity in preclinical and clinical testing [Duncan et al., 1998 and Thomson et al., 1999]. In vitro studies undertaken by Kopecek and co-workers using the human ovarian carcinoma cell line, A2780, showed activity against cells expressing p-glycoprotein. Most importantly, PK1 was found to be active against MDR positive tumours *in vivo* without the associated

systemic toxicity often observed with free doxorubicin [Minko et al., 1999, Muggia, 1999].

1.4.5 The enhanced permeability and retention (EPR) effect

In addition to differences in the mechanism by which PK1 and doxorubicin enter cells (fluid phase pinocytosis and diffusion, respectively), another component thought to be relevant to the antitumour activity of PK1 is the enhanced permeability and retention (EPR) effect. The EPR phenomenon has been postulated as the predominant mechanism by which PK1 and other macromolecular prodrugs accumulate in tumours [Minko et al., 2000]. Maeda [Maeda et al., 2000, and Noguchi et al., 1998 proposed the concept of the EPR effect over a decade ago. It is a phenomenon that uses the hyperpermeability of tumour vasculature as an advantage in retaining macromolecules following their extravasation. Most low molecular weight anticancer agents such as doxorubicin extravasate tumours by diffusion into both normal and tumour tissue. Consequently the drug accumulates in organs and normal tissues, which compete with the tumour for drug. Relatively little drug remains for the tumours, hence the lack of targeting.

As discussed in section 1.1.1, tumour vasculature is severely disorganised and hyperpermeable relative to normal vasculature. Being 3-10 times more leaky, tumour vasculature has wide inter-endothelial junctions which are thought to aid the accumulation of macromolecules following extravasation.

Furthermore, tumours lack functional lymphatic drainage, therefore, once extravasated, macromolecules are thought to be retained within the tumour before being taken back into the circulation. Thus, the accumulation and trapping of macromolecules within tumours is the principle behind the EPR effect. Studies by Seymour et al., [1997] showed accumulation of HPMA copolymers in S-180 sarcoma and B16F10 melanoma models *in vivo*. Duncan and Sat [1998], again using the B16F10 melanoma and the L1210 mouse leukaemia model, suggested that the accumulation of macromolecules is dependent on tumour size.

The exact mechanism by which the EPR effect is mediated is not known. However, possible mediators have been proposed (Table 2). There is evidence to suggest that vascular permeability factor (VPF) in mice and its human homologue,

vascular endothelial growth factor (VEGF), may be involved. VEGF is a 38 KDa protein normally produced by epithelial cells, macrophages and smooth muscle cells for the induction of angiogenesis, endothelial cell proliferation and vascular permeability. VEGF has been shown to be secreted by human tumour cell lines [Baban and Seymour, 1998]. In addition to VEGF, Maeda and colleagues, have also proposed a role for the kinin cascade in the EPR effect. The VEGF mechanism of enhancing vascular permeability is via endothelial cells, while the kinin cascade is said to be via the smooth muscle layer, resulting in gap junctions between endothelial cells for the increased fluid translocation across tumour vasculature.

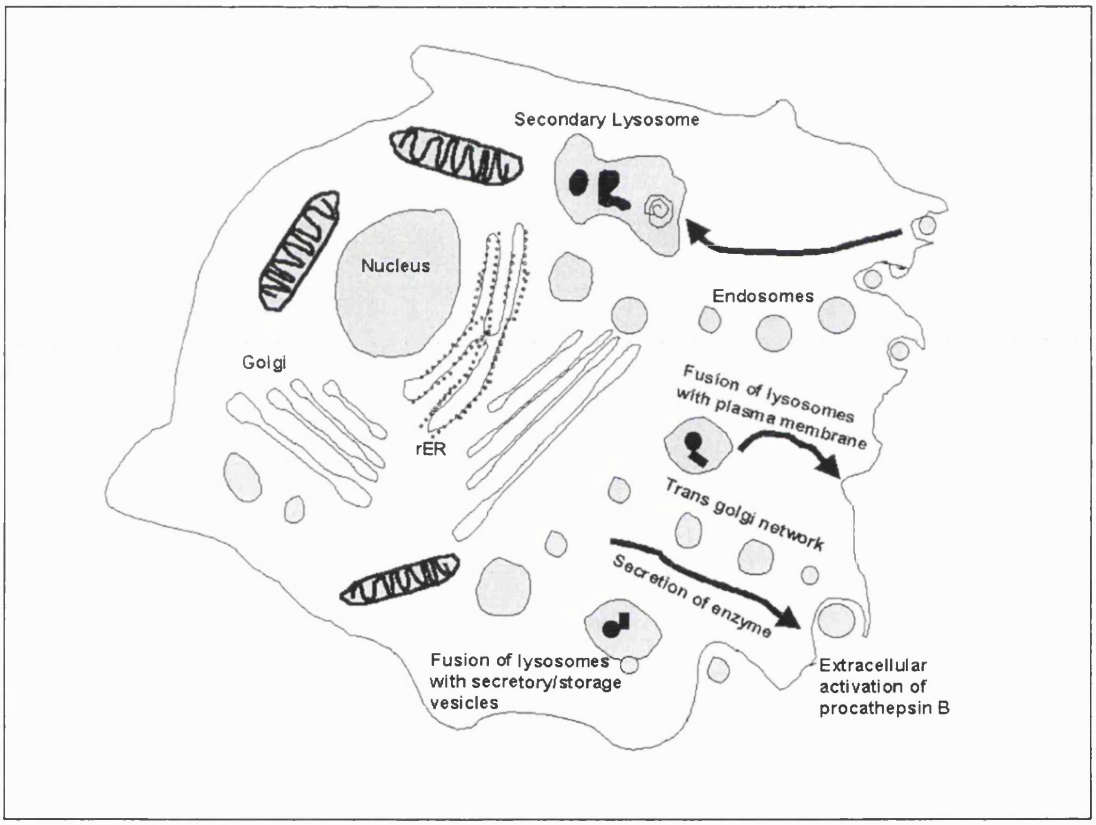

Figure 1.12 - Pathway of cathepsin B synthesis. Preprocathepsin B is synthesised on the rough endoplasmic reticulum. Following transport to the Golgi, the enzyme is glycosylated for recognition by mannose-6-phosphate receptors located in the trans-Golgi network. Procathepsin B is transported to an acidic compartment where the enzyme is activated. The acidic compartment form by fusion with primary lysosomes, secondary lysosomes or endosomes. Cathepsin B can also be secreted as a proenzyme and activated extracellularly. Adapted from Mort and Buttle, 1997.

Nitric oxide synthase (NOS), an enzyme expressed by tumour cells has also been implicated in tumour pathophysiology. Nitric oxide (NO), a potent vasodilator, induces the expression of VEGF and neovascularisation in tumours. Hence, NO is an

initiator of inflammation, cancer and angiogenesis. Furthermore, the involvement of NO in the EPR effect is evidenced by the ability of NOS inhibitors to reduce tumour volume [Fakumura and Jain, 1998].

1.5 Scope of this thesis

The purpose of this study is to firstly investigate the time-and dose-dependence of PK1 and doxorubicin-induced cytotoxicity. Despite its use in the clinic for over 30 years in the treatment of many solid tumours and soft tissue sarcomas, not enough is known with regards to the time- and dose-dependency of doxorubicin-induced cell death. Several mechanisms, as discussed under section 1.2 have been shown to contribute to the cytotoxic effects of doxorubicin. However it is unclear to what extent each of these mechanisms contribute to cell killing. Muller et al. [1997] have shown that doxorubicin-induced apoptosis and oxidative DNA damage are dependent on dose. However, the authors failed to take into account the effect of time since current treatment regimes depend on both effective concentration and time for optimal plasma levels without evidence of cumulative dose-dependent cardiomyopathy.

The doxorubicin polyHPMA conjugate, PK1, is currently undergoing phase II clinical testing and has been reported to have significant antitumour activity [Vasey et al., 1999]. Although the design of PK1 was based upon the prediction that its mechanism of activity would be equal to that of doxorubicin following cleavage of the GFLG linker, it has not been confirmed which mechanism(s) are involved in PK1 cell killing *in vitro* and *in vivo*. Furthermore, very little is known about the effects of PK1 *in vitro*, although preliminary results suggest that the conjugate is relatively non-toxic to cells growing in culture [Wedge, 1991, Duncan et al., 1992]. However, if the proposed mechanism of PK1 internalisation as shown in Figure 1.11 is indeed the route taken by the conjugate for the manifestation of cytotoxicity, one would expect cathepsin B competent cells growing in culture to show sensitivity towards PK1. For these reasons, we aimed to characterise the cytotoxic effects of PK1 on various cancer cell lines growing in culture and compare them with those of doxorubicin (chapter 2). Also, the intracellular fate of PK1 and doxorubicin would be investigated using fluorescence microscopy (Chapter 3).

Finally, we wished to investigate possible explanations for the observed differences between the relative toxicity of PK1 *in vitro* and *in vivo* in relation to the effects of doxorubicin for the future of drug design and for understanding tumour biology (Chapter 4). This was done using C57 mice bearing s.c. B16F10 murine melanoma, a model which has been demonstrated to exhibit the EPR [Seymour et al., 1994]. The ability of PK1 to induce DNA damage in tumours at the single cell level was investigated using the quantitative comet assay, which allows assessment of DNA damage at the single cell level.

CHAPTER 2 - PHARMACODYNAMICS OF DOXORUBICIN AND PK1 AGAINST HUMAN BREAST ADENOCARCINOMA CELLS *IN VITRO*.

2.1 INTRODUCTION

Doxorubicin induces a myriad of biochemical effects on exposed cells. As described in chapter 1, these effects have been proposed as contributing factors to the antitumour activity of the anthracycline antibiotic. Being an amphipathic molecule with polar and non-polar characteristics, doxorubicin is able to interact with cell membranes. In addition, as shown in Figure 1.4, its planar aromatic structure with a net positive charge enables interaction of doxorubicin with DNA. The documented effects contributing to the cytotoxic effect of doxorubicin are dependent on concentration. For example, induction of apoptosis is observed at concentrations below 1 μM, whereas lipid peroxidation and the production of free radicals are observed only at relatively high concentrations ranging from 25 -100 μM [Keizer et al., 1990]. The complex interactions involved in antitumour activity are dependent on doxorubicin concentration, and these have been well documented. However there are relatively few reports on these effects in relation to time.

Upon administration of a therapeutic agent, response is never obtained immediately; it is often delayed and may only manifest itself hours, days or sometimes weeks following administration. There are several reports in the literature on time-dose relationships of anticancer agents that correlate therapeutic response and pharmacokinetic parameters in individual patients [Evans, 1988]. However, our knowledge on concentration and time dependent relationship is rudimentary both *in vivo* and *in vitro*. Understanding the pharmacokinetics and pharmacodynamics will undeniably improve cancer therapy by optimising therapeutic response and decreasing toxicities.

Since its introduction into clinical use, doxorubicin has been administered by bolus injection at 50-60 mg/m^2 every 3-4 weeks. The rationale for this dosing regimen was solely based on the long elimination half-life of doxorubicin [Beilack et al.,

1989]. As discussed in chapter 1, the associated life threatening cardiotoxicity characterised by progressive congestive heart failure compromises doxorubicin efficacy by restricting cumulative doses to 450-550 mg/m^2. In the mid 1970's, evidence began to accumulate that weekly administration of doxorubicin maintained drug efficacy but produced less cardiotoxicity [Barranco, 1975, and Smith 1985]. These results raised questions in terms of which scheduling of doxorubicin should be used. Smith [1985] proposed that a reduction and fractionation of dose would improve the therapeutic index of doxorubicin by decreasing toxicities. On the other hand, Hryniuk and Bush [1984] stressed the importance of dose intensity to achieve increased response rates in metastatic breast cancer. However the use of long-term continuous infusion of 5-Fluorouracil (5-Fu) in the treatment of adult leukeamia has shown improved efficacy over the initial use of bolus administration [Bodey et al., 1976]. With conflicting results in the case of doxorubicin, there is no agreement between clinicians on which dosing schedule of doxorubicin to use. Despite a reduction in doxorubicin-associated toxicities, there is not enough evidence to suggest that continuous infusion is superior over bolus injection.

In vitro cytotoxicity studies of 5-Fura against human epithelial cancer cells [Calabro-Jones et al., 1982] showed a linear relationship between concentration and time, with an increase in drug exposure resulting in increased cytotoxicity. The product of concentration and time (c x t) is regarded as an important pharmacokinetic parameter in determining drug efficacy *in vitro,* and therefore its use may be useful in predicting the response to anticancer agents *in vivo* [Broder and Carbone, 1976]. The product of c and t is the same as area under the curve (AUC) from time zero to infinity. According to Gillette [1974], compounds that interact with a specific receptor, like many anticancer agents, often show a response that is a function of c x t. In common with many chemotherapeutic agents, when the concentration of doxorubicin is increased, common toxicities are also escalated, thus the view that administering agents at the maximum tolerated dose (MTD) for optimal response is not always the case. A study by Eichholtz-wirth [1980], documented that the cytostatic effect of doxorubicin against Chinese hamster and Hela cells was proportional to the product of extracellular drug concentration and exposure time.

Haber's rule [Hayes, 1991] states that the smaller the product of c x t for a given response, the greater is the toxicity for that agent/drug. Thus ct = k where k is a constant characteristic of a particular compound. When analysing data to plot log dose

log time, values for c and t that give rise to a defined response (e.g. 50% cell death) are determined. The log C is plotted vs log T or logdose vs logtime is plotted. These graphs are usually characterised by three distinct segments (Figure 2.1) thought to represent the different mechanisms of drug action at a given concentration. The first segment (**A**) reflects the fact that a certain amount of time must pass for the defined response to be seen following addition of the drug, no matter how high the drug concentration. The second segment (**B**) represents time of incubation/exposure required to cause the defined response and increases as drug concentration is decreased. Typically this part of the graph is linear. Haber's rule states that (over this range) c x t is a constant. The third and final segment (**C**) represents a dose of drug at which no additional response is observed irrespective of how long one waits. Hence c x t = k represents the second segment of the logtime vs logdose curve on a log scale with a slope of 1.

Therefore Haber's rule is a special case of the second segment, where each time defines level/concentration of exposure.

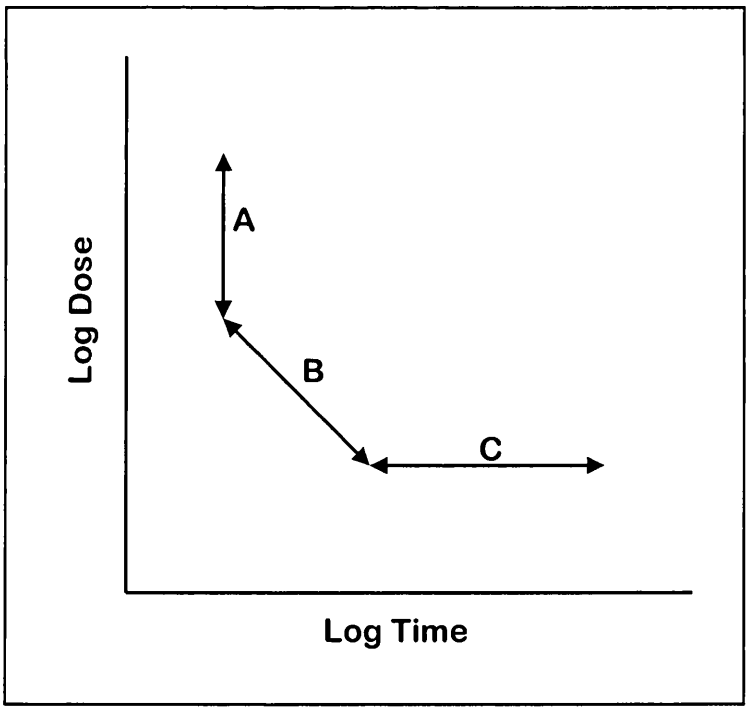

Figure 2.1 – *Model of the logtime logdose plot.*

One must bear in mind that not all compounds exhibit all three segments, with the exception of warfarin and a few others. Some compounds exhibit the 1st and 2nd,

while most exhibit the 2nd and 3rd segments. Crucially, not all compounds obey Haber's rule, because not all show a slope of -1 for the second segment ct = k. Some compounds have slopes which are less or greater than 1 and thus applying Haber's rule will lead to inaccuracies in data interpretation. According to Adams [1989] drug action is not always a function of c x t. Antitumour activity is not related to c x t simply because cytotoxicity is not a constant. According to Adams [1989] and Skipper [1965], for a specified drug efficacy, log transformation of concentration and time values yields a straight line whose slope is defined as the concentration coefficient, n, and whose intercept is the exposure constant, k, for that level of cell kill. This pharmacodynamic principle:

$$C^n x\ T = k$$

was originally used by Skipper in 1908 to determine the $C^n\ x\ T$ relationship for nitrogen mustards and 1,3-bis(2-chloroethyl)-1-nitrosurea against various strains of *E.coli*. Despite the importance of this principle in the development of anticancer agents, $C^n\ x\ T = k$ is rarely used. In 1989, Adams applied the concept of $C^n\ x\ T = k$ to the DNA intercalator, Crisnatol, and, as expected, found that its action is a function of $C^n\ x\ T$ and that drug retention by tumour cells is directly related to both antiproliferative and cytotoxic effects. Adams noted the importance of the concentration coefficient, n, in drug action, especially when comparing antitumour agents. This led to the empirical derivation of the minimum concentration x time parameter, ($minC\ x\ T$), which provides a useful profile for new anticancer drugs.

To improve the therapeutic index of doxorubicin, attempts have been made to modify its means of delivery to tumours. One of these approaches is the covalent conjugation of doxorubicin to HPMA via a proteolytically cleavable bond [Duncan et al., 1982, Lloyd et al., 1986 and Rihova et al., 2000] (Figure 2.2). The concept is that following pinocytic capture of the whole molecule, the linker is cleaved by cathepsin B, allowing intracellular drug release. This prevents systemic exposure to doxorubicin and hence adverse drug effects. PK1 is currently in phase II testing, and, given the proposed mechanism of antitumour activity, toxicity and antiproliferative activity should be apparent *in vivo* and *in vitro* depending of course on the availability, specificity and concentration of the lysosomal protease, cathepsin B. With regards to the importance of C^n x T and minC x T in understanding the action of anticancer drugs, we applied these principles for comparing cytotoxicity and antiproliferative effects of the parent compound doxorubicin and its conjugated form, PK1.

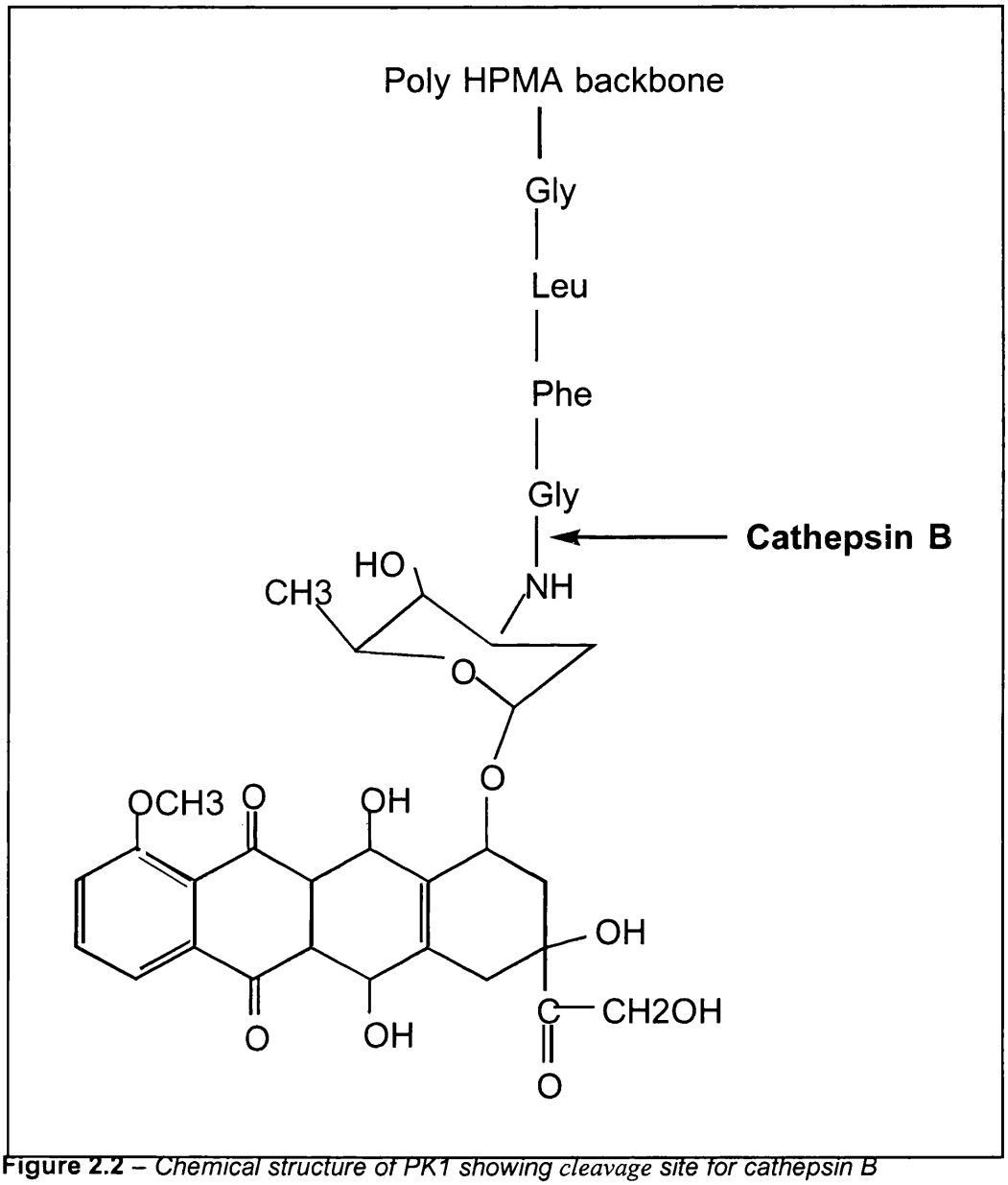

Figure 2.2 – *Chemical structure of PK1 showing cleavage site for cathepsin B*

The present study is therefore aimed at dissecting the pharmacodynamics of doxorubicin and PK1 *in vitro* against the MCF-7 human breast adenocarcinoma cell line, employing two well-established assays for measurement of cell survival. A detailed investigation of the dependence of cytotoxicity on time and drug concentration for doxorubicin and PK1 was carried out. Previous studies by Duncan et al [1992] for incubation times no longer than 72 hours did not result in cytotoxicity of PK1. Therefore to see whether PK1 is cytotoxic after prolonged incubations, a systematic investigation of relation between concentration and time is necessary.

2.2 EXPERIMENTAL APPROACH

2.2.1 3-(4,5-dimethylthiazol-2-yl)-2,5-diphenyltetrazolium bromide (MTT) assay

Principle of methodology

The MTT assay is a colourimetric assay based on the chemical reduction of the yellow water soluble tetrazolium salt, MTT, which forms a coloured insoluble formazan upon reduction (Figure. 2.3). Electron donors such as NADH and NADPH readily reduce MTT at the ubiquinone and cytochrome b and c sites of the mitochondrial electron transport chain. Mossman [1983] was the first to use MTT to quantitatively measure cell growth and cytotoxicity, and in 1986, the NCI (National Cancer Institute) investigated the feasibility of the assay in their *in vitro* drug screening program. The assay is a versatile and quantitative technique based on the ability of viable cells performing glycolysis and the TCA cycle to metabolise MTT, whereas dead cells are not metabolically active and therefore unable to metabolise MTT. MTT is believed to be taken up by cells through the endocytic route. Following reduction, the formazan product is then exocytosed to the cell surface [Liu et al., 1997]. Based on this observation, the MTT assay can also act as a measure of endocytosis or as mitochondrial respiration.

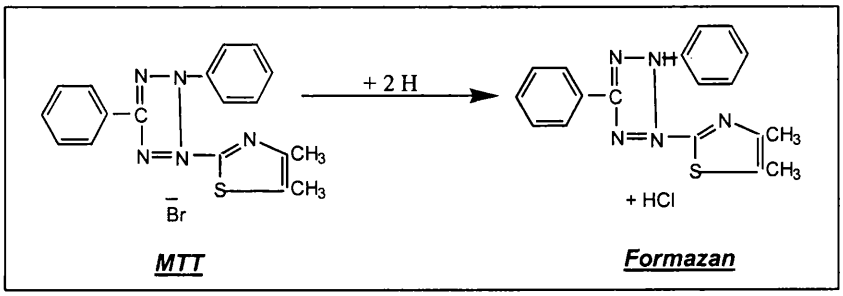

***Figure 2.3** - Chemical structures of MTT tetrazolium and formazan*

The end result of MTT metabolism is the production of an insoluble purple/dark blue formazan. A range of solvents such as DMSO, DMF, and isoproponol have been used to solubilise the formazan product. The amount of formazan produced correlates with

the number of viable cells present as determined by the optical density of the coloured formazan.

Materials

All chemicals were of reagent or analytical grade certified by the manufacturer. MTT (Sigma) was dissolved at room temperature in sterile PBS at a concentration of 5 mg/ml. The solution was sterilised through a 0.45 μm filter and stored at –20^{O}C in 2 and 4 ml aliquots. MTT solubilisation solution was prepared by dissolving 20% w/v SDS in 50% DMF and 50% dH_2O. pH was adjusted to 4.7 by adding 2.5% of an 80% acetic acid solution and 2.5% 1N HCl. Dulbecco's modified eagle's medium (DMEM) with Glutamax-1, fetal bovine serum (FBS), EDTA, phosphate buffered saline (PBS) and hanks balanced salt solution (HBSS) were purchased from Life Science International. T-25 and T-75 culture flasks were purchased from Greiner Labortechnik Ltd. Nunc 96 well microtitre plates were purchased from Fisher Scientific, UK. Doxorubicin hydrochloride was obtained from Sigma and dissolved at room temperature in sterile dH2O at a concentration of 1.72 mM. Aliquots of 500 μl were stored at –20^{O}C following filtration through 0.2 μm filters.

2.2.2 Cell line and culture conditions

The MCF-7 human breast adenocarcinoma cell line was obtained from Prof. Dallas Swallow, University College London. The cells were cultured in DMEM with glutamax-1 supplemented with 10% FBS in a humidified atmosphere of 5% CO_2 in 95% air at 37^{O}C. Cells were routinely grown in T-25 flasks and split twice a week at varying densities according to the standard procedures using HBSS and trypsin-EDTA for washing and trypsinisation respectively. Cells were used for up to ten passages after thawing to minimise genetic drift.

All cell lines tested negative for mycoplasma contamination (performed at The Rayne Institute, King's College London by Dr Ian Trayner) using a commercially available kit (Gen-Probe Incorporated, San Diego). Briefly, the test is based on hybridisation of a tritium-labelled DNA probe to mycoplasma DNA, with sequences corresponding to mycoplasma ribosomal RNA. Samples were prepared by removing cells from conditioned media; the media was then centrifuged to pellet mycoplasma which was then mixed with a lysis and hybridisation buffer. After which double

stranded DNA was isolated from the mixture by binding to an ion exchange resin and any unbound probe was washed off. The beads were then added to scintillation fluid for counting.

2.2.3 Determination of cell viability: trypan blue dye exclusion test

Trypan blue is a water soluble blue dye whose charge prevents penetration into the membrane of viable cells, whereas dead cells or cells with damaged membrane are permeable, hence its use for the determination of cell viability. Trypan blue was prepared as a 0.4% (w/v) stock solution in sterile PBS and stored at room temperature. Following trypsinisation, a 1:1 dilution of cell suspension with trypan blue were thoroughly mixed and viable cell number was determined by counting using a Neubauer haemocytometer under a light microscope. The percentage of viable cells was expressed as 100 x (number of blue cells/total cell number).

2.2.4 Seeding of cells and treatment

Approximately 800 viable cells/well were seeded in 96 well microtitre plates in a final volume of 100 µl of standard culture medium. Cells were allowed to attach and enter exponential growth for 48h. Serial stock dilutions of doxorubicin were prepared in culture medium and administered to cells in a volume of 20 µl, 8 replicates per concentration (0 to 10 µM). Cells were further incubated for predetermined time points before assaying for MTT reduction.

2.2.5 MTT assay

20 µl of 5 mg/ml MTT stock solution were added to each well and incubated for 3 hours at 37^{O}C. Following MTT reduction, 150 µl of the solubilisation solution were added and incubated at 37^{O}C overnight for complete solubilisation of the formazan product. The optical densities (OD) were measured at 570 nm using a Labsystems Multiscan microplate reader. Cytotoxicity of doxorubicin was expressed as 100 x (treatment OD/control OD) following subtraction of blank (without cells).

2.2.6 Data analysis

The relationship between concentration and effective response for doxorubicin on MCF-7 cells was determined with non-linear regression analysis. Concentration versus effect data for each treatment duration was fitted to the widely used mathematical equation for modelling concentration effect relation, the Hill equation:

$$E = B + (E_{con} - B)\ (C^y/(C^y + IC_{50}^y)$$

Where **E** is measured effect, **B** is background effect at infinite concentration, $\mathbf{E_{con}}$ is effect of untreated controls, **C** is drug concentration, $\mathbf{IC_{50}}$ is concentration of drug to give 50% inhibition of the maximal effect, and **y** is the slope parameter of the concentration effect response. When y has a negative slope, the curve falls with increasing drug concentrations.

Following non-linear regression analysis, we applied the 95% confidence interval of the best-fit estimate. The width of the confidence interval gives an estimate/indication of where the true population mean lies. All curves were prepared using Fig.P for Windows (Version 2.7; Biosoft).

2.3 In situ clonogenic assay

Principle of methodology

The colony forming assay is a well known technique for measuring reproductive cell survival following exposure to genotoxic agents. Cells were plated and exposed to test agents for a specified time, followed by a further 10-14 days incubation, without test agent. Cells that sustain genotoxic insult will be expected to become committed to programmed cell death whilst cells that were able to initiate a repair mechanism, and those that were unaffected by the drug, engage in normal cell cycle events to proliferate and form colonies. Colony size is determined by the rate of population doubling. The relationship between cytotoxicity and the number of colonies formed is linear up to a certain seeding density. Cytotoxicity was defined as a percentage of control (untreated) cell survival thus;

Cytotoxicity (%) = 100 (No. of colonies after drug treatment/ no. of colonies without treatment)

Materials

May Grunwald-Giemsa stain, and methanol was purchased from Merck Eurolabs. Nunc 6 well plates were purchased from Fisher Scientific, UK. Cells were routinely cultured in T-25 flasks as described in section 2.2.3.

2.3.1 Colony forming assay

Exponentially growing cells were seeded in duplicate wells in a 6 well plate at a density of 2000 cells/well in a final volume of 3 ml. Following 48 h incubation, cells were incubated with a range of doxorubicin concentrations (0 to 1 μM) for a specified period of time. Then cells were washed three times with HBSS to remove extracellular drug and further incubated in fresh drug free culture medium for 10 to 14 days or until colonies were formed. Colonies were fixed with 70% methanol at room temperature for 30 minutes and stained with 10% Giemsa stain for 30 minutes at room temperature. Colonies comprising of 50 cells or more were scored and the mean survival fraction was scored as a percentage relative to that of controls.

2.4 RESULTS

2.4.1 Standardisation of MTT and colony forming assays

The MTT assay is a well established assay for measuring cell proliferation and cytotoxicity. It has been demonstrated that colour production upon MTT reduction is proportional to viable cell number up to a certain density, and differs with different cell lines [Hansen et al., 1989]. It was therefore necessary to establish whether there was a linear relationship between MTT reduction and viable cell number with the MCF-7 cell line. Briefly, a range of cell densities (100-20,000 cells/well) was seeded in a 96 well plate and assayed for MTT reduction following 72 hour in culture. There was a good correlation between formazan production and viable cell number, as determined by trypan blue exclusion, with cell densities up to 1 x 10^4 cells/well (Figure 2.4). To maintain linearity in our experiments, cells were seeded at initial densities that would not exceed 1 x 10^4 per well at the end of the experimental procedure.

A major disadvantage of the MTT assay is the lack of discrimination between healthy cells and those that have obtained genotoxic insult following treatment resulting in cell cycle arrest, but not cell death. Arrested cells are still capable of reducing MTT as they are still metabolically active. However, these cells are unable to divide and to form colonies. Thus, we chose a complementary assay, the colony-forming assay, which measures reproductive cell survival by colony formation. As was the case with the MTT assay, we had to establish a seeding density that would lead to the formation of distinctive colonies at the end of 10-14 day incubation. This was done by setting up a range of cell densities in our culture vessels in duplicates. Once cells had entered exponential growth (following 48 hours in culture), they were washed in PBS and post–incubated for a further 10-14 days. Plates were then processed as described in materials and methods. Cell densities that gave the maximum number of colonies with more than 50 cells per colony were chosen as the seeding densities in our CFA (Colony forming assay) experiments. The initial seeding density was chosen to fall between 1-2 x 10^3 cells per well.

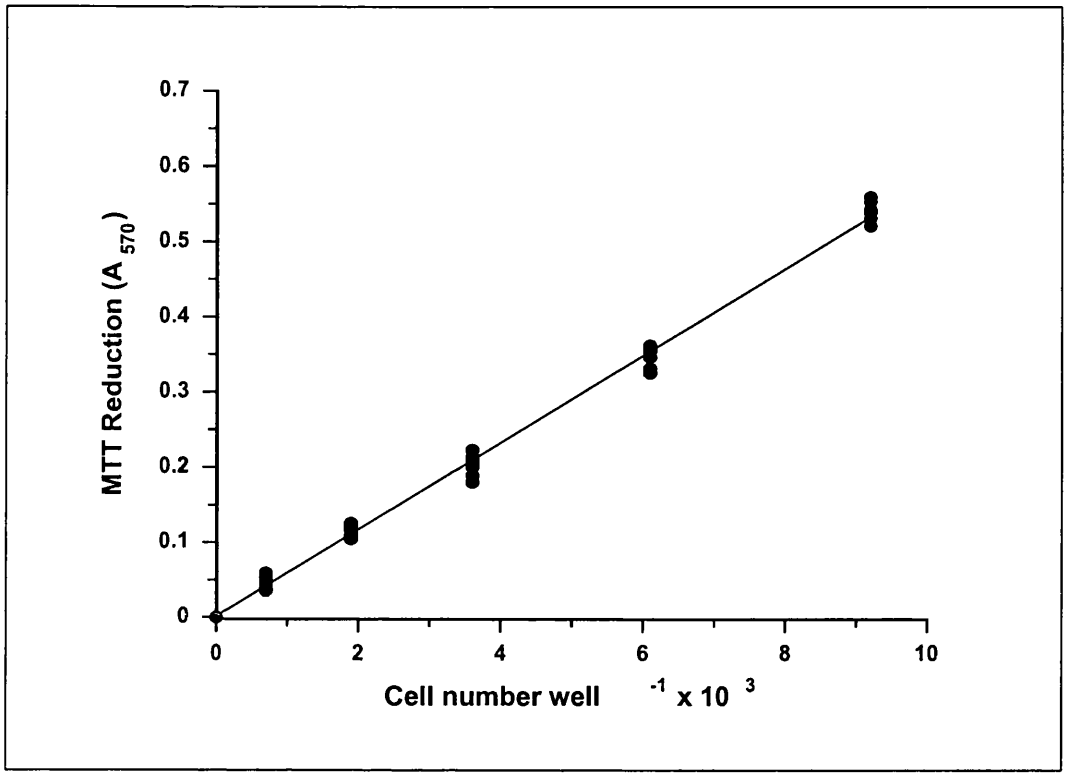

Figure 2.4 Correlation of MTT reduction with viable cell number. MCF-7 cells were seeded at a range of cell densities (100 to 20,000) per well by 2-fold serial dilution, in a 96 well dish. Cells were incubated for 48 hours, after which time the MTT assay was performed on six wells from each seeding density. Cells in the remaining two wells were resuspended by trypsinisation, and the number of viable cells present was determined by counting the cells in the presence of trypan blue. MTT reduction (n=6) is plotted as a function of viable cell density (n=2). First order regression analysis gave rise to a straight line (r^2= 0.99).

2.4.2 Toxicity of doxorubicin to MCF –7 cells using MTT reduction.

Figure 2.5 shows the dose-response curves for MCF-7 cells incubated with a range of doxorubicin concentrations for 4 to 120 hours of continuous drug exposure. As the exposure time increased from 4 to 120 hours, toxicity also increased, as can be seen by the shift of the corresponding curves to the left towards smaller concentrations. However the toxicity of doxorubicin to MCF-7 cells seemed to reach a plateau at 96 hours of incubation. Further extensions of treatment time did not lead to increases in toxicity as can be seen from the graph for 120 hours, which overlaps with the the 96 hour data. Intriguingly, there was an increase in cell survival (48-120 h) at concentration between 2.5-10 μM doxorubicin. This phenomenon has also been observed in a hepatoma and prostate cancer cell lines in our lab (unpublished results).

B

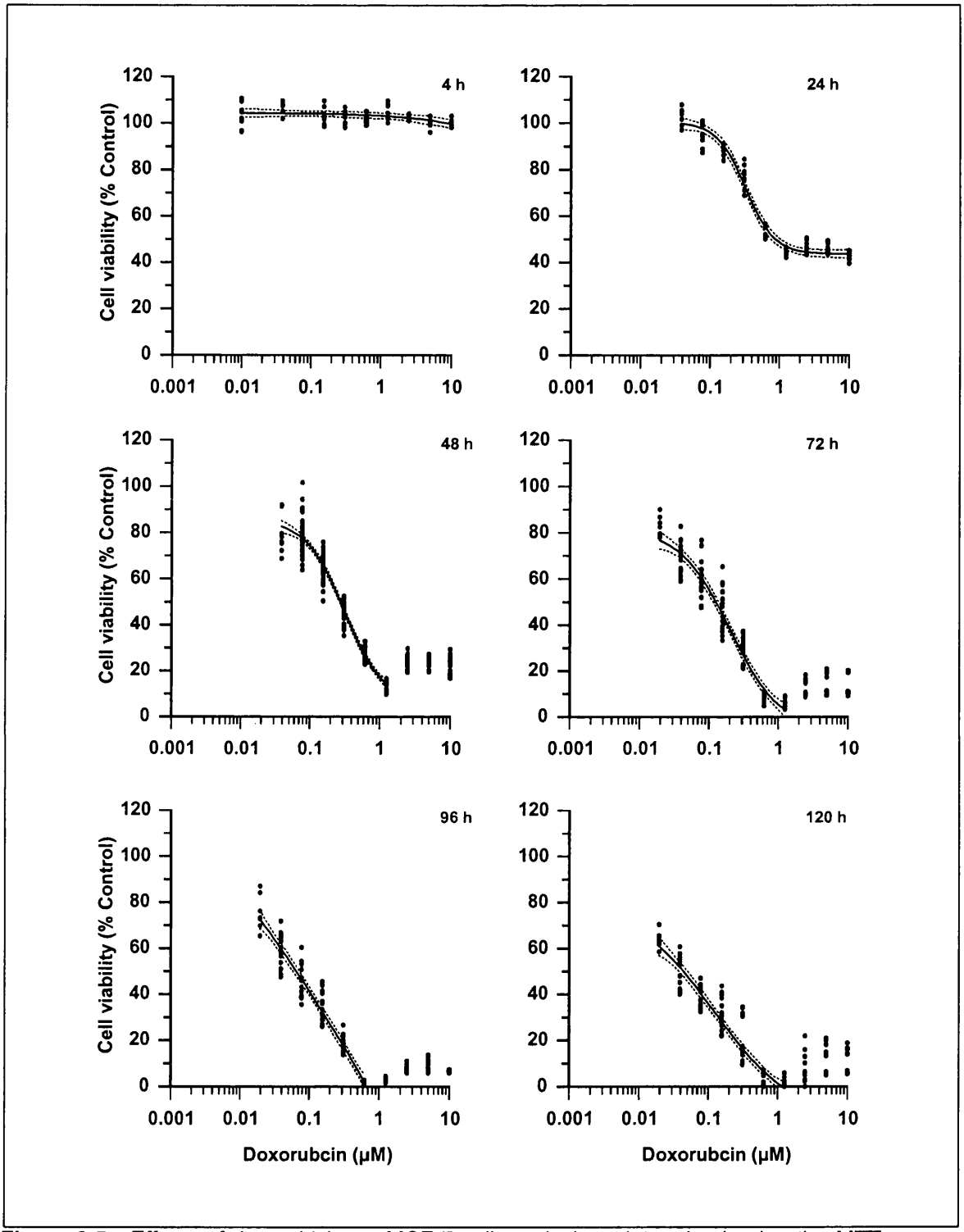

Figure 2.5 - Effects of doxorubicin on MCF-7 cell survival as determined using the MTT assay. Cells were seeded at 1000 cells and after 48 hours of incubation, a 2-fold serial dilution of doxorubicin in 100 µl medium was added. Cell survival was determined after incubation for 4, 24, 48, 72, 96 and 120 hours as indicated. The data combines the results of three independent experiments, with 8 wells at each concentration in each experiment. The combined results are expressed as a percentage of control and fitted to the Hill equation. Shown is the 95% confidence interval (dotted lines) of the best fit regression line (solid lines). Viability of control cells was 99%.

As discussed in chapter 1, the mechanism of doxorubicin cytotoxicity is dose dependent, and there is some evidence that at 2.5-10 μM, the mechanism of doxorubicin antitumour activity is mediated by free radical production. A study by Muller et al., [1997] using an acute lymphoblastic leukaemia cell line also revealed toxicity of doxorubicin to plateau at 1 μM for the induction of apoptosis. Above this concentration levels of DNA damage remained more or less the same up to 100 μM.

Figure 2.6 shows dose-response curves for MCF-7 cells, using MTT reduction, after treatment with PK1 and its free doxorubicin content. The batch of PK1 used in this study had an unbound doxorubicin fraction of 0.02% of polymer-conjugate weight. This unbound percentage of doxorubicin was calculated for PK1 doses used and set up as controls in parallel. For ease of comparison, the effects of unbound doxorubicin, in concentrations equivalent to those present in wells containing PK1 are shown on the same graph as PK1, but corresponding to the second concentration axis, as labelled. Note that PK1 incubation times were longer than those shown in Figure 2.5 for doxorubicin. Figure 2.6 shows that at equitoxic doses PK1 toxicity is lower than the parent drug, doxorubicin. After 3 and 5 days of incubation there was no significant apparent toxicity of PK1 to MCF-7 cells, excluding that attributable to the 0.02% unbound fraction of doxorubicin on the polymer. However, as the incubation time increased to 9-10 days, a contribution to toxicity by PK1 manifested itself as a successive shift of the PK1 curves relative to each other to the left, towards lower concentrations and furthermore, the separation of their 95% confidence intervals. Despite this contribution to cytotoxicity, the effect observed was relatively low considering the amount of doxorubicin bound to the polymer. In absolute terms, only a 30% killing by PK1 was observed after 9-10 days of continuous incubation at a concentration of 50 μM doxorubicin equivalent.

2.4.3 Clonogenic survival of MCF-7 cells exposed to doxorubicin and PK1.

Most *in vitro* cytotoxicity data on doxorubicin published in the literature are based on short-term assays such as the MTT reduction for a maximum exposure time of 72 h. These short-term observations are thought to underestimate overall cytotoxicity simply because cells may require several hours or days to complete pathways leading

to cell death. Measurement of short-term cell survival does not reflect cytotoxicity accurately as we have clearly demonstrated with the extended incubation times used for doxorubicin and PK1.

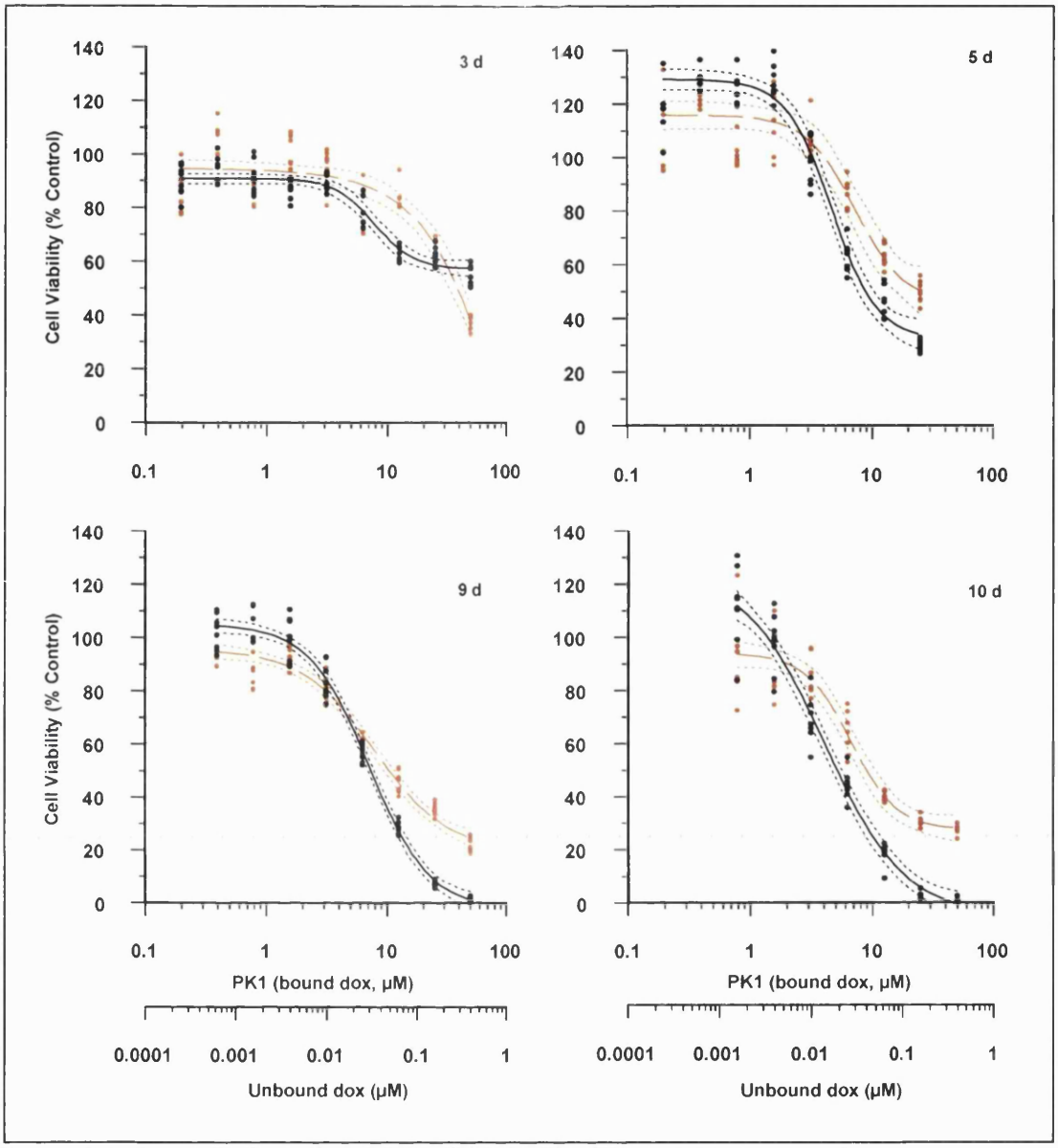

Figure 2.6 Concentration effect curves following 3, 5, 9 and 10 days continuous exposure of MCF cells to PK1 (black) and its free doxorubicin content (brown) as determined using the MTT assay. The data combines the results of two independent experiments, with 8 wells at each concentration in each experiment. The combined results are expressed as a percentage of control and fitted to the Hill equation with the 95% confidence interval (dotted line) of the best-fit regression line (solid line). Cell survival in the presence of PK1 is plotted as a function of the concentration of doxorubicin bound to HPMA (upper x axis), and also as a function of the concentration of the 0.02% unbound doxorubicin present in the PK1 preparation (lower x axis). The two x axes have been purposely aligned in order to compare the potency of bound and unbound doxorubicin. Viability of control cells was 99%.

Having characterised the toxicity of doxorubicin and PK1 using the MTT assay, we decided to re-examine the cytotoxicity profile of both doxorubicin and PK1 in the clonogenic assay. This assay measures the ability of single cells to survive toxic injury, and then proliferate to form a colony. Cells were treated with different

concentrations of doxorubicin, PK1 with doxorubicin and its free doxorubicin content at pre-determined times. Following this, extracellular drug was removed and cells were washed and further incubated in fresh culture medium for 10-14 days. Colonies were fixed, stained and scored as a percentage relative to untreated controls. Figure 2.7 shows a concentration response curve for a 10 h doxorubicin exposure. As expected, cytotoxicity was more pronounced in the colony forming assay in comparison to the MTT assay. However, despite the low IC_{50} values obtained with this assay, a direct comparison between the two assays cannot be made as the total incubation times differ.

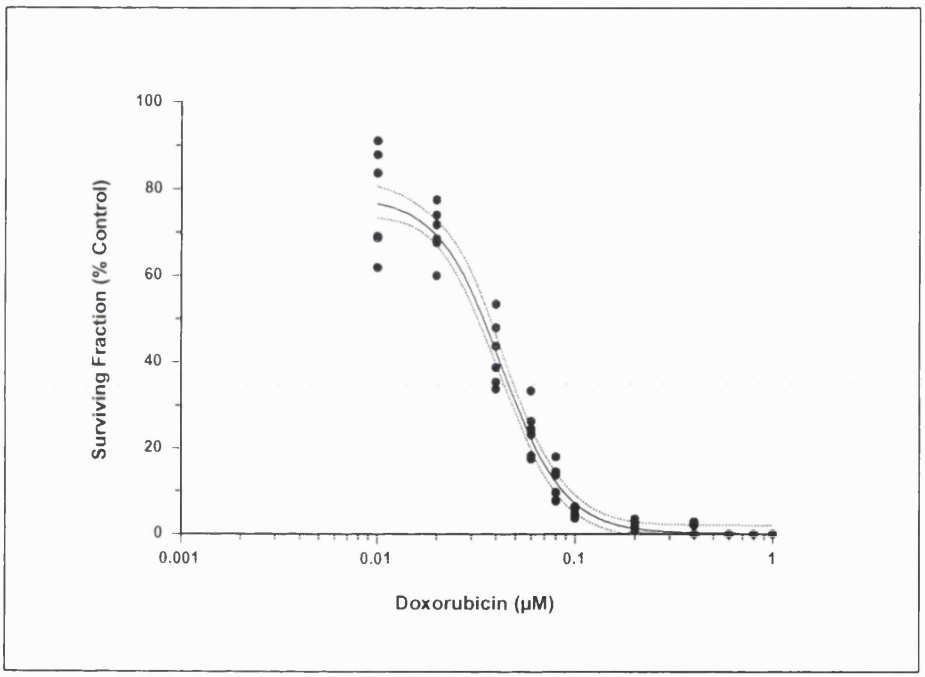

Figure 2.7 Effects of doxorubicin on MCF-7 cells using the colony formation assay. MCF-7 cells were seeded at 2,000 cells per well in 6 well dishes and incubated for 48 h. Various concentrations of doxorubicin was added and incubated for 10 hours. Subsequently drug-containing medium was removed, and cells were washed, incubated in fresh culture medium for a further 8 days, after which time colonies were fixed and stained for counting. Data represents the number of colonies obtained from three independent experiments run in duplicates, expressed as a percentage of control (i.e. cells incubated without doxorubicin) and fitted to the Hill equation. Shown is the 95% confidence interval (dotted line) of the best fit regression line (solid line).

In Figure 2.8 is a dose response for PK1 by colony formation. Following 5 days (120 hours) of continuous drug exposure, the cytotoxicity of PK1 was more pronounced than after 10 days of continuous exposure in the MTT assay, with an IC_{50} of 0.5 and 5 μM doxorubicin equivalent and free unbound doxorubicin respectively. MTT reduction, prior to 120 hours of continuous drug exposure resulted in an IC_{50} of

9 μM doxorubicin equivalent. Following this observation, we decided to apply the conditions of the colony-forming assay to the MTT assay by removing the extracellular drug and by introducing an additional, drug-free, incubation period prior to MTT reduction.

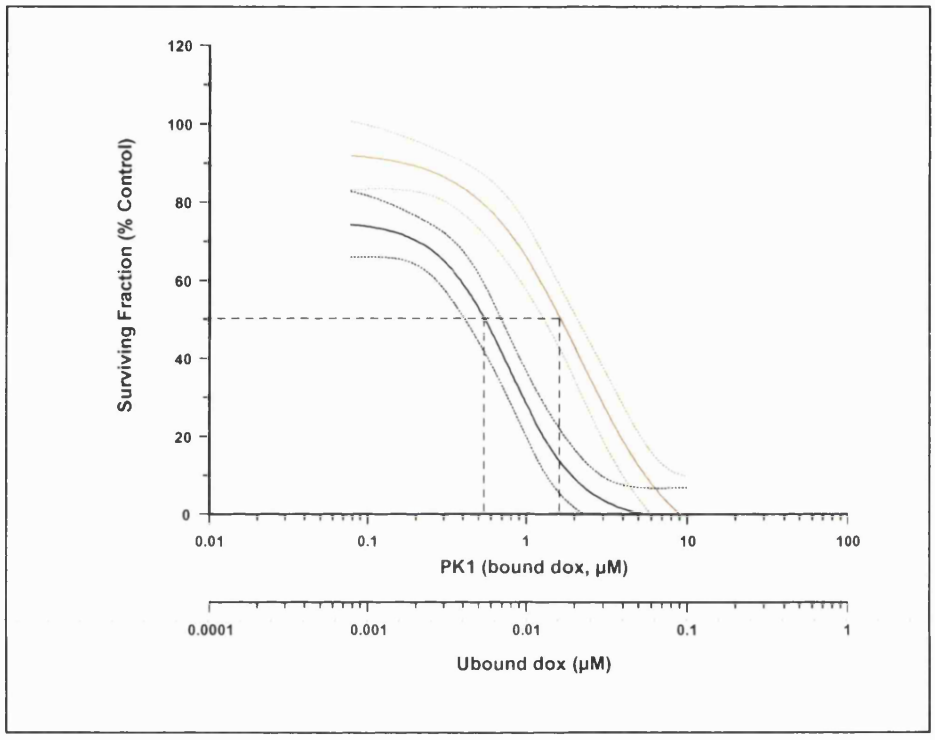

Figure 2.8 Colony forming ability of MCF-7 cells following exposure to PK1 and unbound doxorubicin. Cells were seeded at 1,000 cells per well in 6 well dishes and incubated for 48 h. PK1 and its free doxorubicin content were added to different dishes in parallel and further incubated for 120 hours. Drug-containing medium was subsequently removed; cells were then washed and incubated in fresh culture medium for 8 days, after which time colonies were fixed and stained for counting. For clarity, data points have been omitted. The plot represents the number of colonies obtained from two independent experiments, expressed as a percentage of control (i.e. cells incubated without drug) and fitted to the Hill equation. Shown is the 95% confidence interval (dotted line) of the best fit regression line (solid line).

2.4.4 Effect of post-incubation on the toxicity of doxorubicin and PK1

Figure 2.9 compares 24, 48 and 72 hours of continuous incubation with doxorubicin followed by a further 72 hours incubation in the absence of the drug. Evidently, the introduction of a drug-free incubation period led to a marked enhancement of toxicity. Interestingly, the survival of cells at higher drug

concentrations (2.5-10 μM) which we observed during continuous drug exposure (Figure 2.5) was abrogated following post incubation treatment. Thus, it is apparent that doxorubicin induced cell death is not only dependent on drug concentration, but also on incubation time. Having observed enhanced toxicity of doxorubicin to MCF-7 cells with prolonged incubation times, the cytotoxicity of PK1 was re-examined with the same experimental procedure. In Figure 2.6, it is evident that the toxicity observed with PK1 for 3-5 days of continuous drug exposure could be attributed almost to the 0.02% unbound doxorubicin fraction on the polymer. However, following 72 hours of post-treatment in free drug medium (Figure 2.10), the contribution of the unbound doxorubicin to PK1 toxicity increased, resulting in a complete overlap of both curves after 96 and 120 hours of continuous exposure. Despite a separation of the two curves after 72 hours, the IC_{50} for all three incubation times as shown on the right of Figure 2.10 were identical. 4 μM was the IC_{50} value estimated from the three dose-response curves. More so astonishing was the fact that these curves completely overlapped with that of the 10 days continuous PK1 exposure (Figure 2.6). Thus, there is no difference between the cytotoxicity of PK1 and the 0.02% unbound doxorubicin contained in the polymer preparation. Hence, the cytotoxicity of PK1 can be explained entirely in terms of its 0.02% unbound doxorubicin. It appears that the polymer itself contributes very little if at all, to cytotoxicity.

2.4.5 Relation of concentration and exposure time to the antitumour activity of doxorubicin and PK1

Having ascertained that the *in vitro* antitumour activity of PK1 is comparable to that of 0.02% free doxorubicin, and several orders of magnitude less potent than the parent compound, further detailed analysis of both doxorubicin and PK1 were undertaken to characterise the effect of concentration and time on antitumour activity. We analysed the data using the pharmacodynamic principle described earlier; $C^n \times T = k$ *[Adams, 1989]*. The basis for this comparison is evidence [Evans, 1988] that antitumour activity is not always related to the product of concentration and time. Response is indirectly related to drug concentration and therefore correlation between cytotoxicity and C x T is often imperfect.

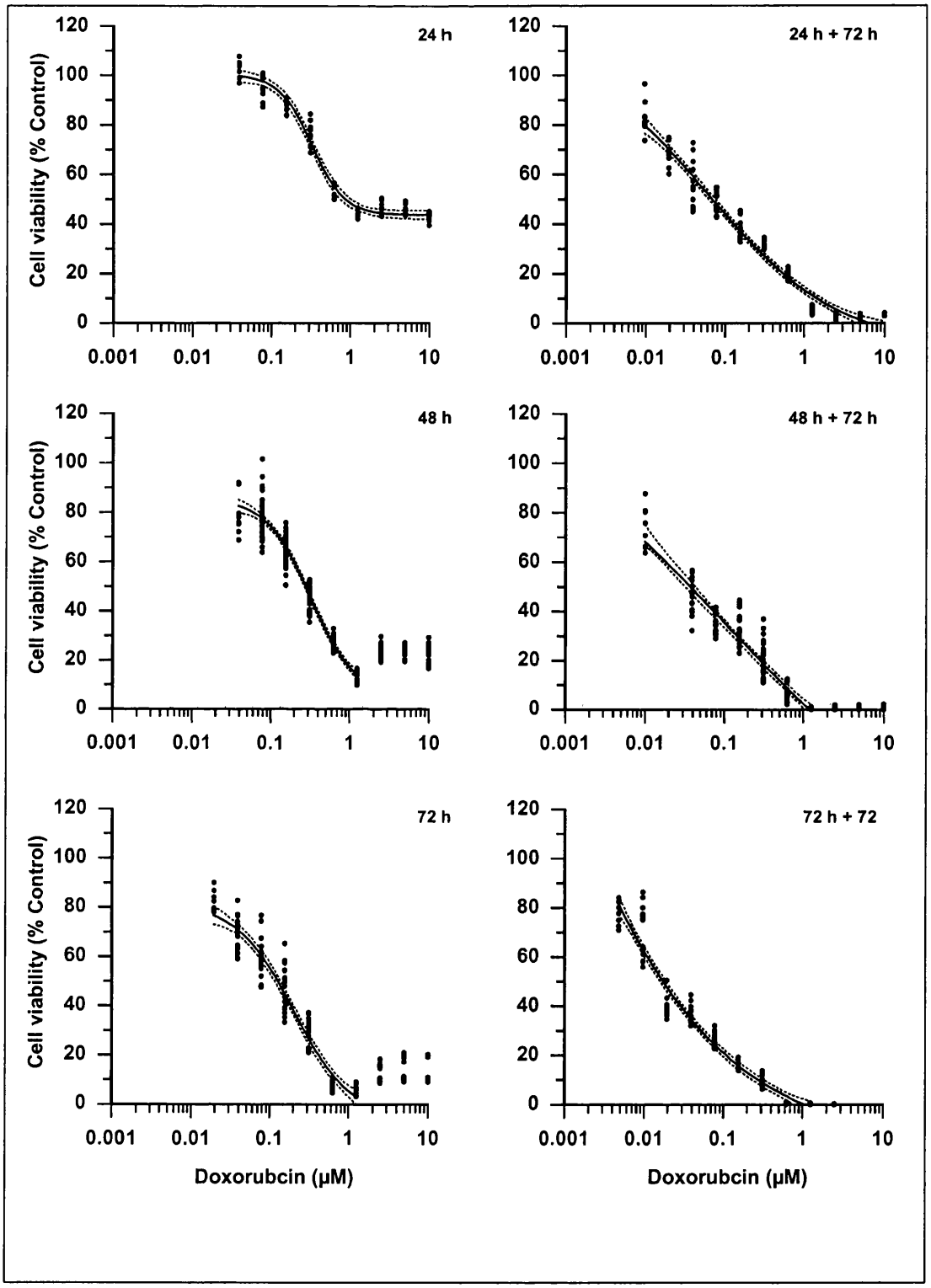

Figure 2.9 Effect of post-incubation on doxorubicin cytotoxicity following 24, 48 and 72 hours of exposure to PK1 and free doxorubicin content. Cells were cultured in 96 ell dishes and treated after 48 hours of incubation. Cells were then washed 3x in PBS and incubated for another 72 hours before assaying for MTT reduction. Cell survival (as defined by MTT reduction) is plotted as a percentage of control. Viability of control cells was 97%.

A log transformation of the $C^n \times T = K$ principle yields the linear relationship:

$$LogT = -nlogC + LogK$$

The general equation for a straight line is $y = ax + b$ where a = n (-slope for a particular surviving fraction) and b = k (the antilog of the intercept for a particular surviving fraction).

Shown in Appendix 1.1 and 1.2 are individual logT vs logC plots for doxorubicin and PK1 and its 0.02% of free unbound doxorubicin. The values for which were obtained by determining concentrations that produced a particular surviving fraction from the dose-response curves at each of the exposure times investigated. The concentration coefficient, n, was found to decrease with increasing toxicity from 10-50% cell kill for continuous doxorubicin exposure, but remained constant following 72 hours of post treatment in drug-free medium (Table 2.1). Conversely, between 50 and 90% cell kill, n increased with increasing cytotoxicity for both continuous and post incubation. Crucially, the exposure constant, k, for both conditions of doxorubicin exposure increased as cell survival decreased with r^2 of 0.96 and above. Thus the $C^n \times T = K$ principle appears to apply only to levels of 50% cell kill or greater.

With respect to PK1 there was no evidence in terms of the n values obtained that $C^n \times T = K$ is applicable as there was no trend for the calculated values. However, 5 of the r^2 values were below 0.95 (0.81-0.93). Disregarding n values for which r^2 was less than 0.95, the exposure constant, k, increased with increasing drug toxicity for the 0.02% unbound doxorubicin. Thus, the importance of k is further emphasised to the action of doxorubicin. Hence, the concentration coefficient, n, is not crucial in the antitumour action of doxorubicin and its conjugate, PK1. However to allow comparison between $C^n \times T = K$ and $C \times T = K$, further analysis was performed to determine the minimum concentration (minC) and minimum time (*minT*), i.e. the minimum concentration and time required that are required for a specified efficacy.for anticancer agents [Adams, 1989]. Thus this parameter can provide a useful comparison of new drugs to established anticancer agents, such as PK1 to doxorubicin.

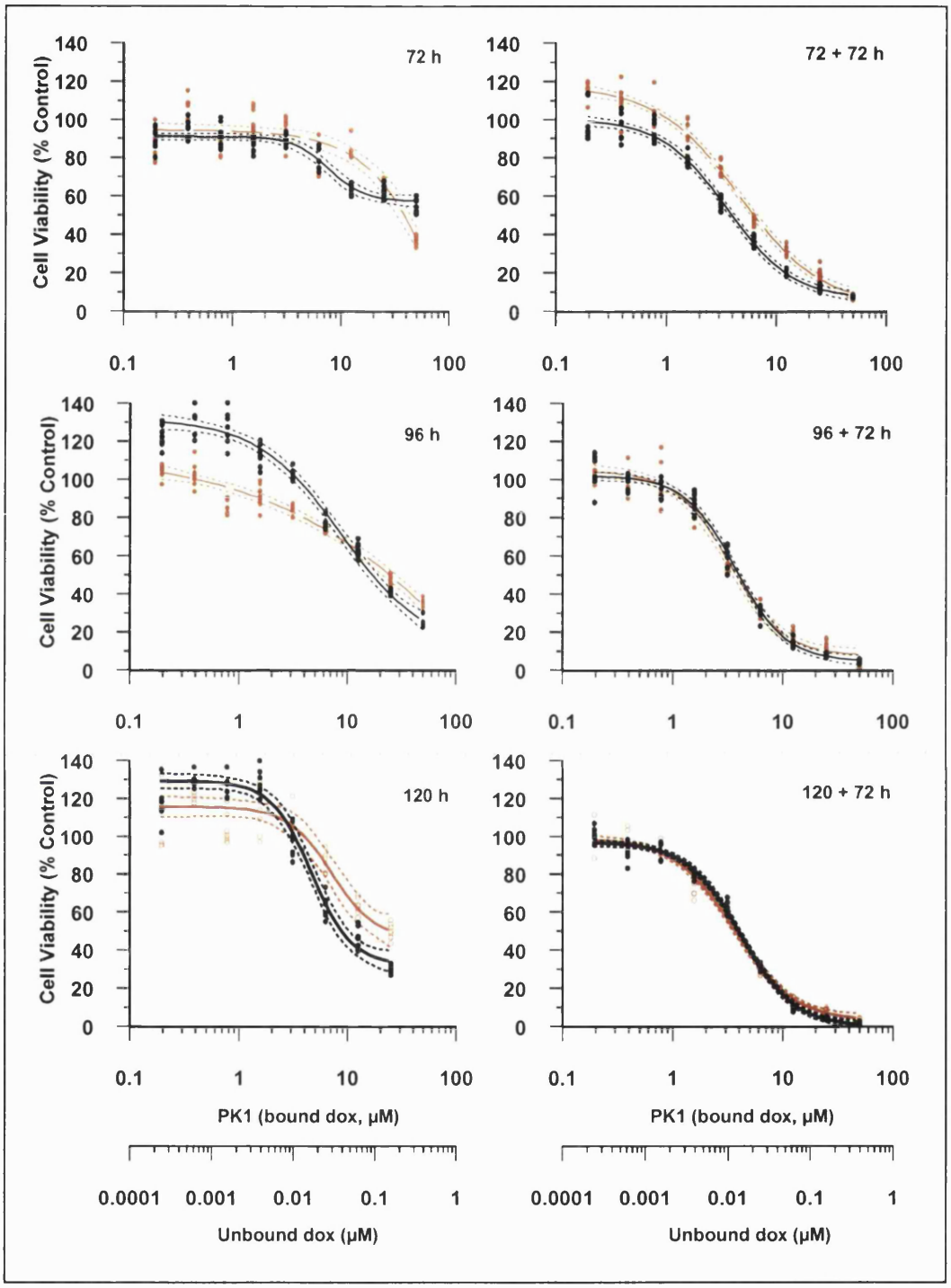

Figure 2.10 Effects of post-incubation on the survival of MCF-7 cells exposed to PK1 or free unbound doxorubicin for 72, 96 or 120 hours. Cell survival in the presence of PK1 (black) is plotted as a function of the concentration of doxorubicin bound to HPMA (upper x axis), and also as a function of the concentration of unbound doxorubicin (lower x axis). Results have been fitted to the Hill equation with the 95% confidence interval (dotted lines) of the best fit regression line (solid lines). Viability of control cells was 99%.

Table 2.1- *Concentration and time relationships for doxorubicin and derivation of the minimum C x T. The concentration coefficient,* n, *and the exposure constant,* k, *were estimated from the log C versus log T plots in Appendix 1.1 and 1.2 and the minimum C x T from Appendix 1.5 and 1.6.*

	Doxorubicin				***Doxorubicin + post incubation***			
% Cell Kill	*n*	*Log k*	R^2	*Minimum CxT (μM-h)*	*n*	*Log k*	R^2	*Minimum CxT (μM-h)*
20	0.49	1.13	0.96	20	0.13	0.84	0.97	0.587
30	0.45	1.28	0.99	30	0.14	0.98	0.99	7.197
40	0.4	1.4	0.99	65	0.14	1.09	0.99	12.5
50	0.39	1.49	0.99	84	0.14	1.18	0.99	14.924
60	0.43	1.53	0.99	90	0.3	1.23	0.99	45.625
70	0.47	1.61	0.99	105	0.33	1.42	0.99	81
80	0.47	1.68	0.99	157	0.31	1.55	0.99	127
90	0.61	1.79	0.99	160	0.34	1.75	0.99	300

Table 2.2 *- Concentration and time relationships for PK1 and its free doxorubicin content, and derivation of the minimum C x T. The concentration coefficient,* n, *and the exposure constant,* k, *were estimated from the log C versus log T plots in Appendix 1.3 and 1.4 and the minimum C x T from Appendix 1.7 and 1.8.*

	Unbound Doxorubicin				***PK1***			
% Cell Kill	*n*	*Log k*	R^2	*Minimum CxT (μM-h)*	*n*	*Log k*	R^2	*Minimum CxT (μM-h)*
20	0.75	2.6	0.98	135.675	0.56	2.25	0.94	112
30	0.66	2.7	0.98	240	0.71	2.6	0.92	150
40	0.59	2.71	0.97	70.7	0.54	2.52	0.83	60
50	0.75	3.07	0.96	65	0.54	2.52	0.82	60.6
60	0.69	3.07	0.81	84	0.48	2.68	0.98	190
70	0.38	2.74	0.93	200	0.58	2.98	0.93	180
80	N/A	N/A	N/A	N/A	0.089	2.25	0.97	N/A
90	N/A	N/A	N/A	N/A	0.65	3.16	0.86	N/A

Utilising data from the linear regression analysis of the logC vs logT plots in Appendix 1.1 and the equation $C= (K/T)^{1/n}$, a concentration vs time plot was constructed on a linear scale to reveal the pattern of change with time (hyperbolic relationship between concentration and time). The *minC x T* lies at the intersection of the line $C= nT$ (derived from $C^n \times T = K$), the minimum concentration and time for an observed effect. The products of minC and T parameters from appendix 1.5 at different levels of cell kill are shown in Table 2.1 for doxorubicin and Table 2.2 for PK1. The product of *C* and *T* for doxorubicin with both continuous and post incubation conditions was found to increase with increasing cell kill. Figure 2.11 gives a summary of the minimum exposure conditions required for doxorubicin and PK1 action against MCF-7 cells at different levels of cell kill. Based on the data analysis, there is no definitive association of *minC x T* with increasing cell kill for PK1 and its free doxorubicin content (Table 2.2). A minimum concentration of 6 μM doxorubicin for a minimum incubation time of 14 hours will result in 50% cell death (*minC x T* of 84 μM-h). PK1 at the same concentration of 6 μM doxorubicin equivalent for 10.1 hours of incubation will also result in 50% cell death (*minC x T* of 60.6 μM-h). Thus suggesting that PK1 is more efficacious than doxorubicin.

Having established a disparity between the dose-response profiles and the pharmacodynamic principle, a logtime versus logdose plot was constructed from the initial dose response curves at 50% effect level for doxorubicin and PK1 (Figure 2.12). The minimum concentration and time estimated from these plots did not correlate with that of $C^n \times T = k$. As described earlier (Table 2.1), the 1st segment of the logtime-logdose plot represents the minimum time required for an observed effect irrespective of drug concentration. In addition, the second segment corresponds to the time of incubation/exposure necessary to cause the defined response with smaller doses. Note that not all compounds display all three segments of the defined curve. Both doxorubicin and PK1 display only the 1st and 2nd segments of the plot. From Figure 2.11A the following conclusions can be drawn: (1) at concentrations of 1 μM doxorubicin and above, a minimum of 30 hours is required to observed a 50% cell kill. (2) a linear relationship exits between logdose and logtime for concentrations between 1 and 0.05 μM. Hence, within this concentration range, a reduction in cytotoxicity of doxorubicin due to lower concentrations can be compensated by increasing exposure time. (3) Concentrations below 0.05 μM doxorubicin will simply result in less than 50% cell kill even if incubation times are extended.

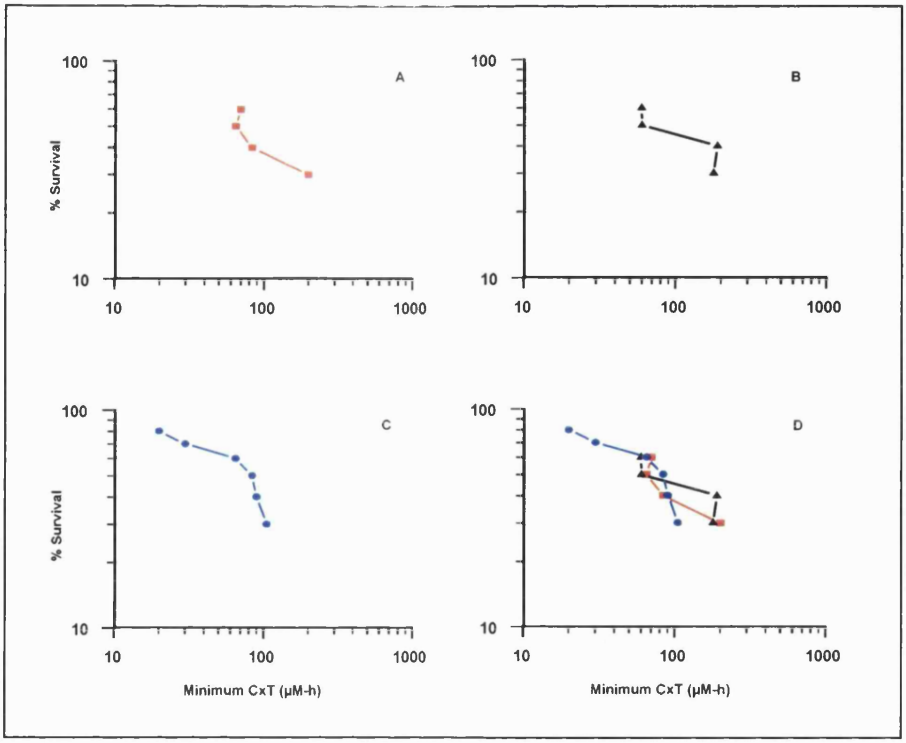

Figure 2.11 - Minimum concentration versus time survival plots for the action of doxorubicin and PK1 against MCF-7 cells. Log concentration (log C) vs log time (log T) plots were constructed utilizing data from the initial dose-response curves in figures 2.5 and 2.6. Log C vs log T plots was constructed at different surviving fractions (appendix 1.1) for determination of the concentration coefficient, n, and the exposure constant, k at any given surviving fraction. To determine minimum C x T that will give a particular surviving fraction, a value for C and T that fulfils both was obtained. Values were used to plot the above graph of minimumC (minC) x minimum T (minT) vs cell survival. See appendix 1.5 for different surviving fractions of minC x minT plots. (A) Unbound doxorubicin, (B) PK1, (C) doxorubicin and (D) A, B, and C superimposed.

From Figure 2.12B, (1) the minimum time required for 50% PK1 induced cell death is 80 hours with a minimum concentration of 50 μM doxorubicin equivalent. (2) We cannot confidently state that there is a linear relationship between PK1 dose and exposure time between 5 and 50 μM doxorubicin equivalent. (3) However, we can confidently hypothesize that concentrations below 5 μM PK1, doxorubicin equivalent will result in less than 50% cell death regardless of the exposure time. The products of C and T for doxorubicin and PK1 from the logdose-logtime plots in Figure 2.12 are 30 and 4000 μM-h doxorubicin and PK1 respectively. Hence, as Haber's rule states; the smaller the product of C x T, the more toxic is the agent. Thus doxorubicin is relatively more cytotoxic in its free form than when conjugated to HPMA.

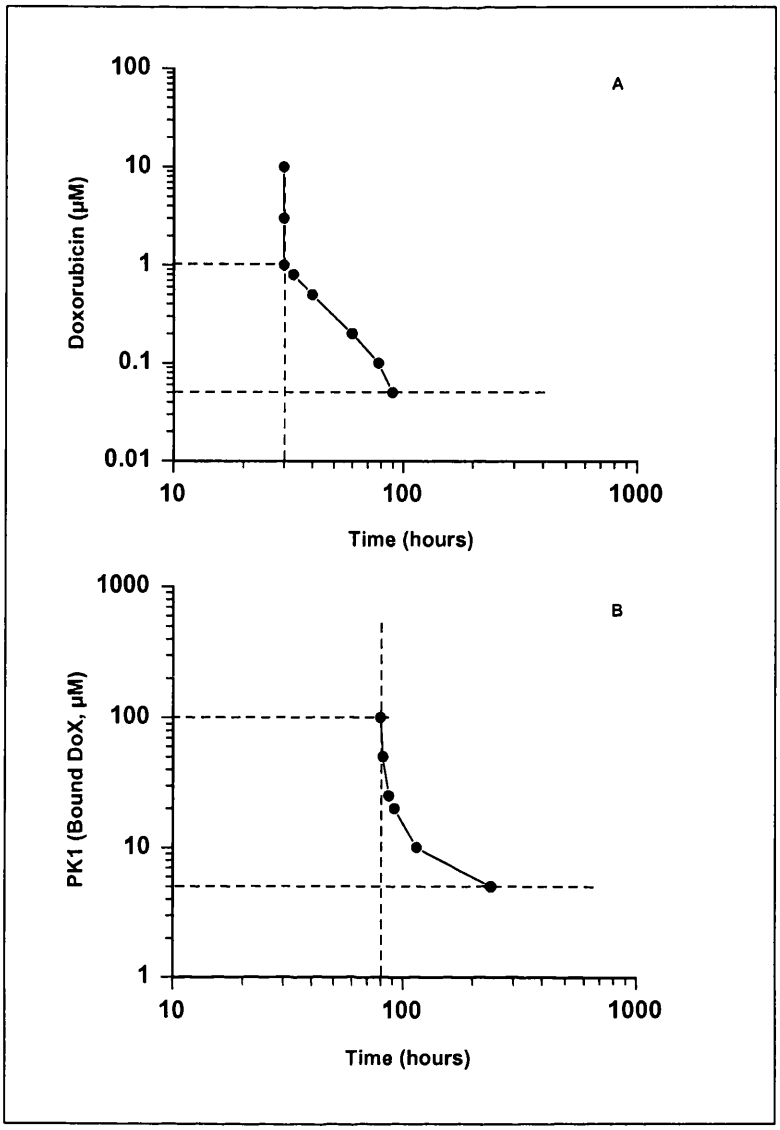

Figure 2.12 - Log time versus log dose plots for doxorubicin and PK1. The exposure time at which 50% growth inhibition occurred for a given concentration of (A) doxorubicin, or (B) PK1 (doxorubicin equivalent), were estimated from Figures 2.5 and 2.6 respectively. These values were subsequently used to construct graphs of concentration versus time, using logarithmic axes [Adams].

2.5 Discussion

It is important to know the relation between therapeutic or toxic response and drug concentration, pharmacodynamics, when determining dosing schedule of antitumour agents. For successful therapeutic objectives both pharmacokinetic and pharmacodynamic parameters of a drug must be known. However, there are very few studies of pharmacodynamic characteristics in the literature. Doxorubicin is a well characterised antitumour agent which displays a concentration and time dependent

rate of cell kill. The rationale for the use of polymers as drug carriers is based on the mechanism of cell entry to limit systemic toxicity often associated with doxorubicin. Although much is known about the biochemistry, pharmacology and clinical use of doxorubicin, its conjugation to a polymer alters these properties, and as such a new drug entity is produced, irrespective of the fact that the active constituent is the same. Both Kopecek and his group [Dvorak et al., 1999, Minko et al., 1999a and 2000], and Duncan et al., [1998, 1992 and 1987] have done numerous *in vivo* and *in vitro* studies using PK1; but comparative pharmacodynamic studies of doxorubicin and PK1 are missing.

As expected, a concentration dependent toxicity was observed for doxorubicin with an IC_{50} of 0.05 μM for a total incubation of 96 hours. IC_{50} values for doxorubicin quoted in several reported investigations with the MCF-7 cell line vary considerably with each other and indeed with those reported here. This could be due to the different treatment protocols. Having systematically investigated doxorubicin induced cell death at various incubation times and concentrations, cytotoxicity was observed to reach a plateau after 96 hours of treatment. Thus, toxicity of doxorubicin was not enhanced with prolonged incubation times. The increased survival of cells in the concentration range between 1.25 and 10 μM doxorubicin following 48 hours of treatment could be due to different mechanism of drug action. Studies by Muller et al., [1999] reported a maximum response of cytotoxicity and apoptosis induction at 1 μM doxorubicin in the mouse leukaemia cell line MOLT-4. They found that above 1 μM, levels of DNA strand breaks remained unchanged up to 100 μM with a decrease in growth inhibition after 24 hours. Other studies have also reported apoptosis in P388 cells at 1 μM doxorubicin, which was not evident at 10 μM[Ling et a., 1993]. Doxorubicin has been shown by Zukier and Tritton [1991] to upregulate epidermal growth factor receptor at very low concentrations. This phenomenon is thought to be due to growth suppressive activity of doxorubicin and consequently an effort made by cells to counteract death is to stimulate growth. At high doxorubicin concentrations, it is also possible that certain growth factors such as IL-3 which has been shown to promote cell survival is being secreted into the growth medium at higher concentrations than normal especially in prolonged culture incubations. If IL-3 is not the autocrine growth factor involved, other potential candidates must exist solely based on the observation that following removal of the drug containing medium with subsequent washes and post incubation, cytotoxicity becomes more enhanced and

interestingly, the increased survival at high concentrations is completely abrogated. Further investigations must be carried out to fully understand this phenomenon of increased cell survival at such high concentrations of doxorubicin.

The initial dose-response profile obtained for PK1 following MTT reduction revealed low cytotoxicity relative to the 0.02% unbound doxorubicin on the polymer-conjugate. As previously mentioned, the rationale for conjugating doxorubicin to HPMA is to reduce systemic toxicity and to enhance tumour targeting. The results of our *in vitro* cytotoxicity profile of PK1 correlated to that reported by Duncan et al. [1992]. However, they see or regard this lack of *in vitro* cytotoxicity as beneficial (what will be seen *in vivo* as lack of systemic toxicity). Following continuous exposure of MCF-7 cells to PK1 for 10 days, there appears to be some contribution to cell kill by PK1. This effect was more pronounced when cytotoxicity was assessed by the colony forming assay. However the results obtained (Figure 2.10) suggests that there is no difference in terms of cytotoxicity between PK1 and the 0.02% unbound doxorubicin on the conjugate. This is evidenced by the complete overlap of the two curves following post-incubation. Further proof that the observed cytotoxicity of PK1 at prolonged incubation times is due to the free unbound doxorubicin is shown in Figure 2.13, with the actual concentrations of free doxorubicin plotted on the same x-axis. Note that the IC_{50} estimations following 120 hours continuous exposure with 72 hours post incubation are 0.03 μM for the free unbound doxorubicin and 10 μM PK1, doxorubicin equivalent. The observed apparent contribution to cytotoxicity by PK1 (Figure 2.6) could possibly be due to differences in the rate of cell kill by the free 0.02% unbound fraction and the 0.02% used for reference. Another possible explanation for this phenomenon of PK1 cytotoxicity at high doxorubicin equivalent concentrations may perhaps be due to cell death induced by protein denaturation. This is based on our observation of crystal formation at concentrations of 25 uM bound doxorubicin and above under a normal light microscope. Thus, protein denaturation could account for the earlier observed cytotoxicity of PK1.

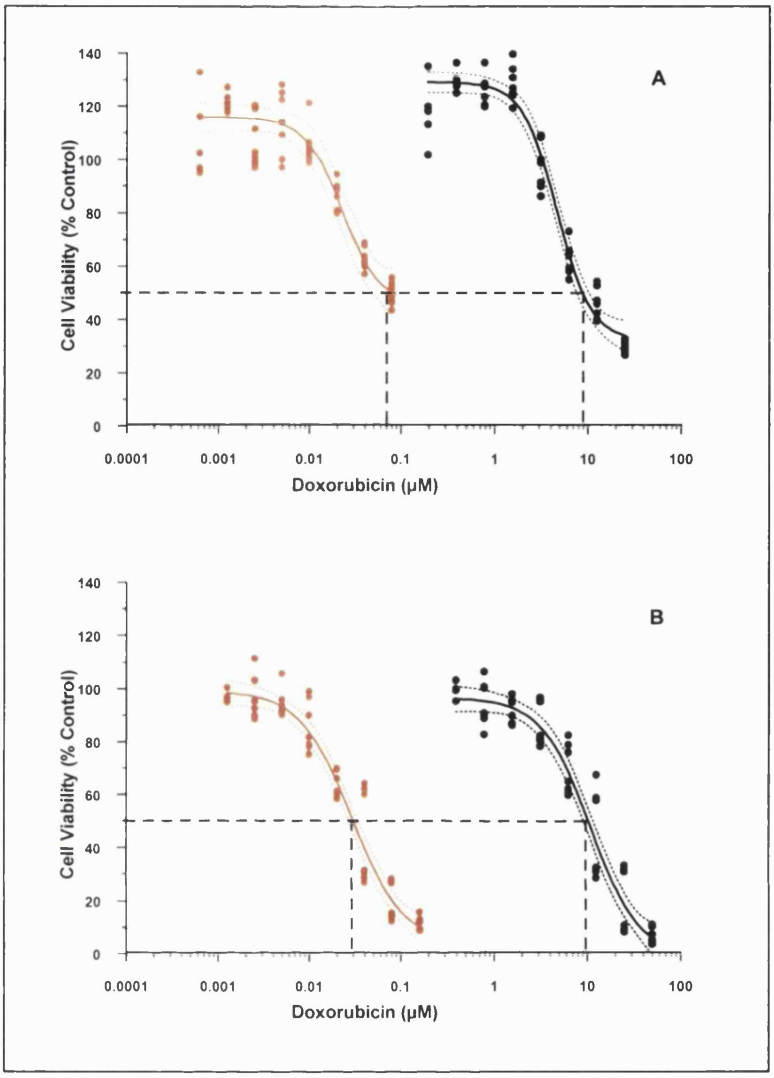

Figure 2.13 Concentration effect curves for doxorubicin covalently bound to HPMA, PK1 (black) and the 0.02% unbound doxorubicin (brown) after (A) 120 hours of continuous exposure, and (B) 120 plus 72 hours post incubation against MCF-7 cells. Cell survival is plotted as a function of doxorubicin concentration.

According to the pharmacodynamic principle used by Adams [1989], if one calculates the product of concentration and time for any antitumour agent whose slope is less or greater than 1on a plot of log concentration vs. log time, this will lead to inaccuracies when comparing antitumour agents in terms of efficacy. Secondly, as cytotoxicity is not a constant, the products of C and T become meaningless. We applied data obtained for doxorubicin and PK1 to this principle on the basis for comparing drug efficacy. Although the slope for both compounds at different surviving fractions were either less or greater than 1, the interpretations from this

analysis did not compare with the actual observations for PK1. Thus doxorubicin and PK1 antitumour action is not a function of $C \times T$ (Haber's rle) and does not strictly conform to the $C^n \times T = K$ principle. On the other hand we have shown that the exposure constant, k, is crucial for doxorubicin action.

However, we have evidently demonstrated that too short an exposure time may result in cell cycle arrest from which recovery is possible and therefore prolonged exposure times are necessary to induce cell death. In addition, the duration of drug exposure and to an extent concentration is an important factor in determining the degree of cytotoxicity elicited by that drug. Although doxorubicin is metabolised, it is not known how long the products generated remain active. It is possible that antioxidants such as glutathione, which is present in millimolar levels inside cells can bind to low levels of doxorubicin being released from the conjugate, thereby inhibiting cytotoxicity.

In conclusion, PK1 appears to be inert *in vitro* against the MCF-7 human breast cancer cell line. However the limited toxicity of PK1 could be due to lack of cellular uptake, and lack of cathepsin B activity necessary for the intracellular release of doxorubicin for intercalation. Therefore further investigations are warranted to decipher the lack of PK1 toxicity *in vitro*.

CHAPTER 3 – Subcellular localisation of PK1 and assessment of cathepsin B activity *in vitro*

3.1 INTRODUCTION

Currently there are seven polymer drug conjugates in clinical trials. These include 1) PK1, 2) HPMA copolymer–paclitaxel, 3) HPMA copolymer camptothecin, 4) polyethyleneglycol-camptothecin, 5) polyglutamic acid-paclitaxel, 6) an HPMA copolymer-platinate and 7) HPMA copolymer-doxorubicin bearing galactosamine (PK2). All these conjugates have been developed in an attempt to enhance the therapeutic response and to effectively reduce toxicity to normal tissues. In addition, these conjugates have been shown to possess anticancer activity in pre-clinical testing.

It has been proposed that the efficacy of PK1 is due to a difference in the uptake of the conjugate compared to that of doxorubicin [Etrych et al., 2001]. Being a low molecular weight compound with a net positive charge, doxorubicin readily diffuses across most biological membranes distributing into the cells of most tissues. In contrast, following intravenous administration of PK1, the covalently bound doxorubicin is biologically inactive and therefore requires activation. As previously mentioned, PK1 is thought to enter cells both *in vitro* and *in vivo* via fluid phase pinocytosis with subsequent hydrolysis of the GFLG tetrapeptide spacer by cathepsin B. This spacer was chosen based on the considerable amount of evidence that many metastatic tumours have elevated levels of cathepsin B, and this was found to correlate with the ability of primary tumours to invade normal tissues [Sloane and Dunn, 1981].

As clearly demonstrated in chapter 2, the *in vitro* cytotoxicity of PK1 can to a large degree be ascribed to the 0.02% free drug present within the polymer preparation. According to Duncan et al., [2001], due to the mechanism of internalisation of PK1 and other HPMA copolymer conjugates, routine *in vitro* cytotoxicity assays are not suitable for assessing the antitumour activity of polymer drug conjugates containing free unbound drug, because they give rise to false positive results. However, one can make the assumption that if this free unconjugated drug is allowed for, or used as a reference, false positives should not occur. In contrast to the results described in chapter 2, *in vitro* studies by Kopecek (who was involved in the design and synthesis of PK1) and his group have suggested that there is *in vitro* activity of PK1 in the A2780 human ovarian carcinoma cell

line (IC_{50} of 36.34 μM doxorubicin equivalent) [Minko et al., 1998]. However, they failed to account for toxicity of free drug. Furthermore, the same group [Minko et al., 1999] also observed that chronic exposure of PK1 to the same ovarian carcinoma cell line *in vitro* does not induce expression of the multi-drug resistance protein (MDR).

As shown in Figure 2.13, PK1 was poorly active in MCF-7 cells in culture. It is however possible that these cells are not enzymatically capable of activating the conjugate. Therefore with the aim of understanding the mechanism of PK1 at the cellular level and for the design of future polymeric drug conjugates, we investigated possible reasons for the observed differences between doxorubicin and PK1. The questions addressed were 1) is PK1 being internalised by cellular systems, 2) if so, do cells have cathepsin B activity for subsequent hydrolysis of the linker, and 3) if doxorubicin is cleaved, is it able to diffuse out from the lysosome for DNA intercalation that is believed to be necessary for antitumour activity [Gewirtz, 1999]. To achieve these aims and to obtain comparative data, various cell lines with differing levels of cathepsin B were employed in these studies. Thus, in addition to MCF-7 cells, HepG2 human hepatoma, DU-145 human prostate carcinoma and the B16F10 murine melanoma cells lines were used.

As described in chapter 1, cathepsin B is found in the lysosomes of cells, the cellular equivalent of the digestive tract, and is involved in the normal turnover of cellular components and other molecules. Following synthesis, cathepsin B and other lysosomal proteases are sorted from other newly synthesised proteins by binding of their phosphomannosyl residue to mannose-6-phosphate receptors (MPRs). This directs transport of the newly synthesised proteinase to lysosomes. Once within the lysosomes, the highly acidic environment initiates dissociation of the receptor enzyme complex. MRPs are recycled either via the Golgi apparatus or the cell surface [Brown et al., 1986]. The form of cathepsin B synthesised depends upon the species and tissue of origin, as different tissues express different forms of the protease. Mature cathepsin B can exist as a single chain, double chain, or both single and double chain forms together. In humans, cathepsin B is encoded for by a single copy gene on the short arm of chromosome 8, (8p22), and the entire gene is 27 kb in size. The proenzyme has a predicted molecular weight of 46,000, and in HepG2 cells is glycosylated to give rise to a 33,000 dalton mature single chain form. This single chain form is further processed to give a 27, 000 + 5,000 double chain form, and then to an unglycosylated form of 24, 000 + 5, 000 double chain form [Koblinski et al., 2000 & Agarwal, 1993].

3.2 EXPERIMENTAL APPROACH

3.2.1 Fluorescence microscopy

Fluorescence microscopy is a technique used to visualise fluorescent probes within biological structures. Due to its quinone moiety, doxorubicin is a naturally fluorescent compound and can therefore be utilised without modifications for uptake studies.

Materials and Method

10^3 cells/chamber (using 4 well Nunc treated chamber slides) were seeded and incubated for 4 days for exponential growth. PK1 or doxorubicin diluted in fresh culture medium was added to give a final concentration of 50 μM (doxorubicin equivalent or doxorubicin respectively). At appropriate time points, prior to visualisation, drug containing medium was removed and cells were washed three times with 0.5 ml PBS. Chambers and gaskets were subsequently detached from the slide without disturbing the monolayer culture. Slides were then covered with coverslip (No. ½ thickness) and images were captured using a rhodamine filter at 488 nm excitation using a Leitz Dialux 20 fluorescence microscope.

3.2.2 Extracellular hydrolysis of the Gly-Phe-Leu-Gly tetrapeptide.

Materials and method

Cells were seeded into chamber slides and allowed to enter exponential growth for 3 days. 24 hours prior to treatment with hydrolysed PK1, 60 μM (doxorubicin equivalent) of the conjugate, was pre-incubated with 100 μg of bovine cathepsin B (Sigma) in the recommended buffer (50 mM NaAc, 0.5 mM MgCl, 1 mM EDTA and 0.2 M NaCl, pH 5.0) at 37^{O}C in 1.5 ml microfuge tubes for 24 hours. The following controls were also set up and incubated in parallel in the same buffer solution. (1) 60 μM doxorubicin, (2) PK1 at 60 μM doxorubicin equivalent, (3) 100 μg cathepsin B. Following three days in culture, cells were treated in duplicate wells with the pre-incubated PK1 with cathepsin B and all relevant controls in a final volume of 120 μl/well giving a PK1 concentration of 20 μM doxorubicin equivalent. Cytotoxicity of the hydrolysed PK1 against MCF-7 cells was determined by MTT reduction as described in section 2.2.6.

3.2.3 Protein expression of cathepsin B using SDS-PAGE

Principle

SDS-polyacrylamide gel electrophoresis (SDS-PAGE) is a rapid and inexpensive technique for resolving proteins on the basis of differences in molecular mass (Sambrook *et al.*, 1989).

Cell extracts are prepared in the presence of protease inhibitors in an SDS containing buffer. If required, a reducing agent such as β-mecaptoethanol or dithiotreitol (DTT) is added to break disulphide bonds. Denatured proteins bind to SDS to form detergent protein micelles. Because the bound SDS contains a negatively charged sulphate group, it confers a net negative charge to most proteins and they migrate towards the anode. The amount of SDS that binds a protein is dependent on the size of the polypeptide, which affects migration during electrophoresis. The size of each protein is estimated using protein markers with known molecular mass. The percentage of polyacrylamide gel used determines the size of proteins that can be resolved. For example, low percentage gels are used for high molecular weight proteins and vice-versa. Proteins are separated according to size by sieving; small proteins migrate faster than larger proteins.

The resolving gel is a three dimensional matrix of randomly cross-linked polymers of an acrylamide and bis-acrylamide. Polymerisation is initiated by APS (ammonium persulphate), which provides free radicals that drive the polymerisation reaction. Temed (N, N, N', N-tetramethylethylenediamine) accelerates the reaction by stabilising the radicals produced by APS. The pore size and rigidity of the gel depends on the concentration of acrylamide and the proportion of cross-linking agent used.

Preparation of cell lysate

Materials

Laemli sample buffer (LSB) stock

- 62 mM(v/v) Tris base pH 6.8
- 10% (w/w) Glycerol
- 2% (w/v) SDS
- 5% β-mecapto-ethanol

Protease inhibitors (purchased from Sigma)
- Aprotinin

- Leupeptin
- PMSF (Phenylmethylsulfonyl fluoride)

Working LSB solution

To 1 ml LSB stock solution, 2 µl of saturated bromophenol blue was added followed by aprotinin, leupeptin and PMSF to give final concentrations of 1 µg/ml, 1 µg/ml and 100 µg/ml respectively.

Method

Culture medium was removed from monolayer cultures growing in T25 flasks, washed twice with Hank's solution (HBSS) and following trypsinisation, cells were kept at $4^{O}C$. They were washed once with HBSS and then pelleted by centrifugation at 1000 rpm for 5 minutes at $4^{O}C$. On ice, the supernatant was removed; the pellet was washed with HBSS to remove traces of culture medium which might otherwise inhibit protease activity. It was lysed with 300 µl of LSB (working solution). DNA was sheared by repeatedly passing the lysate through a 25-gauge hypodermic needle (Becton and Dickinson) until viscosity was reduced. Samples were then boiled for 5 minutes and stored at $-20^{O}C$.

3.2.3.1 Bradford assay

Materials

- Bradford reagent (Bio-Rad)
- dH_2O (deionised water)
- 96 microtitre plate
- 2 ml microfuge tubes
- BSA protein standards (Sigma)
- Plate reader

Method

In Eppendorf tubes containing 0.5 ml dH_2O, BSA standards were prepared by adding the appropriate volume of BSA to a range of concentration from 0-10 µg total protein. In another set of tubes containing 0.5 ml dH_2O, 1 µl of each cell lysate (samples) were mixed. To each sample and BSA standards, 0.5 ml of Bradford reagent was added and thoroughly

mixed by vortexing. 200 µl of each standard and samples were pipetted into a 96 well plate in duplicates wells and the optical density was measured at 570 nm on a Labsystem Multiskan plate reader. The concentration of protein in each sample was calculated from a standard BSA curve.

3.2.3.2 Electrophoresis and protein transfer

Materials

1X Running/ transfer buffer (250 mM Tris base, 2.5 M glycine and 1% SDS)
1.5M Tris base pH 8.8
10% SDS
1.0 M Tris Base pH 6.8
30% acrylamide (Bio-Rad)
Temed
10% APS
Protein standards (Bio-Rad)
Saturated butanol

Method

A Mini Protean II gel casting apparatus was set up according to the manufacturers instructions (Bio-Rad). 10-12% (depending on size of protein of interest) resolving and stacking gels were prepared according to Sambrook et al. [1989]. Gels were then secured onto the electrophoresis apparatus and the upper and lower chambers were filled with 1X running buffer. Samples were loaded and resolved at 90V for 2 hours. Following electrophoresis, resolved proteins were transferred through a 0.45 µm pore nitrocellulose membrane at 40 V for 1 hour.

3.2.3.3 Immunoblotting

Materials

Tris-buffered Saline (TBS)
TBS + Tween-20 (TBS-T)
10% non-fat milk powder in TBS-T (blocking buffer)

Following protein transfer, the nitrocellulose membrane was incubated for 30 minutes at room temperature with gentle agitation in blocking buffer. Subsequently, the membrane was incubated with the primary antibody in 5% milk in TBS-T for 1 hour. The membrane was then washed 3X for 10 minutes in TBS-T followed by incubation with the secondary antibody (goat polyclonal IgG, Santa-Cruz)conjugated with Horse-radish peroxidase (HRP) for 1 hour. The membrane was then washed 1X 30 minutes and 2X 15 minutes in TBS-T.

3.2.3.4 The Enhanced Chemi-Luminescence (ECL) detection

The ECL detection system is based on the oxidation of luminol (5-2,3-dihydrophthalazine-1, 4-dione) to produce light. The reaction is catalysed by HRP which effects the hydrolysis of H_2O_2 to H_2O and O_2 thereby providing the oxygen necessary for the oxidation of luminol. The ECL buffer (see below) is a basic solution, which provides OH^- ions; the resulting radicals are scavenged by coumaric acid, which enhances light emission [Thorpe and Kricka, 1986, and Prichard and Cormier 1987].

Materials

ECL solution
- 100 mM Tris-HCL pH 8.5 (ice-cold)
- 90 mM p-coumaric acid in DMSO
- 250 mM luminol in DMSO

Method

To 10 ml of cold Tris buffer, 50 µl of luminol, 25 µl coumaric acid, and 3 µl of 30% w/v hydrogen peroxide were added and thoroughly mixed prior to use. The TBS-T was drained off the membrane by blotting on a paper towel. In the dark (using a yellow Kodak filter lamp), the membrane was placed on a clean smooth flat surface, covered with 5 ml of the ECL solution and incubated for 1 minute. Excess solution was drained off; the membrane was wrapped in cling film and placed on a film cassette (Amersham). Subsequent membranes were exposed to x-ray film (Amersham) between 10 seconds and 15 minutes depending on the primary antibody used.

3.2.4 Fluorescent microplate assay for human liver cathepsin B and cellular cathepsin B activity in monolayer cultures.

Materials

Fluorogenic substrate: Z-Arg-Arg-7-amino-4-methylcoumarin (Z-Arg-Arg-AMC) (Calbiochem)

Human liver cathepsin B (Calbiochem)

Hanks balanced salt solution (HBSS)

Labysystems Fluoroskan II microplate reader

Pericellular assay buffer (PAB)

200 ml PAB

HBSS w/o sodium bicarbonate containing:

0.6 mM $CaCl_2$

0.6 mM $MgCl_2$

2 mM L-cysteine

25 mM PIPES

PAB-T

PAB buffer as above plus 0.1% Triton x-100

3.2.4.1 Enzymatic activity of purified human liver cathepsin B (Standard curve)

A stock solution of human cathepsin B at 1 μg/ml was prepared in PAB buffer. 5 fold serial dilutions of the stock were prepared in duplicate wells in a 96 well plate at 100 μl/well (1000, 200, 40, 8, 1.6, 0.32, 0.064, 0.0128, 0 ng/ml). 100 μl of 1 mM of the Z-Arg-Arg-AMC fluorogenic substrate in PAB-T was added to each enzyme-containing well to a final volume of 200 μl (final substrate concentration of 0.5 mM). Enzyme activity (reaction rate; relative fluorescence/minute) was measured using a fluorescent microplate reader on kinetic mode at 37^{O}C with an excitation filter at 355 nm and emission filter at 460 nm for 20 minutes. Fluorescence values were measured every 2 minutes.

3.2.5 Cellular cathepsin B activity in monolayer cultures.

Cells were seeded in 96 well plates and allowed to reach 80% confluence after 3-4 days. Culture medium was then removed and monolayer cultures were washed with HBSS (0.2 ml). Cells were incubated with 0.2 ml PAB for 30 minutes at 37^{O}C. The buffer was replaced with fresh PAB-T containing 500 μM Z-Arg-Arg-AMC per well to liberate total cellular cathepsin B. Rates of increase in fluorescence intensity normalisation were compared to a standard curve of purified cathepsin B to obtain cathepsin B activity for each cell line following determination of protein content using the Bradford assay.

3.2.6 Localisation and distribution of cathepsin B protein in monolayer cultures

Principle of methodology

A commercially available kit was used (Santa-Cruz, sc-2023). Immunohistochemical staining (IHC) was used to identify specific antigens (proteins) in tissue sections or cells (immunocytochemistry). Sections were appropriately fixed on slides and incubated with a mono- or polyclonal antibody directed to the antigen of interest. The specifically bound antibody was detected by incubation with a biotinylated secondary antibody raised against immunoglobulins of the primary species of animal in which the primary antibody was raised. Further incubation with a strepavidin-horseradish peroxidase conjugate and a DAB substrate (3-3'diaminobenzidine) gave a positive brown precipitate due to the catalysis of DAB by peroxidase if the protein of interest is present in detectable amounts.

Materials

Required solutions and reagents not provided in the kit:

PBS

H_2O_2

Solvents: acetone, xylene, and ethanol

Monoclonal antibody (Anti-goat cathepsin B, Santa-Cruz)

Aqueous mounting medium

Coplin staining jars

Beakers

Slide racks and coverslips

Method

Cells were cultured on chamber slides (Lab-TeK) to reach approximately 80% confluence after 3 days in culture. Cells were then washed twice with PBS to remove traces of medium. Chambers and gaskets were removed and cells were fixed in cold acetone for 5 minutes before allowing to air dry at room temperature. Samples were rehydrated in PBS for 5 minutes and endogenous peroxidase activity was quenched by incubating with 0.2% H_2O_2 (v/v) in PBS for 10 minutes followed by a 5 minutes wash with PBS only. Samples were incubated for 1 hour in 1.5% normal blocking serum in PBS. Serum was removed prior to further incubation with primary antibody (cathepsin B, sc-6493) at a 1:10 dilution in blocking serum for an hour. Slides were washed 3X with PBS for 5 minutes and incubated for 30 minutes with biotin-conjugated secondary antibody. Following incubation with the secondary antibody, slides were washed 3X with PBS for 5 minutes and further incubated for 30 minutes with freshly prepared HRP reagent. Following 3 PBS washes of 5 minutes each, slides were incubated with DAB solution for 10 minutes. After rinsing in dH_2O for 5 minutes, slides were counter-stained for 10 seconds with Gill's Haematoxylin, washed under running tap water for 2 minutes and dehydrated through 95% and 100% ethanol, 10 seconds each and finally in xylene for 2 minutes or until streaking stops. Slides were mounted whilst still wet in histomount and viewed under a light microscope.

3.2.7 Haematoxylin and Eosin staining

Materials

Gill's haematoxylin (Merck)
Eosin yellowish (1 g in 100 ml dH_2O)
1% acid alcohol (99 ml 70% ethanol+ 1 ml conc. HCL)
Scott's tap water 500 ml
- 10 g Sodium bicarbonate
- 1.75 g Magnesium sulphate

Fixed specimens were rehydrated and incubated with haematoxylin for 5 minutes. Slides were washed in tap water and samples blued in Scott's tap water. Slides were subsequently placed in 1% acid alcohol for 2 seconds, washed, and incubated in eosin for 5 minutes followed by a rinse in tap water, dehydration, and mounted as previously described in 3.6.

3.3 RESULTS

3.3.1 Intracellular distribution of free doxorubicin and PK1

The biological rationale for the development of PK1 and other polymer conjugated drugs is based on the mechanism of cell entry. Low molecular weight agents such as doxorubicin enter cells by simple diffusion via the plasma membrane. In contrast, entry of PK1 and other macromolecules is thought to be confined to fluid phase pinocytosis followed by intralysosomal hydrolysis of the linker by cathepsin B (or other lysosomal enzymes) to release the active drug substance. Pinocytosis is a passive process common to most cells and is used to capture fluids and certain molecules essential for certain metabolic processes. As shown in chapter 2, the cytotoxicity of PK1 against MCF-7 cells could mainly be accounted for by the 0.02% unbound doxorubicin on the polymer. We therefore questioned whether PK1 internalisation, which is postulated to be a pre-requisite for the intracellular release of doxorubicin occurs at all in our in vitro system. Having a planar aromatic ring and a positive charge, doxorubicin has a high affinity for double stranded nucleic acids and therefore should accumulate in the cell nucleus. Taking advantage of the natural fluorescence of doxorubicin (free and conjugated) the cellular distribution of PK1 and doxorubicin was investigated in the MCF-7 cell line using fluorescence microscopy.

Following culture and treatment of cells for various time intervals with a single concentration of PK1, 50 μM, (this was the highest concentration of bound doxorubicin used in cytotoxicity studies) internalisation of PK1 was observed as early as 30 minutes after treatment (Figure 3.1). Interestingly, PK1 was distributed throughout the cytoplasm, but was mainly localised in the perinuclear region in vesicles. This pattern of distribution was observed for up to 72 hours of continuous drug exposure to cells, but with little or no fluorescence in the nucleus. As expected, doxorubicin was mainly observed in nuclei with very little fluorescence in the cytoplasm (Figure 3.1 A-B). Untreated cells do not have background fluorescence (not shown). In addition, doxorubicin was also observed to bind to membranes in a transient manner. Hence, doxorubicin has a higher affinity for cellular DNA than membrane components due to its amphipathic nature. Increasing the exposure time of PK1 to 7 days revealed a vesicular pattern of distribution not only around the perinucleus but also within the cytoplasm as shown in Figure 3.1H.

We thus established that there are profound differences in the intracellular fate of doxorubicin and HPMA bound doxorubicin following continuous drug exposure. To rule

out the possibility that the observed distribution of fluorescence was not due to surface binding of the conjugate when cells were incubated with PK1 (despite washing cells prior to imaging) we investigated the distribution of PK1 after removal of extracellular drug followed by post-incubation. As in Figure 3.1, MCF-7 cells were treated continuously with 50 μM doxorubicin equivalent, PK1, for 72 hours. Following this, extracellular drug was removed; cells were washed and further incubated in fresh culture medium for 4-72 hours.

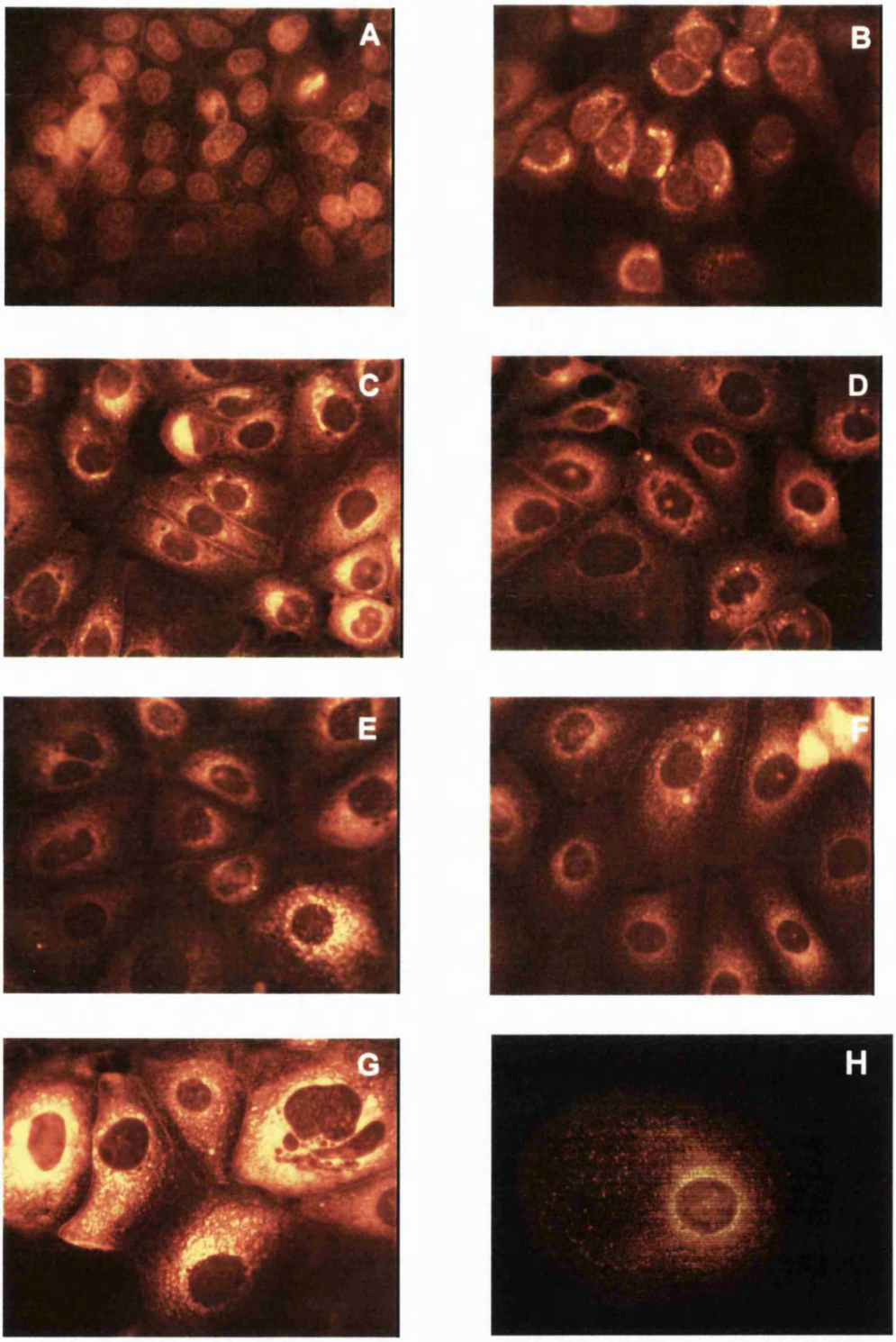

Figure 3.1 – Cellular distribution of doxorubicin and PK1 in MCF-7 cells. MCF-7 cells were treated with 50 μM bound doxorubicin equivalent of PK1 and incubated for various times. (A) Doxorubicin 30 minutes, (B) 4 h (C) PK1 30 minutes (D) 4h, (E) 24 h, (F) 48 h, (G) 72 h. and (H) 7 days. Images were acquired with a Leitz Dialux 20 fluorescence microscope at a magnification of x400. Untreated cells do not fluoresce.

This led to marked decreases in overall fluorescence with increasing post incubation time, but with a more distinct vesicular distribution of PK1 (Figure 3.2). Thus, binding of the polymer to cell surfaces can be ruled out as an explanation for the observed fluorescence of PK1.

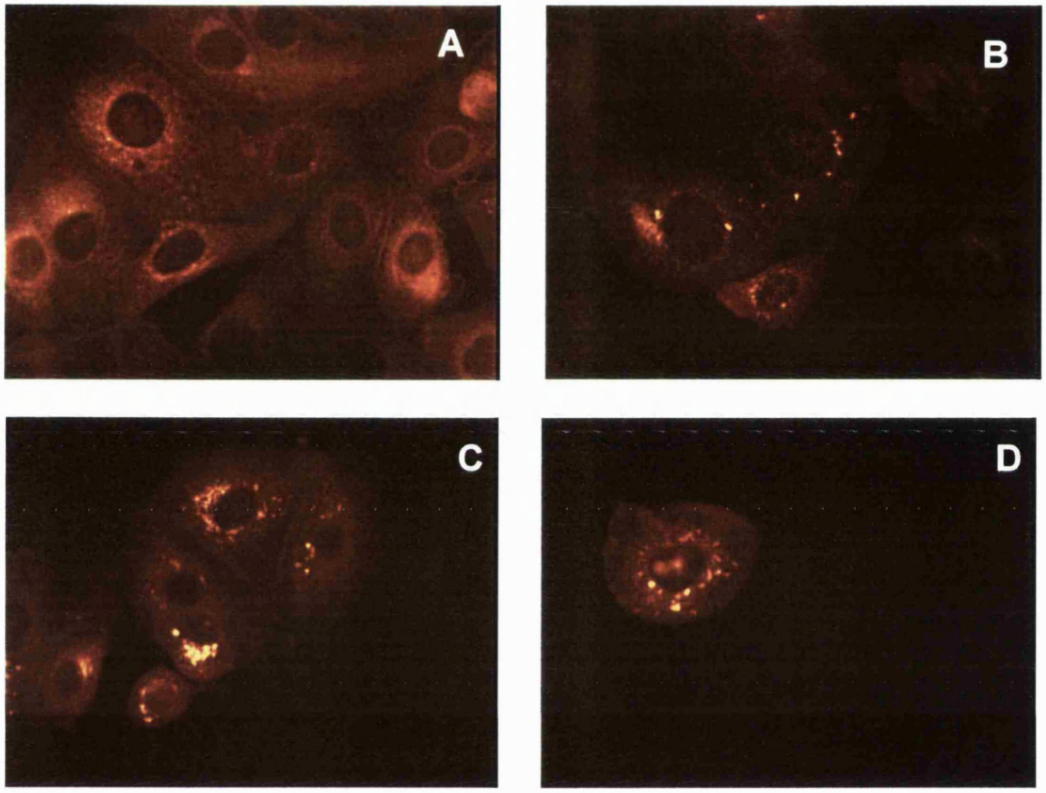

Figure 3.2 - Effect of post-treatment on the cellular distribution of PK1. MCF-7 cells were treated for 72 h continuous and post-incubated for various times: (A) 72 h, (B) 72 + 4 h, (C) 72 + 48 h, (D) 72 + 72 h. Images were acquired at a magnification of x400.

3.3.2 Effect of pre-digestion with human cathepsin B on cytotoxicity of PK1

Having demonstrated clearly that PK1 has been internalised by cells, next we addressed the question as to whether the Gly-Phe-Leu-Gly linker is susceptible to hydrolysis by cathepsin B as proposed [Subr et al., 1988 and Duncan et al., 1982]. As previously mentioned, GFLG was specifically designed to match the specific cleavage activity of the lysosomal protease cathepsin B. Following internalisation, the antitumour activity of PK1 is presumed to be dependent on the availability and activity of cathepsin B in the cell. However, other lysosomal enzymes such as cathepsin H, D and L, have also

been shown to demonstrate some level of specificity for the GFLG linker but to a much lesser extent relative to cathepsin B specificity. In order to establish susceptibility of the linker to hydrolysis by cathepsin B, based on results obtained from preliminary experiments at varying time periods, PK1 was pre-digested for 24 hours with cathepsin B, then administered to MCF-7 cells growing in culture. Cytotoxicity (after 18 hours) as assessed by MTT reduction, was dramatically potentiated by pre-digestion of PK1 (Figure 3.3). Pre-digestion reduced viable cells to 30% of untreated controls, and this was comparable to that obtained with the equivalent of doxorubicin under the same experimental conditions.

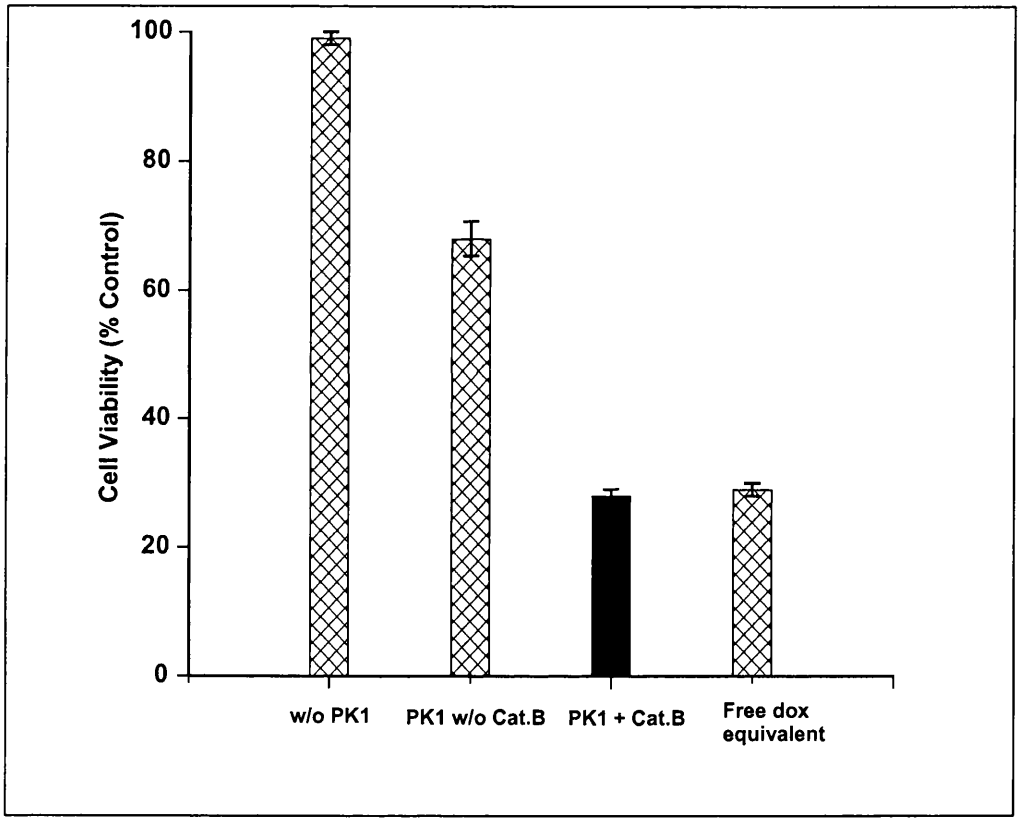

Figure 3.3 – Extracellular hydrolysis of PK1. 60 μM PK1 (doxorubicin equivalent) and 60 μM doxorubicin were incubated with 100 μg of bovine cathepsin B for 24 hours at 37^{o}C and then administered to MCF-7 cells growing in culture. Cell viability was then assessed by MTT reduction after 18 hours of incubation.

3.3.3 Cathepsin B expression

Although informative, the results described above do not in themselves explain the relatively low degree of PK1 cytotoxicity. Cathepsin B is a house keeping gene that is often over-expressed during the process of carcinogenesis. Upregulation of lysosomal proteases is thought to be a mechanism used for tumour invasion and metastases by digestion of extracellular matrices resulting in detachment of cells from the primary tumour [Poole, 1978]. For example, cathepsin B activity in a solid subcutaneous tumour of a variant of the murine B16 melanoma, B16F10, has been correlated with its metastatic potential.

We next investigated whether the limited cytotoxicity of PK1 observed in vitro could be due to low levels of cathepsin B inside cells. In addition to the MCF-7 cell line, the B16F10 variant, HepG2 human hepatoma, and DU-145 human prostate carcinoma cell lines were also tested for cathepsin B protein expression. For these studies we used an antibody that specifically recognises the active form of cathepsin B. The purified enzyme was used as a positive control. As shown in Figure 3.4, mature cathepsin B was highly expressed in HepG2 and DU-145 cells but not in the MCF-7 or the B16F10 cell lines. Thus, the low or no-exiting levels of Cathepsin B in MCF-7 cells, might account for the lack of PK1 cytotoxicity observed against MCF-7 cells. In addition, the results suggest that HepG2 and DU-145 are more metastatic than MCF-7 and B16F10 cells.

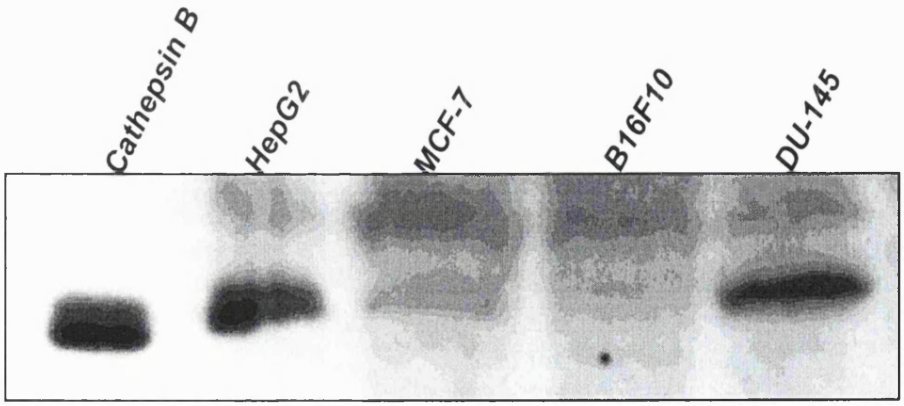

Figure 3.4 – Western blot analysis for cathepsin B. A 1:1000 dilution of anti-cathepsin B polyclonal antibody was used. Lane 1: 100 ng of purified human cathepsin B, lane 2: 50 ug of HepG2 whole cell lysate and lanes 3, 4 & 5: 200 ug of MCF-7, B16F10, and DU-145 whole cell lysates respectively.

Following these observations, it was therefore important to establish the cytotoxicity of PK1 against HepG2, DU-145 and the B16F10 cell lines. Figure 3.5 shows the dose-response curves for the various cell lines after 10 days of continuous treatment.

As previously shown in Chapter 2, PK1 appeared to be slightly more toxic to MCF-7 cells than the equivalent amount of unbound doxorubicin. In contrast, the unbound doxorubicin fraction was more cytotoxic to HepG2, Du-145 and B16F10 cells. There was no significant cytotoxicity of PK1 in any of the 4 cell lines tested bearing in mind the amount of bound and the percentage of unbound doxorubicin. These experiments showed that the cytotoxicity of PK1 did not correlate with cathepsin B levels of the cells studied. Thus, in our in vitro systems there appears to be no relationship between PK1 cytotoxicity and mature cathepsin B expression.

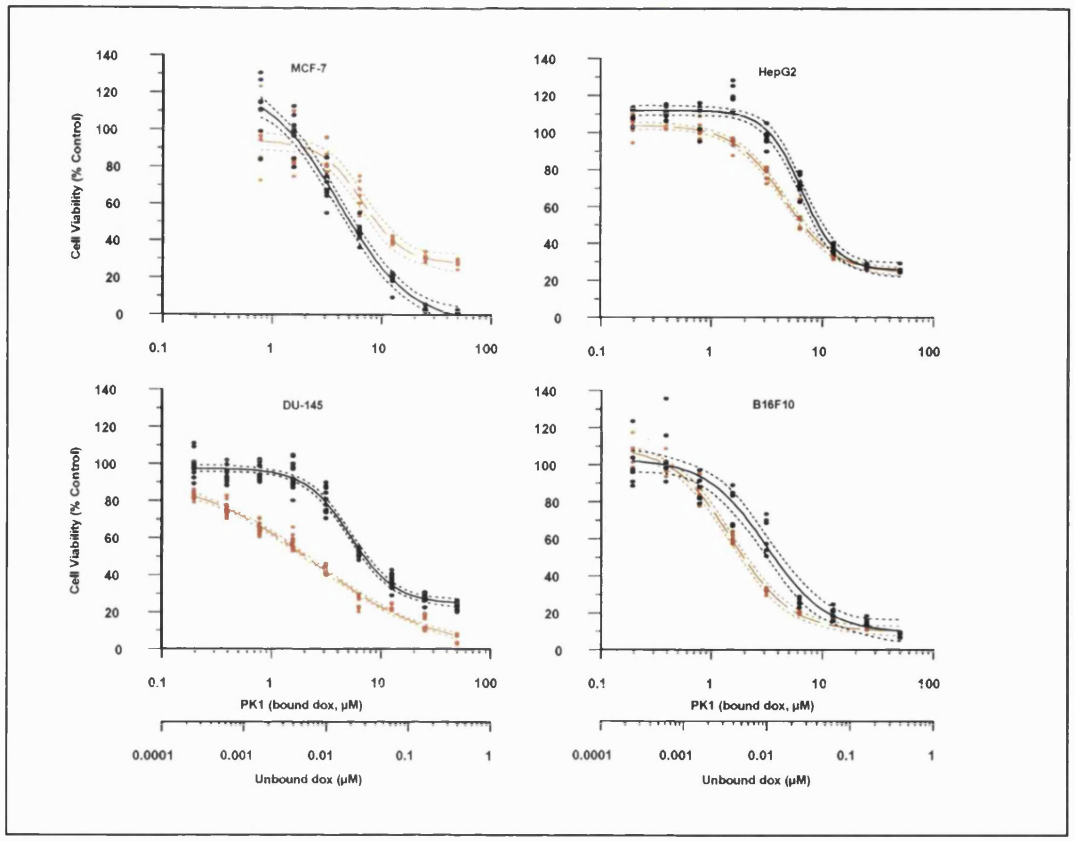

Figure 3.5 - Concentration effect curves for PK1 (black) and its free doxorubicin content (brown) following 10 days of continuous exposure to MCF-7, HepG2, DU-145 and B16F10 cells. Viability was determined using the MTT assay. The data combines the results of two independent experiments, with 8 wells at each concentration in each experiment. The combined results are expressed as a percentage of control and fitted to the Hill equation with the 95% confidence interval (dotted line) of the best-fit regression line (solid line). Cell survival in the presence of PK1 is plotted as a function of the concentration of doxorubicin bound to HPMA (upper x axis), and also as a function of the concentration of the 0.02% unbound doxorubicin present in the PK1 preparation (lower x axis). The two x axes have been purposely aligned in order to compare the potency of bound and unbound doxorubicin.

3.3.4 Cathepsin B activity

Given the relatively high levels of cathepsin B protein in HepG2 and DU-145 cells, the lack of toxicity of PK1 against these lines was surprising. Thus, it became necessary to probe whether the cathepsin B expressed in cell lines was biologically active. To this end, enzyme activity studies were performed using a commercially available synthetic fluorogenic substrate, Z-Arg-Arg-AMC, which is specific for cathepsin B as described by Hulkower *et al.*, [2000].

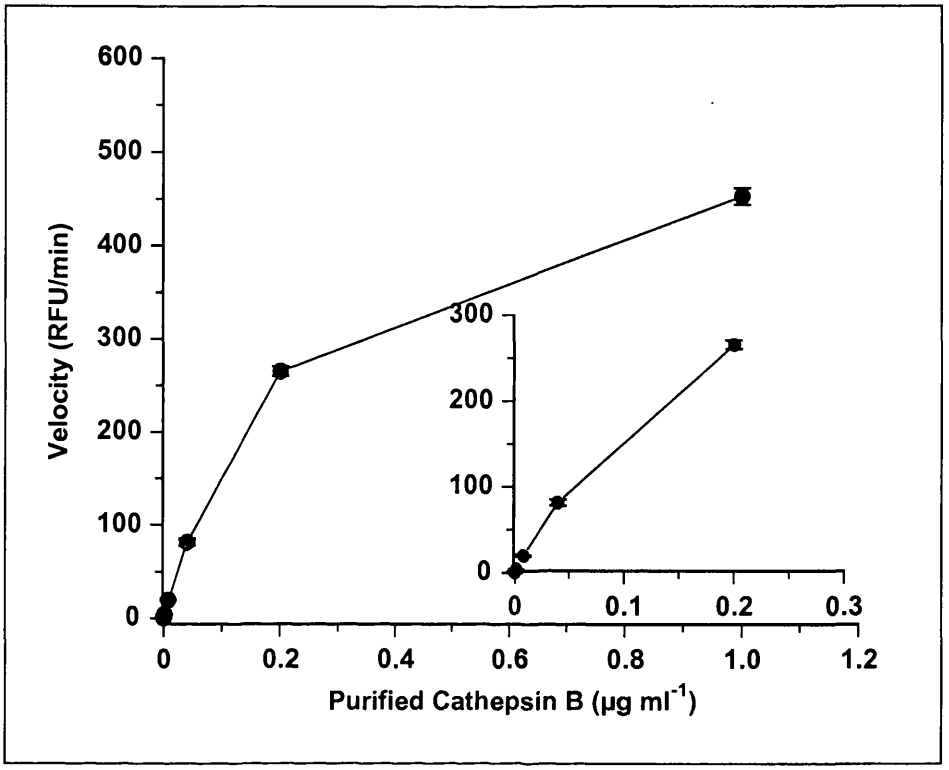

Figure 3.6 – Enzymatic activity of purified human liver cathepsin B. A 5 fold dilution from 1000 ng/ml of human liver cathepsin B was added to 1 mM Z-Arg-Arg-AMC in PAB and fluorescence readings taken every 2 minutes as described in materials and methods.

Before assaying for pericellular (cell surface and secreted cathepsin B) activity in monolayer cultures, the rate of activity of the purified enzyme was established as shown in Figure 3.6 using 540 µM Z-Arg-Arg-AMC. Shown in Figure 3.7 are the relative fluorescence units and rate of cathepsin B in HepG2, DU-145, MCF-7 and B16F10 cells growing in culture.

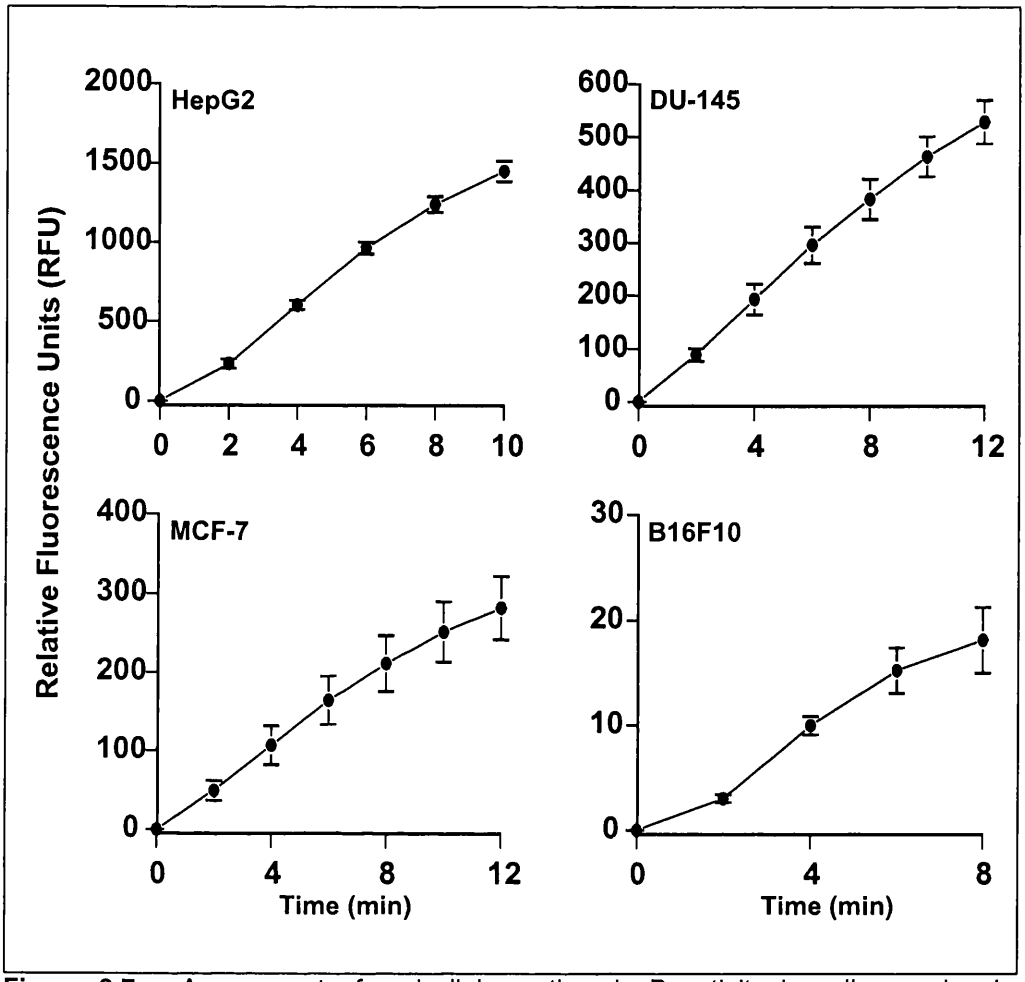

Figure 3.7 – Assessment of pericellular cathepsin B activity in cells growing in culture. HepG2, DU-145, MCF-7 and B16F10 cells were incubated with PAB-T for 30 minutes at 37^{o}C followed with 500 µM Z-Arg-Arg-AMC. Fluorescence readings were taken 2 minutes as described in materials and methods. Data shown are mean ±SEM of two independent experiments where n=4.

It became evident that all lines tested had cathepsin B activity, with HepG2 (150 RFU/min) showing the greatest activity followed by Du-145 (50 RFU/min), MCF-7 cells (25 RFU/min) and the B16F10 (2.5 RFU/min) variant of B16a which has been shown to have a velocity of 10 RFU/min by Hulkower *et al.* Following the enzyme assay, the total protein content of each cell line was determined using the Bradford assay on cells that were set up in parallel to those used for the enzyme assay. The rate of cathepsin activity was then normalised to total protein. Figure 3.8 shows relative cathepsin B activity for each cell line, and Table 3.1 is a summary of protein content, enzyme velocity and activity of each cell line. From these results, HepG2 cells had the greatest cathepsin B activity. Despite a lack of detectable protein expression, MCF-7 and B16F10 cells had low albeit measurable

pericellular cathepsin B activity. Within experimental error, cathepsin B activity correlated with protein levels as determined by Western blot analysis.

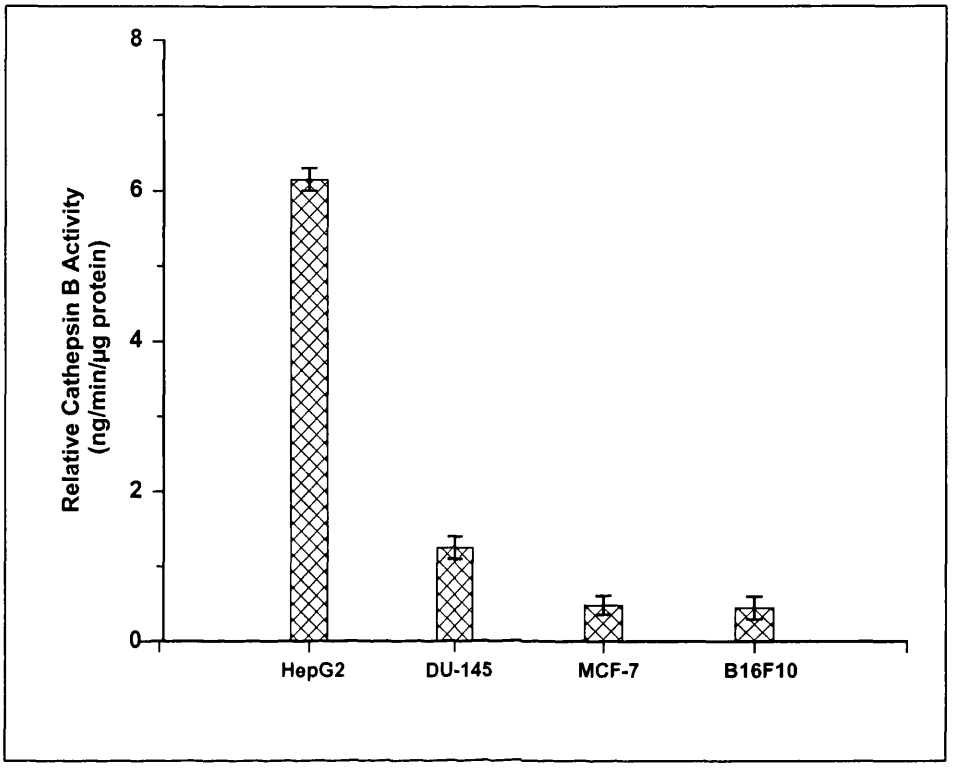

Figure 3.8 – Comparison of cathepsin activity in cell lines relative to purified human cathepsin B and protein content. After assaying for enzyme activity as described in materials and methods the protein content for each cell lines was measured using the Bradford assay and this was used to normalise cathepsin B activity. Results shown are the mean ± SEM of two independent experiments where n = 2.

3.3.5 Immunohistochemical staining for mature cathepsin B

In light of the results obtained so far, it was considered of interest to determine the cellular distribution of cathepsin B. This was done by immunohistochemical staining using DAB as the substrate. The distribution of PK1 observed using fluorescence microscopy and described in section 3.2.1 was compatible to a lysosomal distribution. The lack of cytotoxicity could be due to little or total lack of cathepsin B activity within the lysosome. Alteration in trafficking of cathepsin B and other lysosomal proteases have been reported in human and animal tumours. The distribution of cathepsin B in normal cells is mainly localised in the perinuclear region with a vesicular pattern compatible with a lysosomal distribution.

Table 3.1 - Relative cathepsin B activity.

Cell Line	*Protein (µg/ml)*	*Velocity (RFU/min)*	*Relative Activity (µg/ml)*	*Activity (ng/min/µg protein) ± SEM*
HepG2	17.1	150	0.105	6.15 ± 0.150
DU-145	26.05	50	0.0011	1.25 ± 0.150
MCF-7	34.95	25	0.000362	0.487 ± 0.125
B16F10	16.5	2.5	0.00030	0.451 ± 0.151

The development of the MCF-10 human breast epithelial cell line enabled studies into the redistribution and altered cathepsin B trafficking following cell immortalisation [Soule et al., 1990]. Subsequently, distribution of cathepsin B shifted from the perinuclear region to the plasma membrane [Sloane et al., 1994]. This was also found to be the case in MCF-7 cells [Sameni et al., 1995].

Using a commercially available immunohistochemical staining kit and the primary cathepsin B antibody raised against the mature form of the enzyme, a diffused cytoplasmic staining pattern was observed for MCF-7 and B16F10 cells with increasing staining intensity towards the cell periphery (Figure 3.9). In contrast, DU-145s showed more of a vesicular distribution with slight diffused cytoplasmic staining for cathepsin B, compatible to an extent to lysosomal distribution. A cytoplasmic distribution of cathepsin B was also observed with HepG2 cells.

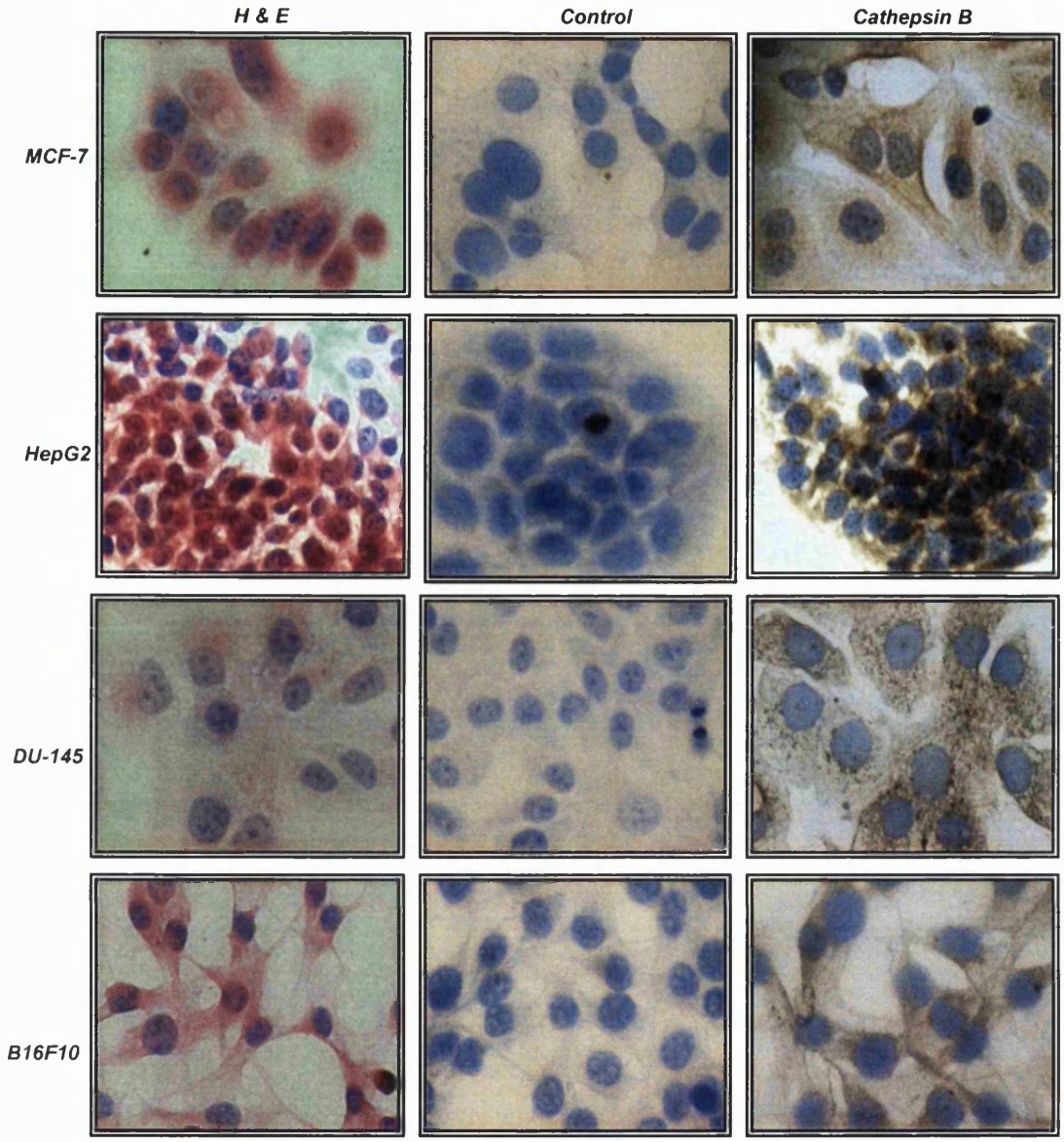

Figure 3.9 - Immunohistochemical staining for cathepsin B *in vitro* (X400). Cells were grown on chamber slides and allowed to reach 80% confluence before staining for cathepsin B with a commercially available kit and an anti-cathepsin B antibody raised against the 27 KDA mature form. Results shown are from a representative experiment out of 3.

3.4 Discussion

In the above studies we examined the cellular distribution of PK1, the levels of cathepsin B protein expression, subcellular localisation and activity in four different cell lines. These experiments were motivated by our observations of a rather low degree of cytotoxicity with PK1 in the MCF-7 breast cancer cell line.

Fluorescence microscopy studies revealed that uptake of PK1 is not a limiting factor in its toxicity. Uptake occurred as early as 30 minutes after incubation. However there was no fluorescence within the cell nucleus suggesting that doxorubicin was not being hydrolytically cleaved from HPMA, which might explain its relative lack of cytotoxicity. It is however important to note that for fluorescence to be observed a saturation point must be reached because when doxorubicin intercalates with DNA, fluorescence is quenched until a saturation point is reached. Therefore if doxorubicin is not cleaved to high enough concentrations, fluorescence will not be observed. Free doxorubicin had a very high affinity for double stranded nucleic acids, which confirmed its preferential localisation within the cell nucleus where intercalation into nuclear DNA occurs. In contrast, PK1 was observed in the cytoplasm and not in the nucleus with fluorescence concentrated in the perinuclear region with a vesicular distribution. This was also observed in HepG2, DU-145 and B16F10 cells (images not shown). Lysosomes are normally found within the perinucleus [Sloane et al.,] and thus, the distribution observed for PK1 suggests a lysosomal localisation [Calendi et al., 1965]. However, a study by Omelyanenko et al. [1998] using OVCAR-3 human ovarian carcinoma cell lines reported release of doxorubicin from the antibody-targeted HPMA into the cell nucleus. We were unable to detect doxorubicin fluorescence in the nucleus of any of the cell lines used after treatment with PK1. However, in agreement with our observations is a recent study by Hovorka et al. [2002] who observed fluorescence in "membrane-limited cytoplasmic structures" but also failed to detect the intrinsic fluorescence of doxorubicin in the cell nucleus released from HPMA in five different cell lines (EL-4 mouse T-cell lymphoma, SW620 human colorectal carcinoma, K562 human erythroblastoma, 38C13 mouse B-cell lymphoma and OVCAR-3). Further experiments by Hovorka et al. also confirmed a lack of lysosomal hydrolysis.

Our experiments showed that extracellular hydrolysis of PK1 using human cathepsin B greatly increased its cytotoxicity. Thus, we confirmed that in the batch of PK1 being used for our studies the linker, GFLG is susceptible to lysosomal hydrolysis, and is able to release toxic doxorubicin. Other factors that were taken into consideration to explain the low toxcity of PK1 in our in vitro systems were that the cells tested may not have the capability to hydrolyse GFLG either based on a lack of cathepsin B activity or a redistribution of cathepsin B from the lysosome during processing.

Initially, we determined protein expression of cathepsin B in all 4 cell lines by Western blot analysis. Surprisingly, HepG2 and DU-145 cells expressed high levels of active cathepsin B protein. On the other hand, expression was not observed in MCF-7 and B16F10 cells which might explain the lack of cytotoxicity in these cell lines. Surprisingly, the lack of toxicity in HepG2 and DU-145 cells was not in line with this idea. To rule out the possibility that cathepsin B, although present, did not possess enzymatic activity, studies were carried out using a fluorogenic substrate specific to cathepsin B. These experiments revealed enzymatic activity in all 4 cell lines to various degrees. The results obtained were in line with Western blot analyses (Figure 3).

It is now accepted that during carcinogenesis trafficking of lysosomal enzymes including cathepsin B is altered, due to its involvement in tumour growth and invasion during the proteolytic process of angiogenesis [Yan *et al.*, 1998, & Koblinski *et al.*, 2000]. Studies to date suggest that in human breast cancer cell lines, cathepsin B is localised at the cell surface by translocation of lysosomal vesicles to the cell periphery at the point of transition between pre-neoplastic and neoplastic state [Sameni *et al.*, 1995]. Immunostaing for mature cathepsin B was evaluated in HepG2, DU-145, MCF-7 and B16F10 cells. All cell lines stained positive for mature cathepsin B at different intensities, suggesting varying amounts of cathepsin B in each cell line. A diffused cytoplasmic localisation was observed in HepG2, B16F10s and MCF-7 with some intense membrane staining in the latter cell line. In contrast, cathepsin B distribution in DU-145s appeared more of a vesicular pattern.

Taken together, our results suggest that PK1 was internalised in all cell lines tested. Crucially, there were no associations between mature cathepsin B expression and PK1 cytotoxicity. Cells that expressed high levels of cathepsin B, such as HepG2 and DU-145, responded poorly to PK1 *in vitro*. However, it has been suggested that current routine *in vitro* cytotoxicity screening methods are not suitable for polymer drug conjugates because of the presence of free drug [Duncan *et al.*, 2001]. Given the proposed mechanism of action and the use of appropriate controls, the lack of PK1 toxicity against cells *in vitro* is astonishing. Thus the question whether doxorubicin cleaved inside lysosomes is able to leave the organelle deserves serious consideration.

CHAPTER 4 – ASSESSMENT OF PK1-INDUCED DNA DAMAGE AND CATHEPSIN B LOCALISATION *IN VIVO*

4.1 INTRODUCTION

The pharmacodynamics of doxorubicin is significantly modified by its conjugation to the vinyl polymer HPMA, as shown in Chapter 2. This modification, unlike free doxorubicin, is thought to be based on the inability of the copolymer conjugate to diffuse through biological membranes. As a result, the conjugate displays a lower volume of distribution and prolonged plasma half-life than doxorubicin [Seymour et al., 1990]. Studies by Duncan et al. [1994] show that PK1 is non-toxic to cells growing in culture, which is in agreement with our own results obtained using PK1 *in vitro*. However PK1 and other HPMA bound anticancer agents have been shown to mediate anticancer activity in a range of animal tumour models [Duncan et al., 1992 and 1998, and Seymour et al., 1995]. It has been suggested that the efficacy of PK1 *in vivo* is mediated by proteolytic activation of the conjugate within tumour tissues [Vasey et al., 1999].

Cathepsin B activity has been detected in culture media from tumour cell and explant cultures [Poole et al., 1978]. Activity has also been detected in the ascites fluid of women with ovarian cancer [Mort et al., 1981]. In metastatic tumours Cathepsin B is thought to be mainly associated with the plasma membrane, rather than the lysosomes, in metastatic tumours [Sloane et al., 1986]. This altered trafficking of cathepsin B is thought to be a result of defective intracellular processing where the enzyme is delivered to the plasma membrane rather than to the lysosome. In the last 10 years inhibitors of cathepsins, in particular cathepsins B, L and D, have been recognised as potential anti-metastatic agents. Currently in phase III clinical trials is the matrix metalloproteinase inhibitor, marimastat, in the adjuvant treatment of breast cancer. In normal cells cathepsin B is localised to the lysosome, whereas in cancer cells, levels of this protease are elevated 4-30 fold and there is an increase of cathepsin B in the plasma membrane at the cell surface [Keppler et al., 1996]. Cathepsin B has been implicated in several cancers including brain, bladder, breast, pancreas, prostate, stomach and thyroid.

Due to its amphipathic character, doxorubicin self-associates in aqueous solutions. As a result, there will always be a fraction of free unbound doxorubicin present in polymer-drug conjugates. This fraction of free drug accounts for the *in vitro* cytotoxicity of

PK1, as shown in Chapter 2. However it is thought to have negligible effect when PK1 is administered *in vivo*, as it constitutes 1% of the total weight of the conjugate.

PK1 is thought to be internalised by pinocytic capture, and consequent exposure to the intracellular lysosomal enzymes is postulated to be necessary for the release of active doxorubicin from the linker Gly-Phe-Leu-Gly. This was designed to be sensitive to degradation by cathepsin B and to a smaller extent cathepsins H and L [Duncan et al., 1984], and this is consistent with our own data (pre-digestion of PK1 with cathepsin B). If the linker is indeed susceptible to hydrolysis by cathepsin B, then the possibility that active doxorubicin is unable to traverse the lysosomal membrane needs consideration. As shown in Chapter 3, HepG2 cells expressing high levels of cathepsin B protein and enzyme activity were insensitive to PK1, even after prolonged incubation following internalisation of the conjugate. This would suggest that PK1 may lack cytotoxic activity against cancer cells growing *in vivo*. However, since *in vitro* data cannot be reliably extrapolated to *in vivo* situations, we decided to investigate the ability of PK1 to induce DNA damage *in vivo*. Furthermore, if doxorubicin is released inside cells from PK1, DNA strand breaks should be induced following intercalation of the doxorubicin in the DNA. Furthermore, if the conjugate is hydrolysed inside lysosomes preferentially within tumour cells, toxicity should be confined to tumour tissue and therefore damage to host tissue and other organs should be less apparent. Therefore, in addition to tumour samples, damage to bone marrow was also assessed.

In this chapter we investigated the ability of PK1 to induce DNA damage in individual tumour cells using the single cell gel electrophoresis (comet) assay. The tumour model chosen for this study is the well established and aggressive B16F10 murine melanoma. Over the years, B16F10 tumour cells have been shown to express elevated levels of cathepsin B, and most importantly, have been used to study tumour uptake of macromolecules (the EPR effect) [Seymour et al., 1995], and the pre-clinical efficacy of PK1 [Duncan et al., 1992].

DNA damage was chosen as a parameter of drug efficacy to investigate instead of cell death because 1) induction of DNA damage does not always lead to cell death and 2) the comet assay can detect the effect of PK1 on a heterogeneous population of cells following genotoxic insult.

The comet assay is a powerful and sensitive tool for measuring DNA damage in single cells. The assay is named for the microscopic appearance of DNA following electrophoresis. Its strength lies in its ability to measure the response of individual cells

within a population, thus allowing characterisation of tumour heterogeneity and, most importantly, prediction of the effects of cancer therapy on tumour cells and normal tissues. To our knowledge, this is the first study to investigate the genotoxic insult of macromolecules in single cells *in vivo*.

4.2 EXPERIMENTAL APPROACH

4.2.1 Preparation and treatment of cells growing in culture for single cell gel electrophoresis

MCF-7 and B16F10 cells were routinely cultured in DMEM supplemented with 10% foetal calf serum (FBS). DU-145 cells were cultured in RPMI 1640 supplemented with 10% FBS and 2 mM L-glutamine. HepG2 cells were routinely cultured in Minimal Essential Media, MEMα supplemented with 10% FBS. All cell lines were routinely cultured in T-25 Greiner flasks for 4 days prior to treatment in a total volume of 5 ml growth medium. Flasks were protected from light by covering with aluminium foil 24 hours prior to treatment. Cells were then treated with either doxorubicin (5 μM) or PK1 at equivalent concentrations in duplicates flakes for varying times. After treatment, cells were rinsed with HBSS, and dislodged with trypsin-EDTA. Following trypsinisation, cells were resuspended in fresh culture medium, pelleted by centrifugation and resuspended in HBSS to give 10^4 viable cells in 10 μl.

MCF-7 and DU-145 cells were obtained from Professor John Masters, Urology Department, University College London. B16F10 and HepG2 cells were obtained from Professor Ruth Duncan, Centre for Polymer Therapeutics, Welsh School of Pharmacy, Cardiff.

4.2.2 Inoculation of C57BL/6 mice with B16F10 cells

All *in vivo* studies were done in collaboration with Ruth Musila and Professor Ruth Duncan. All animal experiments were conducted according to the UK Coordinating Committee on Cancer Research (UKCCCR) (1998) and Home Office Guidelines (Animals Scientific Act, 1986).

B16F10 cells were seeded in T-75 tissue culture flasks to reach 80% confluence after 3 days. Male C57 black mice (6-8 weeks old, approx. 25g) were then lightly anaesthetised and injected subcutaneously with B16F10 melanoma cells (10^5 cells/mouse in 0.1 ml of 0.9% saline). Tumours were often palpable after 10 days of injection when they were 9-10 mm in size (the product of orthogonal diameters) (Figure 4.1). Animals were randomly distributed into dosing groups (3 per group) and on day 11, mice were weighed and a single dose of either saline (control), doxorubicin (7.5 mg/kg of animal body weight) or PK1 (15 mg/kg, doxorubicin equivalent) was administered intravenously in 0.1 ml saline via the lateral tail vein. At various times (5-72 hours) mice were killed by CO_2 asphyxiation followed by careful removal of tumour and femur on ice under UV safe light. Isolation of single tumour and marrow cells were performed as described below.

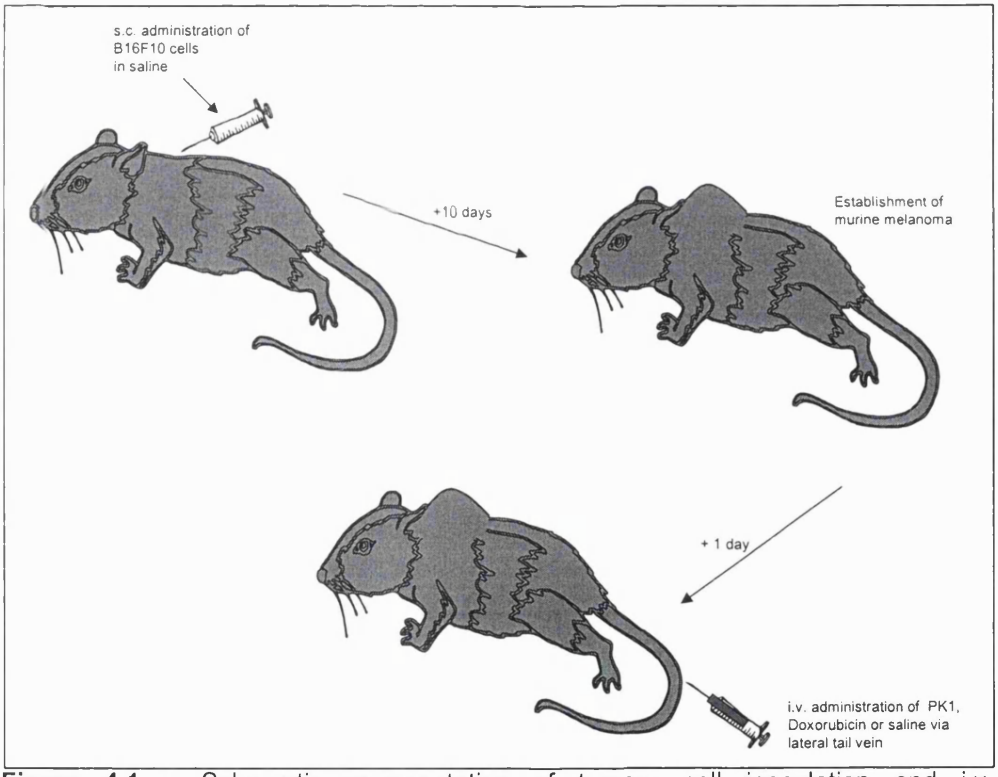

Figure 4.1 – Schematic representation of tumour cell inoculation and i.v. administration of antitumour agents. Male C57 black mice (6-8 weeks old, approx. 25g) were lightly anaesthetised and injected subcutaneously with B16F10 melanoma cells. Tumours were often palpable after 10 days, animals were then randomly distributed into dosing groups (3 per group). On day 11 mice were weighed and a single dose of saline, doxorubicin, or PK1 was administered intravenously via lateral tail vein.

4.2.3 Preparation of single cell suspensions

Samples were protected from light to prevent further DNA damage by working under yellow light. On ice, tumours were carefully removed, weighed, washed twice in ice-cold HBSS and cut into pieces in 5 ml ice-cold HBSS to produce a single cell suspension. The resultant cell suspension was strained through a sterile 70 μm Falcon cell strainer. This was repeated by using a 40 μm pore Falcon cell strainer to further remove cellular debris without losing cells.

4.2.4 Preparation of single bone marrow cell suspensions

Bone marrow cells were prepared from the femur. After cutting off the epiphyses, femur contents were aspirated with a 23 gauge needle attached to a 1 ml syringe filled with ice-cold HBSS. The resultant suspension was strained through a 40 μm pore strainer (Falcon) to remove other cellular components of marrow.

4.2.5 Alkaline single cell gel electrophoresis (comet assay)

Methodology

Ostling and Johanson developed the comet assay or single cell gel electrophoresis in the early 1980's to directly visualise and quantitate DNA damage in individual cells. The original method was subsequently modified by Singh and Olive [ref]. The assay is based on the micro-electrophoretic mobility of DNA fragments from the nucleus of a single cell. Treated or untreated cells are embedded in a thin agarose sandwich and lysed in an alkaline solution to remove all cellular content but leaving nuclear material intact. This is then subjected to electrophoresis in a neutral buffer to detect single strand breaks or in an alkaline buffer (pH > 10) to quantify both single and double strand breaks including alkali labile sites. After electrophoresis, slides are stained with a fluorescent DNA binding dye for visualisation and quantification of strand breaks.

Because DNA is a negatively charged molecule, relaxed and broken fragments migrate towards the anode during electrophoresis of nuclear material. Therefore, cells

showing high levels of damage to the genetic material display increased migration, thus giving the appearance of a 'comet'. Hence, the greater the strand breaks the larger the comet tail.

Using computer image analysis software, the length of the comet tail relative to the head is captured and measured. Parameters used to quantify the extent of DNA damage include tail length, percentage of DNA in the tail, and tail moment.

As shown in Figure 4.2, a comet consists of a head region, which represents DNA that did not migrate from the nucleus during electrophoresis, and a tail, which represents DNA that migrated out the nucleus due to fragmentation and loss of structure. The Komet software used allows computation of extensive comet parameters following electronic capture of such parameters as comet intensity, percent DNA in tail and head, tail length, tail moment, mean, mode and standard deviation.

Tail moment was chosen as a parameter to express DNA damage because it has been established that combining tail length and distribution of DNA in the tail is the best way to quantify DNA damage with the comet assay. Initially, it was thought that tail length was sufficient for damage evaluation profile, however, it was later realised that tail length alone was inadequate due to the fact that it increases steadily for low levels of damage and then plateaus beyond a certain point. This might lead to underestimation of DNA damaging capacity of agents that are extremely genotoxic, as the amount of DNA migration into the tail still increases. Olive et al. [1990] introduced the tail moment parameter, which takes into account the distance of migration from the comet head centre. As a result, two different comets, where one tail appears longer than the other (denoting more damage), may have the same amount of DNA in the tail. Hence, the use of tail moment parameter allows for this difference.

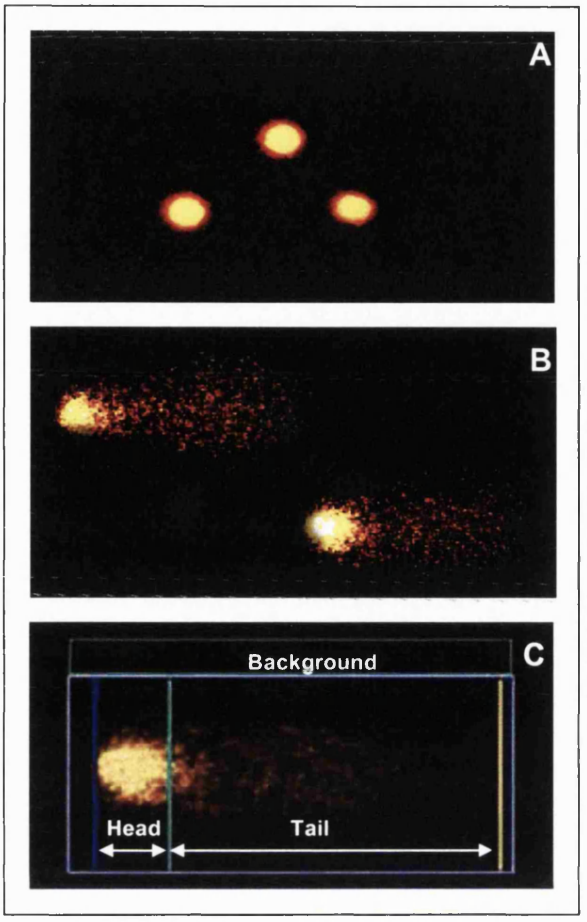

Figure 4.2 – Images of MCF-7 cells subjected to the alkaline Comet assay and stained with ethidium bromide. **(A)** Shows the normal appearance of untreated cells, with most of the DNA retained in the comet head. **(B)** Appearance of MCF-7 cells treated with 1 μM doxorubicin for 2 hours. The presence of the tail indicates DNA damage due to fragmentation of cellular DNA due to single- and double-strand breaks and alkali-labile sites. The greater the number of strand breaks, the larger the comet tail. **(C)** Parameters measured in the analysis window of the computer software, Komet 3.0. Background is automatically selected for correction immediately above or below the chosen cell for analysis.

Method

24 hours prior to experiment, 100 μl of 0.75% normal melting agarose (NMA) in PBS at approximately 50^{O}C was layered onto fully frosted microscope slides, covered with a coverslip and kept on ice for 1-2 minutes to allow the agarose to solidify. Coverslips were removed and slides were left to dry at room temperature. This layer of agarose is essential for the attachment of the second layer of low melting point agarose (LMA).

The following steps until the end of electrophoresis were performed under yellow light in order to minimise additional damage to DNA by radiation. Approximately 10 μl (10,000 cells) of freshly prepared single cell suspension was mixed with 75 μl of 0.75% LMA in PBS at 40^{O}C. The resultant cell suspension was quickly and gently vortex and layered onto the pre-coated slide. This second layered was spread using a coverslip and placed on an ice-cold surface to allow the agarose to solidify.

The coverslip was removed and slides were immersed in ice-cold lysis buffer at pH 10.0 for 3 hours at 4^{O}C to remove membranes and proteins. The lysis buffer contained 2.5 M NaCl, 100 mM EDTA, 10 mM Tris, pH 10 with 10% DMSO and 1% Triton X-100 added 1 hour before use at 4^{O}C. Following lysis, slides were placed on a horizontal gel electrophoresis unit filled with ice-cold alkaline buffer (10 M NaOH, 200 mM EDTA) for 30 minutes to allow unwinding of DNA and expression of alkali labile sites. Slides were subjected to electrophoresis at a field strength of 0.8 V/cm (20 V, 300 mA) for 20 minutes. Subsequently slides were carefully removed from electrophoresis buffer, rinsed with ice-cold Tris buffer (0.4M Tris, pH 7.5) to neutralise the excess alkali, dehydrated in ice-cold ethanol and allowed to dry at room temperature overnight.

4.2.6 Comet image acquisition and analysis

Each slide was stained with 50 µl ethidium bromide (20 mg/ml), covered with a coverslip and incubated for 2 minutes in the dark. Slides were examined under a fluorescence microscope (excitation filter 515-560 nm; barrier filter 590 nm) attached to a CCD video camera connected to a computer based image analysis software (Komet 3.0).

In each individual experiment, duplicate slides were examined. In each slide 50 nuclei were randomly captured, avoiding the edges of the slide and superimposed comets. The parameter used for damage quantification in this study is the Olive tail moment; defined as the product of the percentage of DNA in the tail and length of tail in µm [Olive et al., 1990].

As previously mentioned, the popularity of this assay is based on its ability to measure DNA damage in individual cells. For representation and accurate interpretation of the level of DNA damage in each sample analysed, a 2-D histogram for each treatment was graphed and fitted to the chi-square function (χ^2) described by Bauer et al, 1998, using the computer software Sigma Plot version 5.0. The χ^2-function was applied to our data for the following reasons:

- *Our comet data are asymmetrically distributed (due to low levels of damage).*
- *χ^2-function is more appropriate for fitting asymmetric distributions.*
- *Gaussian distribution assumes symmetry.*

Gaussian statistics were previously used to describe the distribution of tail moments [Speit G and Hartman A, 1995]. However, for distribution of tail moments in samples where damage levels are low, distributions are asymmetrical. Hence, mean tail moments are inadequate for assessing the statistical significance of low levels of DNA damage. Thus, we applied the χ^2-function described by Bauer et al [1998]. The equation below was used to calculate fits in a non–linear regression. The fits were superimposed with tail moment distributions.

χ^2-function equation:

$$\chi^2(x) = \frac{1}{2^{n/2} \cdot \Gamma\left(\frac{n}{2}\right)} \cdot (x)^{\frac{n}{2}} \cdot e^{-\frac{1}{2}x}$$

*where Γ is the gamma-function and **n** is the degree of freedom.*

Whereas the Gaussian distribution is described by the mean and standard deviation, the χ^2 distribution is described by the single parameter 'n' degrees of freedom, which is equivalent to the mean of Gaussian statistics. Importantly, the standard error is calculated during curve fitting and is a measure for the quality of fit to the data. Curves with a χ^2-function ≤ 2 (i.e. untreated samples) did not always correspond to the χ^2-fit, and thus the χ^2-function is not suitable. However, for ease of comparison, the χ^2-function was used to fit data obtained from untreated samples.

To test whether DNA damage observed between treated and untreated samples were statistically different, the non-parametric test, Wilcoxon-Mann-Whitney U test using the statistical computer program STATA, version 7.0 was applied. The Wilcoxon-Mann-Whitney U statistics, the non-parametric version of the t-test, was chosen because our data was not normally distributed. In summary, the test works by first ranking the data. In this case, the tail moments for treated and untreated samples are combined into one dataset (but distinguished) and ranked in ascending order. The rank of each score is recorded and when two or more scores are tied, all the tied scores are assigned the average number of the tied

scores. For example, if 3 scores are tied for position 3, 4,and 5, all would be assigned the rank of 4.

4.2.7 Cathepsin B Immunohistochemical staining

Method

On ice, tumours were carefully removed, weighed and washed twice in ice cold HBSS. Samples were kept moist in ice-cold HBSS and transported for frozen sections to be made. Tumour tissue was cut into 5μm thick sections onto PEG coated microscope slides at the London Royal Free Hospital and stored at –20°C.

Frozen sections were left at room temperature for 20 minutes followed by rehydration with PBS. Endogenous peroxidase activity was quenched by incubating with 0.2% H_2O_2 (v/v) in PBS for 10 minutes. Samples were incubated for 1 hour in 1.5% normal blocking serum in PBS, after which, serum was removed and sections were incubated with primary antibody (cathepsin B, sc-6493, Santa-Cruz) at a 1:10 dilution in blocking serum for an hour. Slides were then washed 3X with PBS and incubated for 30 minutes with biotin-conjugated secondary antibody. During this incubation step, or 30 minutes prior to use, the avidin-biotinylated HRP was prepared according to the manufacturers instructions. Sections were further incubated for 30 minutes with the HRP reagent prepared, prior to washing for 15 minutes with PBS. Following 3 changes of PBS washes, 5 minutes each, slides were incubated with DAB solution for 10 minutes. After rinsing in dH_2O for 5 minutes, tissue sections were counter stained for 10 second's with Gill's Haematoxylin, washed under running tap water for 2 minutes and dehydrated through 95% and 100% ethanol, 10 seconds each and finally in xylene for 2 minutes or until streaking stops. Slides were mounted whilst still wet in Histomount and viewed under a light microscope.

4.2.8 Haematoxylin and Eosin staining

Materials

Gill's haematoxylin

Eosin yellowish (1 g in 100 ml dH2O)

1% acid alcohol (99 ml 70% ethanol + 1 ml conc. HCL)

Scott's tap water 500 ml (10 g Sodium bicarbonate and 1.75 g Magnesium sulphate)

Frozen tumour sections were left out to equilibrate with room temperature, and placed in water for rehydration and incubated with haematoxylin for 5 minutes. Slides were washed in tap water and sections blued in Scott's tap water. After washing in tap water, slides were placed in 1% acid alcohol for 2 seconds, washed, and incubated in eosin for 5 minutes followed by a rinse in tap water, sections were dehydrated, cleared and mounted as previously described.

4.2.9 UV-C irradiation

Background

The genetic integrity of cells depends on DNA repair enzymes that detect, recognise and remove mutagenic lesions from DNA. UV radiation produces lesions in DNA that do not form breaks directly. However, these lesions are converted to breaks when the cell attempts to repair the damage. UV radiation produces base damage by a variety of mechanisms. These include 1) production of oxygen radicals resulting in oxidative damage and 2) generation of photoaddition products. Upon detection of damaged bases, the DNA nucleotide is flipped out of the base stack for recognition by enzymes of the base excision repair (BER) pathway. The BER enzymes are the main defence against major forms of DNA base damage. First, individual DNA glycosylases are targeted (recruited) to distinct base lesions followed by incision and rejoining to restore the correct DNA base sequence.

Method

Working under UV safe light, medium was removed from sub-confluent cells growing on a petri dish and washed twice with HBSS. Cells were then exposed to UVC (254 nm) at 8.8 J/s m^2 for 10-60 seconds. For UVC lesion to be converted to strand breaks, cells were incubated for 1 hour at 37^{O}C in fresh culture medium following irradiation. Samples were then subjected to electrophoresis as described above.

4.3 RESULTS

Although several polymer drug conjugates are currently in clinical trials, none has been characterised for their ability to induce DNA damage at the single cell level *in vitro* and *in vivo*. This is the first study to show that PK1, the first polymer drug conjugate to enter clinical trials, is able to induce DNA damage at the single cell level *in vivo*, but not *in vitro*. Thus, although we have established in previous chapters that PK1 is relatively non-toxic to cells growing *in vitro*, we wished to quantify any DNA damage that might be occurring. Additionally, it is known that intercalation of doxorubicin into DNA results in quenching of fluorescence, therefore the fact that we were unable to visualise doxorubicin fluorescence within the nuclei of cells examined, does not necessarily mean that intralysosomal release necessary for antitumour activity is absent.

4.3.1 Assessment of PK1-induced DNA damage in vitro

Although DNA damage is central to the mechanism of programmed cell death, it does not always result in cell death. Whether a cell undergoes apoptosis, or repair by firstly inducing growth arrest, depends on the level of damage sustained. Quantification of cytotoxicity as assessed by measurement of metabolic activity does not reflect the amount of DNA damage in a cell. If metabolic activity is used as a marker of cell viability, individual cells may be defined as viable even though they are committed to undergo programmed cell death at a later time.

HepG2, MCF-7 and B16F10 cells were incubated with 5 μM doxorubicin equivalent of PK1, the known equivalent of its free doxorubicin content, and the parent compound doxorubicin, for 24, 48 and 72 hours continuously. Following treatment, cells were subjected to the Comet assay as described in section 4.2.5. Shown in Figure 4.3 are histograms of frequency plotted against comet tail moments and fitted to the χ^2-function. As the level of DNA damage increased, a shift of the $\chi 2$-distribution to the right, towards higher Olive tail moment became apparent. Of the three time points investigated, DNA damage was induced by doxorubicin in all three cell lines and peaked at our earliest chosen time point of 24 hours. Using Wilcoxon-Mann-Whitney statistics, the damage observed with doxorubicin was significantly elevated in relation to untreated controls with all cell lines tested ($P<0.0001$). B16F10 cells were the most sensitive (degrees of freedom of 11.60), followed by MCF-7 cells (4.7) and HepG2 (2.7).

The levels of damage observed with PK1 and its equivalent free doxorubicin content, were very low, and not statistically different from each other or untreated controls.

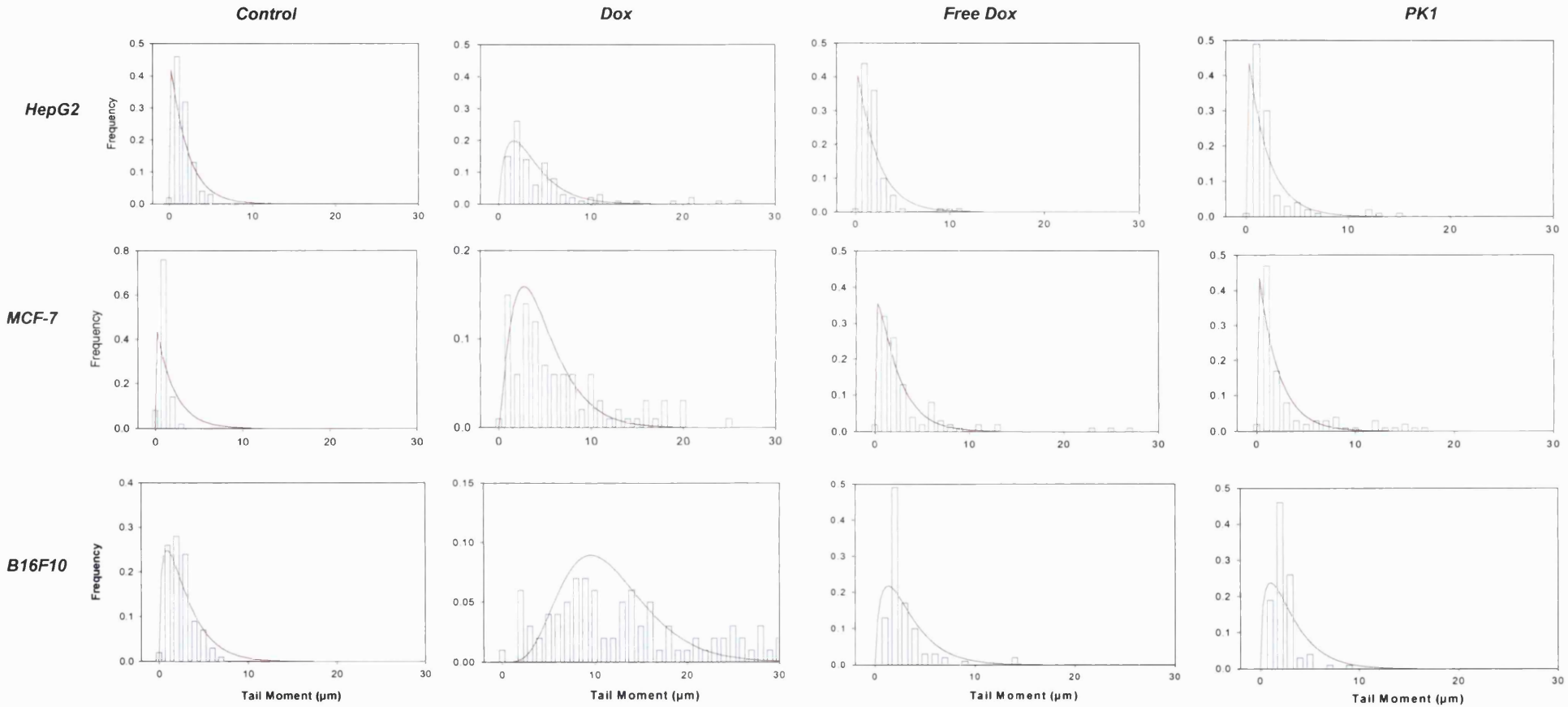

Figure 4.3 – Distribution of DNA strand breaks induced by treatment of cells growing in culture with doxorubicin and PK1. All three cell lines were grown to approximately 70% confluence before treatment with 5 µM doxorubicin, PK1 (doxorubicin equivalent) and doxorubicin 0.02% of dose (free unbound fraction) for 24 hours. All histograms are superimposed with the fitted curves calculated by the function of the χ^2-distribution.

Table 4.1 – Degrees of freedom '*n*' obtained following a 24 hour treatment of cancer cells growing *in vitro* with doxorubicin, PK1 and free doxorubicin.

	Control	*Dox*	*Free Dox*	*PK1*
HepG2	2.052	2.728	2.482	2.221
MCF-7	2.007	4.771	2.275	2.002
B16F10	2.924	11.60	3.321	3.041

Values are from data shown in Figure 4.3.

4.3.2 Assessment of PK1-induced DNA damage in vivo

Several studies have demonstrated an *in vivo* anticancer effect of polymer based doxorubicin conjugates in the murine B16F10 melanoma model [Duncan et al., 1992, Seymour et al., 1994 and 1995]. We have shown that PK1 is inert against tumour cells growing in culture as assessed by MTT reduction and DNA damage, when compared with the damage attributable to relative to the free doxorubicin present within the polymer preparation.

Table 4.2 - Degrees of freedom from χ^2-fit to Tail Moment Distributions and mean tumour weights following doxorubicin and PK1 treatment *in vivo*.

	Degrees of freedom (mean tumour weight in grams)		
Sampling Time (h)	**Saline**	**Doxorubicin**	**PK1**
5	3.26 (0.5)	3.42 (0.86)	3.10 (0.46)
24	2.70 (0.4)	3.91 (0.53)	3.76 (0.5)
48	3.27 (0.5)	3.80 (1.3)	4.01 (0.86)
72	3.17 (1.5)	4.10 (1.16)	4.10 (1.16)

Values are from data shown in Figure 4.4.

Mice bearing established s.c. tumours were treated with doxorubicin (7.5 mg/kg) and PK1 (15 mg/kg, doxorubicin equivalent) for various time schedules and the effects of treatment on DNA damage were investigated (Figure 4.4). At the earlier time points of 5 and 24 hours, doxorubicin induced more DNA damage than PK1. In contrast, after 48 hours of treatment, PK1 caused more DNA damage than doxorubicin. The degrees of

freedom obtained following χ^2-fit to the data were 3.8 and 4.01 for doxorubicin and PK1, respectively (Table 4.2 and Appendix 1.11 for P values). Moreover, after 72 hours of administration, both agents appeared equitoxic as evidenced by the exact χ^2-fit to data with degrees of freedom of 4.10 as shown in Table 4.2. Furthermore, the Tail Moment distributions and χ^2-fits induced by PK1and doxorubicin completely overlapped when superimposed. It is also important to note that the mean tumour weights, shown in brackets in Table 4.2 for doxorubicin and PK1 treatment groups were identical at 72 hours.

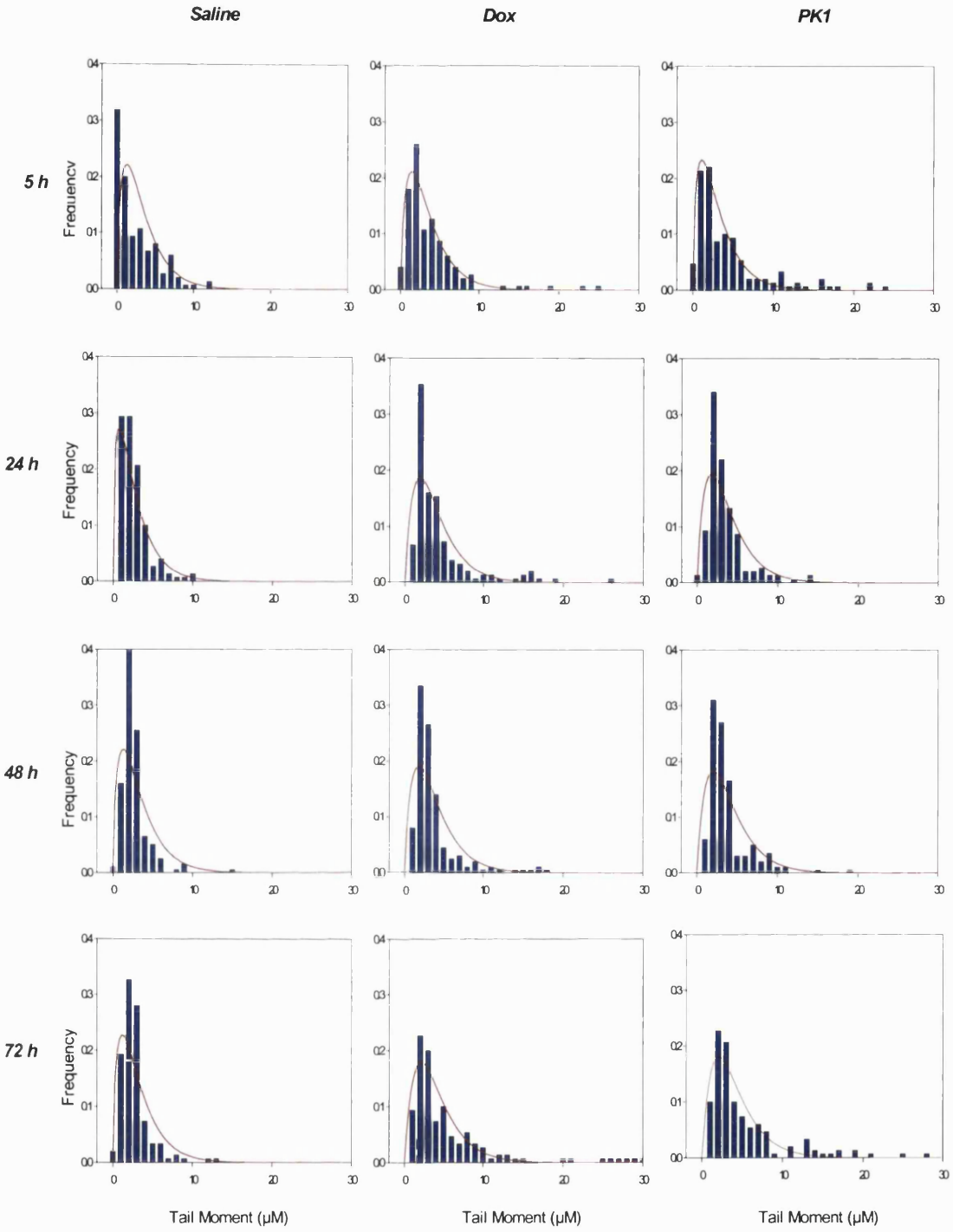

Figure 4.4 – Histograms showing the distributions of DNA strand breaks with time in tumour cells isolated from C57 mice given a single intravenous injection of doxorubicin (7.5 mg/kg), PK1 (15 mg/kg, doxorubicin equivalent) or 0.9% saline. Data represents quantitative frequency distributions superimposed with curve fit calculated with χ2-function (red line). Each histogram contains 300 analysed cells from two independent experiments. (Animal and tumour weights per treatment group are listed in Appendix 4.1 and 4.2).

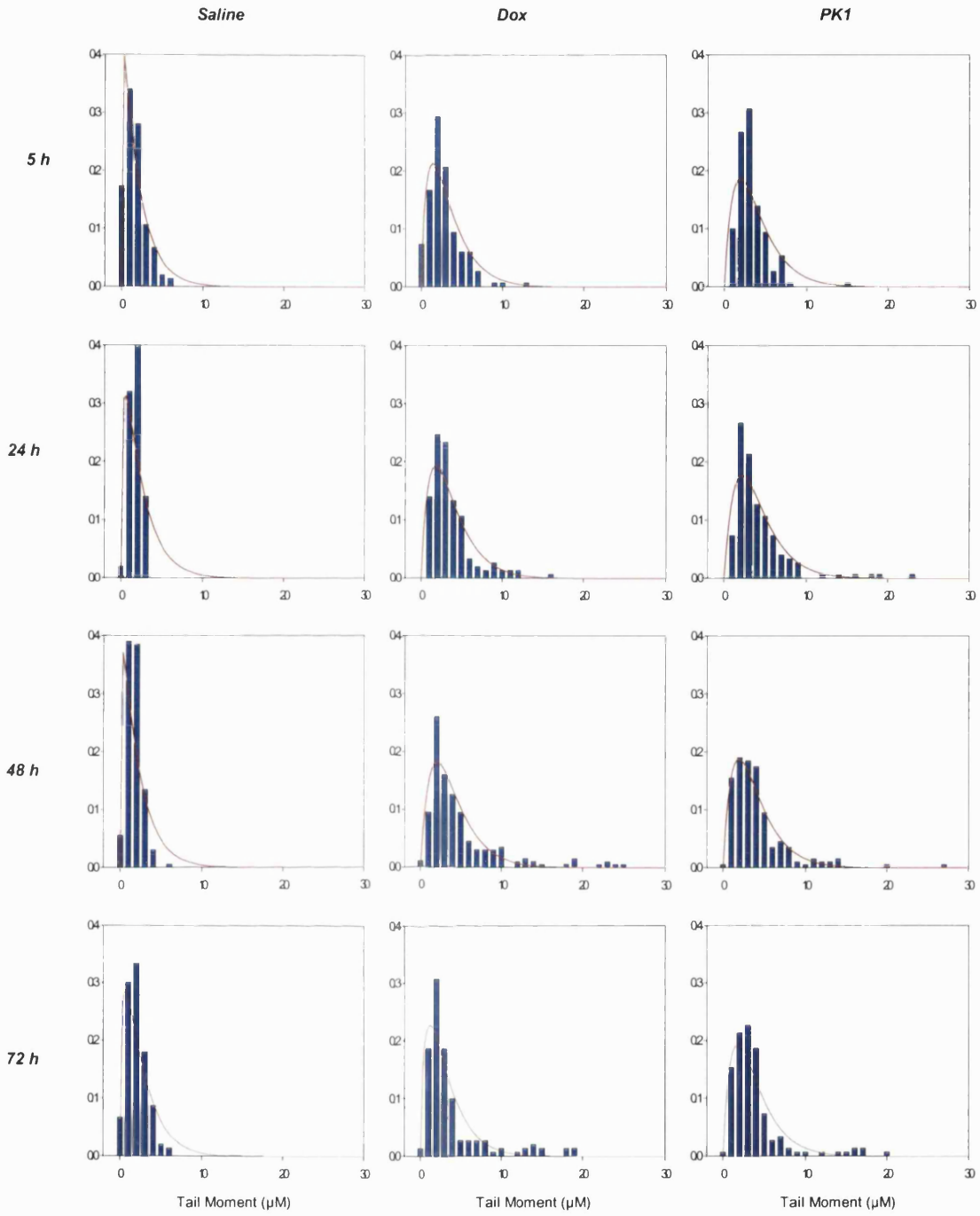

Figure 4.5 – Distribution of DNA strand breaks with time in bone marrow isolated cells from C57 mice given a single intravenous injection of doxorubicin (7.5 mg/kg), PK1 (15 mg/kg, doxorubicin equivalent) or 0.9% saline. Data represents quantitative frequency distributions superimposed with curve fit calculated with χ^2-function (red line). Each histogram contains 300 analysed cells from two independent experiments.

Bone marrow suppression is a well recognised effect following treatment with anticancer agents in general. Therefore, to probe whether there was a reduction of systemic drug toxicity of PK1 compared to doxorubicin, bone marrow samples were isolated after each dosing schedule, and these were assessed for DNA damage, in parallel with the tumour samples. As shown in Figure 4.5, both PK1 and doxorubicin induced DNA damage in bone marrow cells, however DNA damage at this concentration of PK1 was significantly greater ($P<0.0001$) than that seen for 7.5 mg/kg doxorubicin after 48 hours (Table 4.3 and Appendix 1.11).

Table 4.3 – Toxicity of doxorubicin and PK1 to bone marrow as assessed by induction of DNA damage.

	Degrees of freedom		
Sampling Time (h)	**Saline**	**Doxorubicin**	**PK1**
5	2.11	3.40	3.93
24	2.44	3.77	4.17
48	2.22	4.02	3.89
72	2.61	3.18	3.76

Values are degrees of freedom obtained from χ^2-fit to Tail Moment distributions from Figure 4.5.

4.3.3 Immunohistochemical staining for Cathepsin B in subcutaneous murine melanoma

As described previously, we have clearly demonstrated that PK1 induces DNA damage *in vivo,* but not *in vitro*. One factor that may modulate the efficacy of PK1 is variability in the expression and regulation of cathepsin B activity. Thus, it is of utmost importance to characterize cathepsin B expression in the B16F10 melanoma tumour model. It is hoped that this will lead to a better understanding of the anticancer mechanism of PK1.

Male C57 mice, at 6-7 weeks of age, were injected s.c. with $1x10^5$ viable B16F10 cells (as assessed by trypan blue exclusion) in 0.9% saline. After 9-10 days, when tumours were palpable, immunohistochemical studies were undertaken subsequent to sectioning. Figure 4.6 shows the subcellular localisation of cathepsin B in the B16F10 murine melanoma. Cathepsin B staining was mainly localised to the cytoplasm and cell surface.

We also observed an increase in cathepsin B staining with increasing tumour mass, as evidenced by the increase in staining intensity as tumour mass increased from 0.3g to approximately 1g. In agreement with several studies on tumour angiogenesis, we observed tumour angiogenesis (blood vessel formation) as tumour mass increased. Moreover, vessel formation was not observed in sections of tumours that had a mass less than or equal to 0.5g.

Figure 4.7 shows staining for cathepsin B at a higher magnification. Samples are tumour cells grown *in vivo* and cultured B16F10 cells. From the images shown, it appears that the cells undergo some form of morphological transformation when grown *in vivo*. In addition, and, bearing in mind that the antibody concentration and other reagents used for localisation remained unchanged for both *in vivo* and *in vitro* staining, cathepsin B expression appeared to be upregulated *in vivo*.

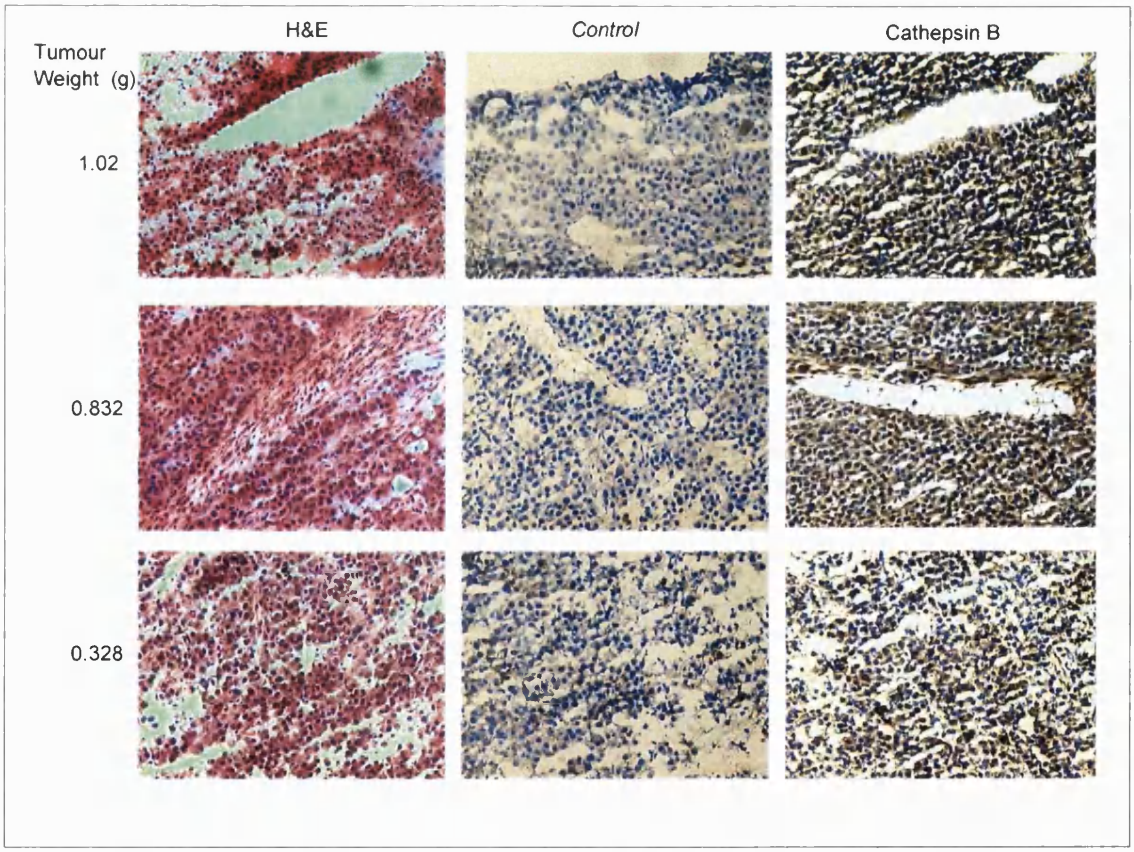

Figure 4.6 – Immunohistochemical localisation of intracellular cathepsin B in various sizes of B16F10 melanoma. Viable B16F10 cells were injected s.c. following the protocol described in section 4.2.7. A commercially available kit was used with an anti-cathepsin B antibody raised against the 27 KDa mature form of the enzyme. Slides are representatives of 2 independent experiments. Magnification = X100.

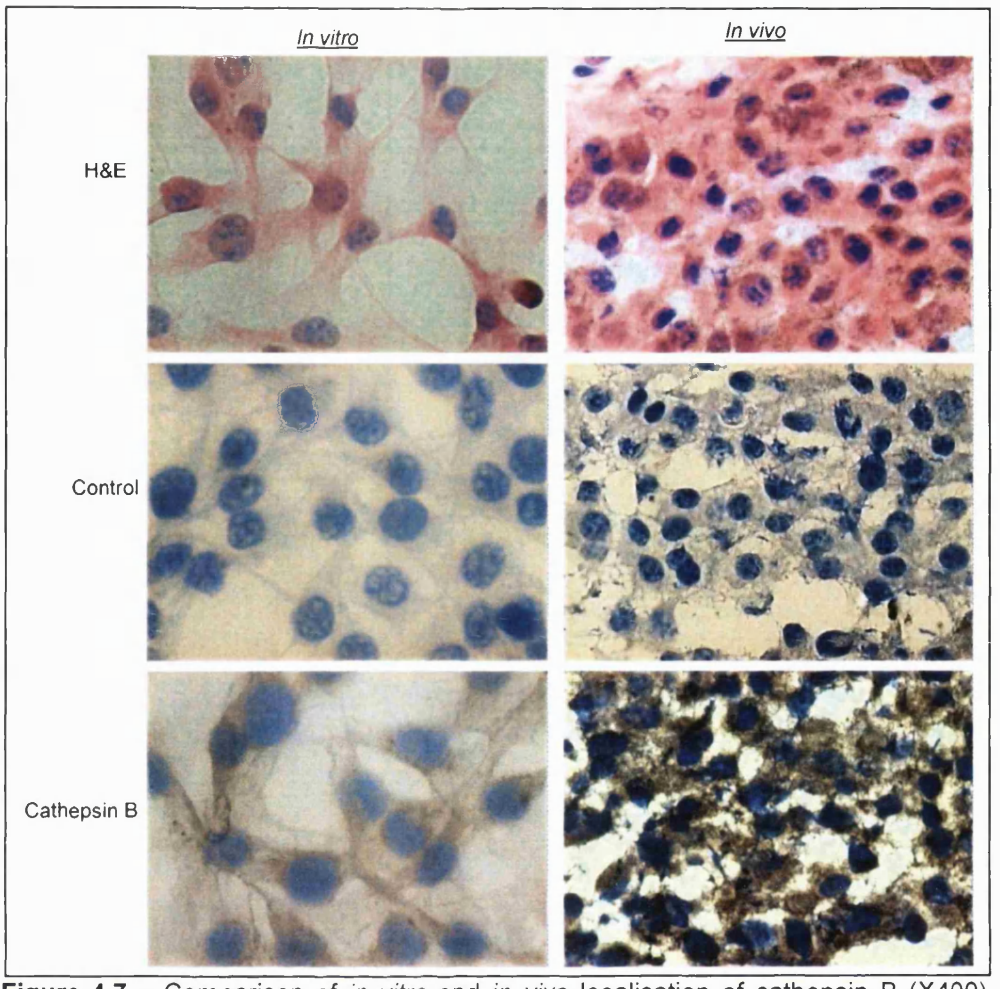

Figure 4.7 – Comparison of *in vitro* and *in vivo* localisation of cathepsin B (X400). Sections show H&E staining, negative control (secondary antibody only) and cathepsin B as labelled. Cathepsin B staining is relatively intense in B16F10 cells *in vivo*.

4.3.4 Differential sensitivity of B16F10 cells to UV-C in vivo and in vitro

To probe whether there are differences between B16F10 cells growing *in vitro* and in *vivo,* freshly isolated tumour cells and cells grown in culture were irradiated with UV-C at 8.8 J/s m^2 for 60 seconds followed by incubation for 1 hour to allow DNA repair to take place. Figure 4.8 shows the distribution of Olive tail moment and χ^2-fit to data obtained from B16F10 cells *in vivo* and *in vitro*. Cells grown *in vivo* were almost 3 times more sensitive to UV induced DNA damage in comparison to those grown in culture with degrees of freedom of 42.63 and 16 respectively.

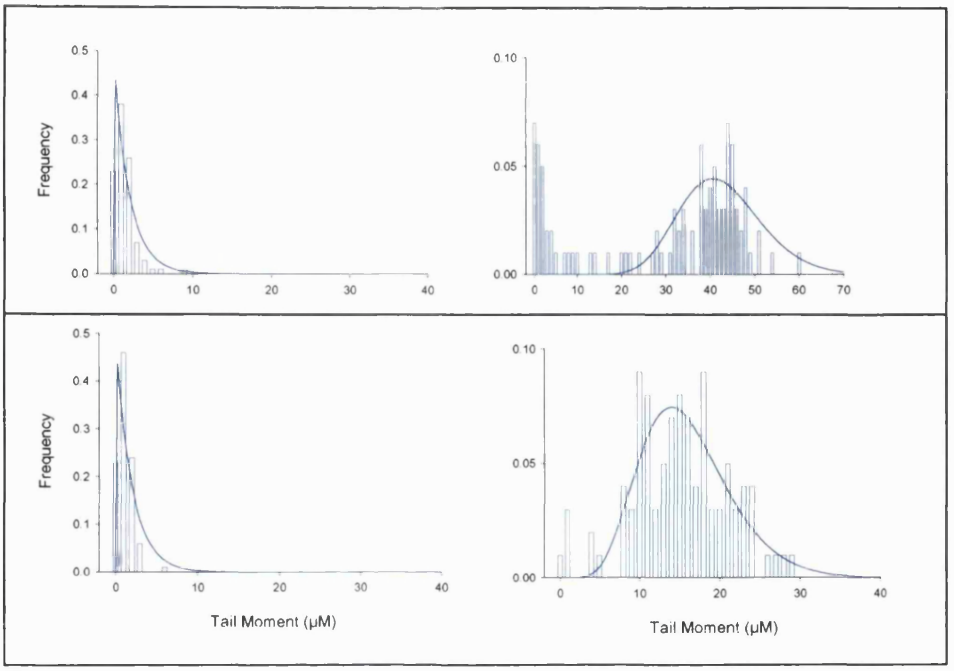

Figure 4.8 - Distribution of UV-C-induced DNA strand breaks in freshly isolated B16F10 cells from C57 B mice (top panel) and cultured (bottom panel). Left-hand side panels are controls and right are UV-C treated. Cells were irradiated with UV-C (254 nm) for 60 seconds and resuspended in fresh culture medium and incubated for an hour at 37^{O}C before assaying for DNA damage. Histograms are from two independent experiments superimposed with the χ^2- distribution fits.

For ease of comparison, the two chi fits have been plotted to overlap in Figure 4.9. The increased sensitivity of B16F10 cells growing in vivo, could be due to increased metabolism, as cells are in their natural environment. Thus the rate of DNA repair will be greater and therefore more strand breaks will be produced as cells attempt to repair. Additionally, solid tumours contain heterogeneous cell types including, macrophages, lymphocytes and stromal cells. Therefore, although, the majority of isolated cells will be that of the tumour. These cells from non-cancerous origin will contribute to the sensitivity of UV treatment depending on their type and other characteristics including the rate of metabolic activity.

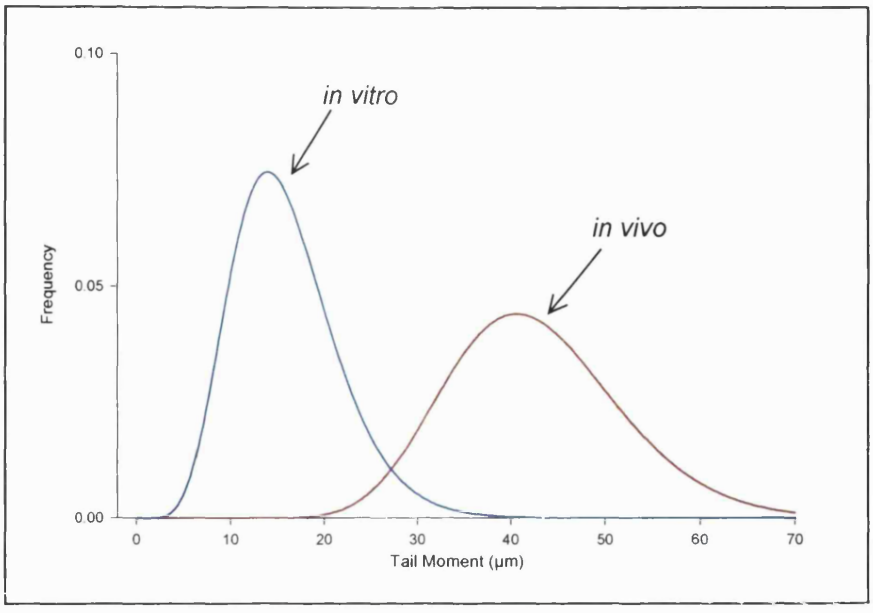

Figure 4.9 – Comparison of UV-C treated B16F10 cells in vitro and in vivo. χ^2-fits are those from tail moment distribution from Figure 4.8.

4.4 DISCUSSION

This chapter describes investigations into the susceptibility of cells to undergo DNA damage following treatment with PK1 or doxorubicin, both *in vitro* and *in vivo*. The results obtained should contribute to our understanding of the mechanisms that mediate cytotoxicity of PK1, and clarify how the pharmacological efficacy of PK1 differs from doxorubicin, both *in vitro* and *in vivo*.

Our results show that PK1 is able to induce DNA damage *in vivo* but not *in vitro*. B16F10 cells grown in culture and exposed to doxorubicin for 24 hours were more sensitive than MCF-7 cells, which were in turn more sensitive than HepG2 cells (Table 4.1). However, it is interesting that the levels of damage for all three cell lines were relatively low, when compared to DNA damage induced by shorter exposure times at equivalent concentrations of doxorubicin. In Chapter 3, we demonstrated that following treatment with PK1 for 120 hours, HepG2 cells were least sensitive, followed by MCF-7 cells, with B16F10s being the most sensitive. Thus, the observed induction of strand breaks is in line with the trends for cytotoxicity. Importantly however, the sensitivity of cultured cells to doxorubicin did not correlate with the amount of cathepsin B activity, since the

least sensitive HepG2 cells expressed the highest level of cathepsin B, and the highly sensitive B16F10 cells expressed the lowest levels (see Chapter 3).

DNA damage observed in B16F10 cells following treatment with PK1 for 24 hours was attributed entirely to the 0.02% of unbound doxorubicin present in the PK1 preparation (Fdox); levels of damage determined in all three cell lines were not statistically different from treatment with Fdox. Studies by Kopecek and his group have demonstrated cytotoxicity of the conjugate *in vitro* against a variety of human cell lines, but these results did not take into account the possible contribution of unbound doxorubicin.

Thus, *in vitro* PK1 is inert, as speculated by Ruth Duncan [Duncan 1992]. However, since PK1 has been shown to possess anticancer effect *in vivo*, we investigated the DNA damaging potential of the conjugate in mice bearing a well established and highly metastatic subcutaneous B16F10 melanoma. Results obtained demonstrated that PK1 does indeed induce significant DNA damage *in vivo,* as does doxorubicin. However, there are differences in the kinetics of DNA damage induction.

The quantity of damage induced by doxorubicin and PK1 peaked at our earliest time point, and then fell markedly over several days, whereas the level of DNA damage induced by PK1 decreased far more gradually. However, if doses are compared directly, the amount of PK1-induced DNA damage was significantly lower than that induced by doxorubicin. This could also explain the prolonged effect on DNA damage (see Figure 4.10).

Because bone marrow suppression is a major side effect of cancer chemotherapy, the toxicity of PK1 on bone marrow cells was evaluated, using DNA damage as a marker for cell toxicity. Due to a lack of time we were unable to assess the levels of DNA damage induced in other organs such as liver, kidney and most importantly the heart. The rationale for conjugating doxorubicin to the HPMA backbone was to reduce toxicity to major organs [ref]. Anthracyclines in general are amongst the most effective chemotherapeutic agents, but are limited by their myelosuppressive and cardiotoxic side effects, which are mediated mainly by free radical damage to cellular membranes.

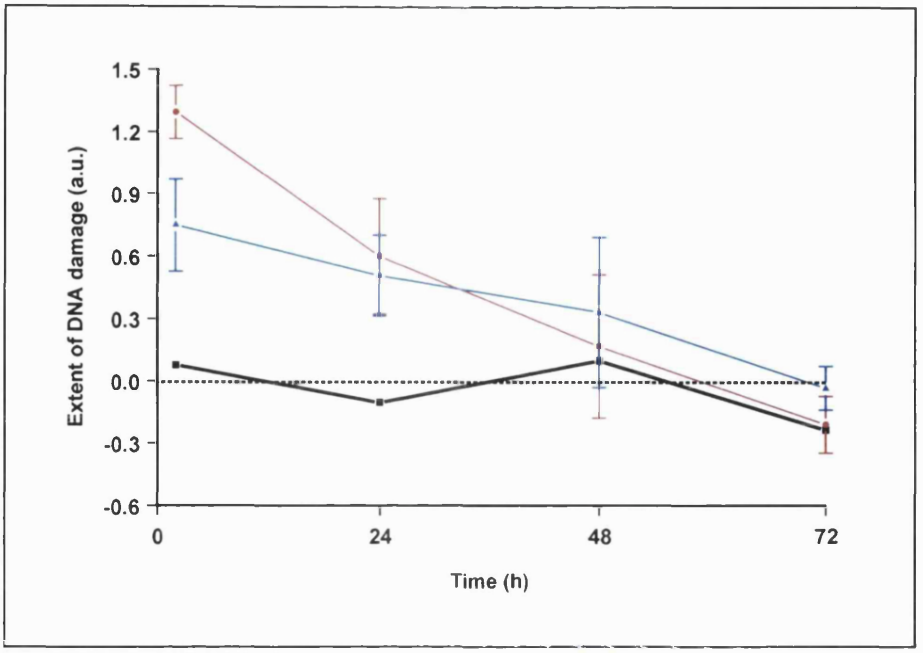

Figure 4.10 – Extent of DNA damage induced by doxorubicin (red line, 7.5 mg/kg) and PK1 (blue line, 15 mg/kg doxorubicin equivalent) in relation to saline (0.9%, black line) *in vivo*. Data points shown were obtained by subtracting the mean '*n*' value from χ^2- fit of tail moment distributions for saline treated mice from that obtained for doxorubicin and PK1 at the various sampling times. Data represents mean ±SEM from two independent experiments.

If indeed PK1 suffers cleavage inside cells and not outside, then DNA breaks should not be induced in cells of bone marrow origin. However, DNA strand breaks were observed in bone marrow cells from as early as 5 hours and were not significantly different from that in control animals treated with parent drug doxorubicin. Thus, doxorubicin is being released into circulation and not solely within tumour cells, a major problem that conjugation was designed to minimise.

It is also important to note that background levels of damage (in untreated mice bearing tumours) were higher in the tumours than in marrow cells. This could be due to DNA damage in necrotic cells that are often found within the core of tumours, where there is lack of oxygen and increased interstitial pressure. The damage induced by PK1 *in vivo* and *in vitro* formed comets with mainly smaller structures with large heads and narrow tails of varying lengths. Therefore, mechanism of PK1 induced cell death unlikely to be via apoptosis, as apoptotic cells tend to have large fan-like tails and small pin-like heads. Hence, the comet assay can be used to distinguish apoptotic from non-apoptotic cells.

An expert panel on the use of the comet assay decided in 1999 that the concept of tail moment as a parameter for measurement of DNA damage eliminates potentially useful information on tail length and percentage DNA in the tail. As such, they advised that when using tail moment as a parameter for DNA damage, data on tail length or percentage of migrated DNA in the tail should also be provided. Shown in appendix 1.12 and 1.13 are data on percentage tail DNA for tumour and bone marrow cells.

Taken together, our results confirm that PK1 is active *in vivo* but not *in vitro*. However, if the proposed mechanism of action, whereby doxorubicin is released from PK1 in the lysosomes is valid, DNA damage should be apparent *in vitro*. Having demonstrated that cells possess cathepsin B activity, essential for intralysosomal release, the inability to observe DNA damage with established pinocytic capture can only mean that the linker is not being cleaved, or if it is, that released doxorubicin cannot escape from the lysosome. It is known that not all molecules can diffuse in and out of lysosomes. In addition, we speculate that the cytotoxic effects of PK1 *in vivo* are not mediated by intralysosomal release of doxorubicin, but are due to extracellular cleavage of doxorubicin by cathepsin B, which is known to be present on the cell membranes of metastatic tumours. Studies by Seymour et al., [1994] and Steyger et al. [996] show localisation of HPMA-FITC and dextran-FITC confined to mainly to peripheral regions. This may account for the reported efficacy of PK1 during phase I trials against metastatic tumours [Vasey et al, 1999]. Also worth mentioning is that aggressive tumours are known to have increased protease activity.

Cathepsin B was highly expressed in tumour sections, and expression increased with increasing tumour weight up to approximately 1g. Cathepsin B activity in B16 melanoma variants have been shown to be at its highest in tumours weighing less than 1g [Sloane et al, 1982]. In addition, Duncan and Sat [1998] also using the B16F10 tumour model show the dependence of tumour size on the localisation of PK1 following administration. In agreement with Steyger et al [1996] is our observation of increased blood vessel formation at the tumour periphery with tumour size as shown in Figure 4.11.

In summary, although the addition of PK1 to cells growing in culture is followed by some cell death, this effect can be fully attributed to the presence of free doxorubicin present in the PK1 preparation. Moreover there is no correlation between the sensitivity of different cell lines to the PK1 preparation and the levels of cathepsin B expressed by these cells.

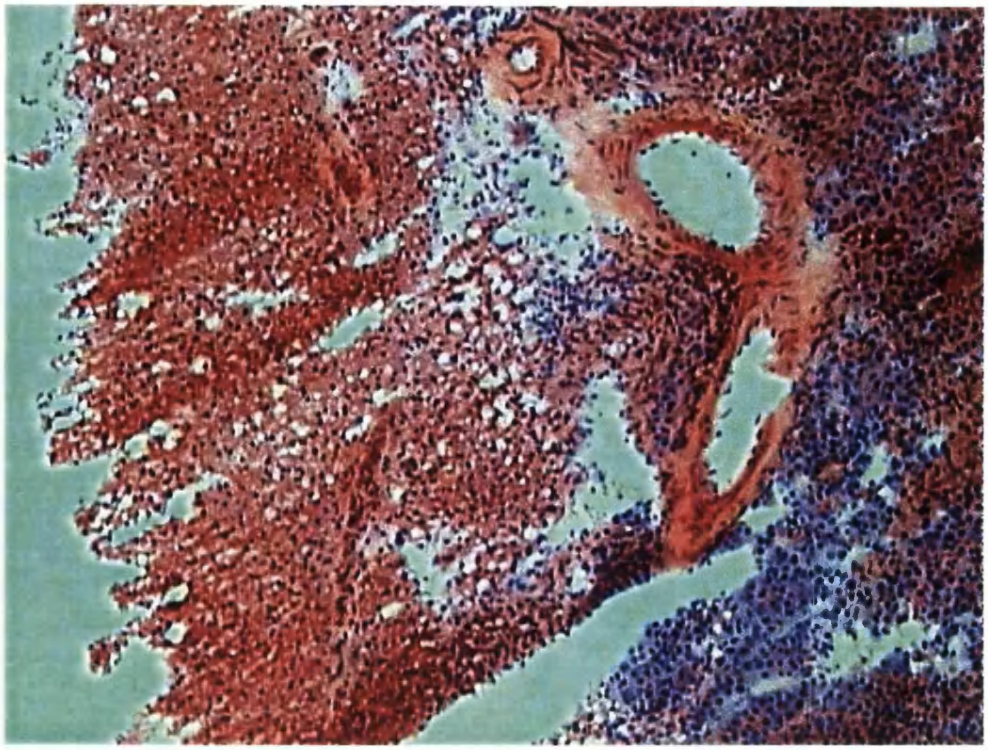

Figure 4.11 – An H&E staining of B16F10 tumour (1.02g) section. Frozen sections were left out to equilibrate with room temperature before staining with haematoxylin for 5 minutes. Slides were washed in tap water and blued in Scott's tap water as described in section 4.2.8. Image shown is a typical observation of increased blood vessel formation at the tumour periphery in all samples.

PK1 itself has no cytotoxic activity on cells growing *in vitro*, even though it rapidly enters these cells, and some of these cells express high levels of cathepsin B activity. The subcellular distribution of internalised PK1 is consistent with sequestration in the lysosomes, but release of doxorubicin (as assessed by release of fluorescence) from the lysosomes is not detectable, even after prolonged incubation. However, PK1 is cytotoxic to cells growing in culture if it is incubated with cathepsin B prior to incubation with the cells, thus demonstrating that cathepsin B will release the doxorubicin.

In contrast, PK1 does have an antitumour effect in mice, but it also causes significant damage to the DNA in bone marrow cells. The rapidity and magnitude of this effect suggests that a substantial release of doxorubicin from PK1 occurs extracellularly, and the released doxorubicin is free to enter the blood circulation.

In light of these results and other reported PK1 studies, as referred to above, we propose that the pharmacokinetics of PK1, and the release of doxorubicin from PK1, depend upon cathepsin B activity on the tumour periphery, and possibly upon increased vascular permeability of tumours. We suggest that intralysosomal, or indeed intracellular,

release of doxorubicin from PK1 does not significantly contribute to tumour toxicity, even though this proposition was the basis for the original design of the drug.

CHAPTER 5 - GENERAL DISCUSSION AND CONCLUSIONS

The use of polymeric delivery vehicles for established anticancer drugs is intended to improve efficacy by increasing bioavailability to target cells. The most exploited carrier for polymeric delivery systems to date is the synthetic non-immunogenic vinyl polymer, HPMA, originally developed as a plasma expander. PK1 is the first HPMA conjugate to be clinically evaluated. It has been shown to possess antitumour activity in pre-clinical and clinical settings [Vasey et al 1999, Duncan et al 1998, Duncan et al 1992] and is currently in phase II testing. Given its advanced status of clinical development, it is surprising that mode of action and toxicological profile of PK1 are relatively poorly understood.

This thesis was intended to make a contribution to improving our understanding of PK1 action at the cellular and physiological levels. The starting point of our investigations was to evaluate the cytotoxicity of PK1 to target cells *in vitro*. A number of reports suggested that PK1 is toxic *in vitro* against the human ovarian carcinoma cell line, A 2780 [Minko et al 1998, Omelyanenko et al 1998, Demoy et al 2000]. However, none of these studies have made any attempts to delineate between cytotoxicity induced by PK1 and cytotoxic effects resulting from the free, unconjugated fraction of doxorubicin that is present in the polymer preparation. This is somewhat surprising, since already in 1991, Wedge showed that the cytotoxicity of PK1 could almost entirely be attributed to the free, unbound doxorubicin, when PK1 was added to HepG2 cells, or the murine leukaemia cell line L1210. To measure cytotoxicity, the MTT assay was used, and treatment times did not exceed 72 hours. Hence, there was the possibility that a genuine contribution of the polymer conjugate to the overall cytotoxicity was obscured because of possible delayed kinetics of uptake and cleavage leading to release of doxorubicin. The present thesis has filled this gap by extending the duration of exposure to PK1 in cytotoxicity studies well beyond 72 hours (Chapter 2). It was found that even after 10 days of treatment the contribution of PK1 to the overall observed cytotoxicity was minimal. The effects could be explained largely in terms of the toxicity of the fraction of unbound, free doxorubicin present in the polymer preparations.

Stability data is not in the public domain, however in appendix 4.6 data on the analytical chemistry of the conjugate is provided by Pharmacia. In addition, if the PK1 was

unstable under the storage conditions and doxorubicin becomes unbound, increased cell toxicity would be apparent.

These observations raised questions as to the uptake and intracellular fate of PK1 *in vitro*. Although contradicting the proposed pinocyctosis/intra-lysosomal cleavage and –release model, it was conceivable that the minimal cytotoxicity of PK1 was due to poor uptake of the polymer in all 4 cell lines used in the present studies. The data presented in Chapter 3 rule out this possibility. Similar to the results obtained in experiments with free doxorubicin, uptake of the polymer conjugate could be observed as early as after 30 minutes of incubation in all cell lines. Pinocytosis is a constitutively active process, and early uptake is therefore not surprising. The pattern of distribution that we observed was consistent with lysosomal localisation in MCF-7 cells, and was similar in DU-145, B16F10 and HepG2 cell lines (data not shown).

If insufficient uptake was not the factor limiting PK1 cytotoxicity, there could have been problems with the intracellular release of doxorubicin from the polymer conjugate due to absent (or low) activity of cathepsin B.

Studies by Uchegbu et al [1996], have shown that doxorubicin polymer conjugates form temperature dependent micelles in solution. This micelle formation could prevent cathepsin B reaching its substrate (Gly-Phe-Leu-Gly), which is necessary for PK1 activity. Furthermore, the natural fluorescence of doxorubicin due to its quinone moiety is often quenched below a certain concentration until a saturation point is reached. Thus, if a relatively low concentration of doxorubicin (<1 μM) was present after cleavage from HPMA, fluorescence would not be evident in the cell nucleus.

For the first time, we have investigated the cathepsin B levels in cell lines in which PK1 cytotoxicity was assessed. The data presented in Chapter 3 show clearly that all cell lines used for cytotoxicity assessment were able to express bioactive cathepsin B, albeit to differing degrees. On the basis of the intra-lysosomal cleavage and –release hypothesis of PK1 action one would expect that PK1 cytotoxicity should increase with rising intracellular levels of cathepsin B. Enhanced activities of the enzyme should lead to larger amounts of doxorubicin being released, resulting in elevated cytotoxicity. Contrary to this expectation, there was no relationship between cathepsin B activity and PK1 cytotoxicity. Even with a cell line that exhibited very high cathepsin B levels, such as the HepG2 line, there were no differences between overall cytotoxicity and the effects attributable to the free, unbound doxorubicin present in the system. Thus, it seems hard to invoke a lack of cathepsin B to explain the absence of a contribution of PK1 to overall cytotoxicity in the

four cell lines tested here. This is further substantiated by our observation of significant increases in cytotoxicity upon pre-incubation of PK1 with cathepsin B. In the right circumstances, the enzyme is well able to release free drug from the polymer conjugate.

In an attempt to further probe the intracellular fate of PK1 after uptake, we carried out studies of DNA strand break induction due to doxorubicin's well-known ability to inhibit topoisomerase II. Here, we made use of the most sensitive assay currently available, the Comet assay (Chapter 4). These studies were also intended to deal with some of the ambiguities in interpretation that were left with the experiments carried out so far:

Thus, on the basis of the uptake studies which made use of the inherent fluorescence of PK1, we could not entirely discount the possibility that small amounts of doxorubicin could have been cleaved off the polymer and reached the cell nucleus. It was therefore essential to employ a very sensitive measure of possible biological activity of PK1. We speculated that doxorubicin escaping from the polymer conjugate by proteolytic cleavage should induce higher levels of DNA damage than would be expected considering the amount of free doxorubicin in the preparation. The results shown in Chapter 4 demonstrate that this was not the case. PK1 failed to induce DNA damage over and above the levels anticipated to occur by the free, unbound amounts of doxorubicin. Similar to the results obtained with our cytotoxicity studies, there was no apparent relationship between the sensitivity of the cell lines and their intracellular cathepsin B levels.

These observations and results force two possible conclusions: (1) PK1, although able to reach the inside of cells, cannot be taken up by lysosomes, and consequently, doxorubicin is not released in its free, active form to cause DNA damage and subsequent cell death. Although we cannot conclusively rule out this possibility, the strong fluorescence we observed in perinuclear structures of cells suggests that PK1 has indeed successfully entered lysosomes. (2) Thus, it appears more likely that PK1 can be taken up by lysosomes during pinocytosis, where it suffers proteolytic cleavage by cathepsin B. However, doxorubicin may not be able to cross the lysosome membrane, enter the cytosol and diffuse into the nucleus to cause DNA damage. Instead, it may remain trapped inside the lysosomes.

It is clear that further studies are required to clearly delineate between these two possibilities. However, in the light of considerations of the properties of lysosomal membranes, we favour the latter conclusion.

A detailed review by Lloyd [2001] on the implications of lysosomal membrane permeability for drug delivery systems explains the physiological role of the lysosome and

how efflux of intralysosomal products is affected by the chemistry of the molecules involved.

The lysosomal membrane is thought to have specific substrate porters for varying metabolites for efflux of products from catabolism. However, the membrane is said to be impermeable to certain molecules such as glucose. Evidence supporting the impermeabilty of the lysosome membrane is in lysosomal storage diseases, for example cystinosis, where cystine accumulates in the lysosome due to a defect in the lysosome membrane porter. Also, in type II glycogen storage disease, lysosomal alpha-glucosidase responsible for the degradation of glycogen is defective. Hence, the inability of molecules to cross the lysosomal membrane results in their excessive accumulation within lysosomes, leading to gross tissue damage. This can impair the function of major organs.

The permeability of lysosomal membrane to molecules for which there are no specific transporters is thought to be dependent on the so-called 'notional hydrogen-bonding capacity' of molecules [Stein 1967, Diamond and Wright 1969, Piqueras et al. 1994, Andrew et al. 1997 and reviewed by Lloyd, 2000]. This property is an inverse correlate of the oil-water partition coefficient of a substance. It is based on the number of functional groups on a molecule capable of hydrogen bonding. On a theoretical basis, following analysis of published data that showed an inverse correlation between permeance of the lysosome and the notional hydrogen-bonding capacity, an aliphatic hydroxy moiety has a hydrogen bonding capacity of 2, because it is able to donate and receive a hydrogen bond. Thus compounds with n hydroxy moiety would have a hydrogen bonding capacity of $2n$ [Lloyd 2000]. Shown in Table 5.1 is a list of some functional groups and molecules with their hydrogen-bonding capacity and the rate at which they permeate the lysosomal membrane. Molecules with notional hydrogen-bonding capacity less than or equal to 7.5 were found to rapidly cross the membrane, those with values between 7.5 and 11 also crossed the membrane but at a much slower rate. Molecules with values of 11.5 to 18 crossed the membrane but at a relatively slow rate, but those with a notional hydrogen-bonding capacity greater than 18 such as sucrose were non-permeant.

As shown on Table 5.1, Lloyd calculated a notional hydrogen-bonding capacity of 14.4 for doxorubicin. Functional groups in the chemical structure with potential hydrogen bonding capacities are: aliphatic hydroxy: 3, primary amine: 1, phenolic hydroxy: 2 and ether/hemiacetyl: 3.

Table 5.1 - Notional-hydrogen bonding capacity of some functional groups and molecules. Permeability of amines decreases when hydrogen-bonding groups are present.

Functional group/molecule	Hydrogen–bonding capacity	Ability to cross the lysosome membrane
C-OH	2.0	Very rapid
C-O-C	0.8	Very rapid
$C \cdot NH_2$	2.0 when uncharged	Very rapid
C—N—C | C	1.0 when uncharged	Very rapid
Charged Nitrogen	11	Rapid to slow
Charged carboxylate	11	Rapid to slow
Polyethyleneglycoi	4	Very rapid
Doxorubicin	14.4	Slow to very slow
Sucrose	18.4	Essentially non permeant

Modified from Lloyd 2000.

Therefore, based on the concept of hydrogen-bonding, doxorubicin's permeability would be predicted to be extremely low in its uncharged form, even if the conjugate is successfully cleaved by cathepsin B within the lysosome. However, should it become protonated, doxorubicin would be unable to traverse the lysosomal membrane.

Taken together, our results indicate that the proposed mechanism for PK1 action at the cellular level is inaccurate. It appears that the idea of intra-lysosomal cleavage of the conjugate is not tenable. Instead, we propose that the documented efficacy of the polymer conjugate *in vivo* may be due to **extracellular** cleavage. This is in line with the fact that PK1 is only efficacious against metastatic tumours [Vasey et al., 1999]. As a consequence of altered trafficking of the protease during tumourogenesis , metastatic tumours have high levels of cathepsin B on the tumour periphery.

Studies by Steyger et al. [1996] showed accumulation of FITC-dextran in s.c. B16F10 murine melanomas 10 minutes following i.v. injection in the vascularised host/tumour interface within intratumoral blood vessels. After 1 hour, a heterogeneous pattern of fluorescence was observed throughout the tumour. However, 24 hours after administration, the majority of fluorescence was relocated to the tumour side of the

administration, the majority of fluorescence was relocated to the tumour side of the tumour/host interface where further movement was observed to be hindered by the presence of the fibrous layer.

Further studies performed by Seymour et al [1994] using the same B16F10 tumour model also showed accumulation of HPMA-FITC fluorescence in the peripheral fibrous stroma of the tumour after ten minutes of administration with the highest fluorescence intensity occurring near major blood vessels on the tumour/host interface. After 72 hours of administration, the observed fluorescence was mainly confined to the peripheral fibrous stromal regions with little or no fluorescence in the interstitium. Thus, our observation of DNA damage as early as 5 hours could be indicative of extracellular cleavage of PK1, with subsequent intercalation into tumour cell DNA. Accordingly, assessment of DNA damage in cells isolated from the tumour periphery would be expected to have sustained more damage in comparison to those isolated within the tumour. It is important to note that the region where HPMA-FITC was confined paralleled cathepsin B staining observed following immunolocalisation [Sloane et al, 1986 and Sameni et al, 1995]. Therefore future experiments that investigate the distribution of PK1 fluorescence in individual tumours will be useful to compare with the observed distribution *in vitro*. This would tell us whether the efficacy of PK1 *in vivo* is due to intralysosomal or extracellular release.

In addition, extracellular cleavage of PK1 near major blood vessels is likely to cause systemic release of free doxorubicin, consistent with our observation of DNA damage to bone marrow cells, which paralleled that of free doxorubicin.

Thus, in conclusion, we propose extracellular cleavage of PK1 by proteolytic enzymes present in tumours as the mechanism by which the conjugate exerts its action *in vivo*.

REFERENCES

Adams D.J. (1989). In vitro pharmocodynamic assay for cancer drug development: application to Crisnatol, a new DNA intercalator. *Cancer Res.* **49**: 6615-6620.

Agarwal, M.L, Taylor, W.R, Chernov, M.V, Chernova, O.B, and Stark, G.R. (1998). The p53 Network. *J. Biochem. Criticism* **273**: 1, 1-4

Agarwal, S.K. (1993). Lysosomal proteases with special reference to cathepsin *B. J. Sci. & Industrial Res.* **52**: 423-431.

Allen, T.M. (1997). Liposomes, opportunities in drug delivery. *Drugs* **54** Suppl. 4: 8-14

Amin, F., Bowen, I.D., Szegedi, Z., Mihalik, R., Szende, B. (2000). Apoptotic and non-apoptotic modes of programmed cell death in MCF-7 human breast carcinoma cells. *Cell Biol. Int.* **24**: 253-60.

Andrew, C.L., Klemm, A.R., Lloyd J.B. (1997). Lysosome membrane permeability to amines. *Biochim. Biophys. Acta* **1330**: 71-82.

Arcamone F., Cassinelli G., Fantini G., Grein A., Orezzi P., Pol C. and Spalla C. (1969). Adriamycin, 14-hydroxydaunomycin, a new antitumor antibiotic from S. peucetius var. caesius. *Biotech. Bioengeneering:* **11**: 1101-1110.

Ashkenazi, A. and Dixit, V.M. (1998). Death Receptors: Signaling and Modulation. *Science.* **281**: 1305-1308

Ashkenazi, A. & Dixit, V.M. (1999). Apoptosis control by death decoy receptors. *Curr. Opin. Cell Biol.* **11**: 255-260

Baban, D.F. and Seymour, L.W. (1998). Control of tumour vascular permeability. *Adv. Drug Delivery Revs.* **34**: 109-119

Barranco S.C. (1975). Review of the survival and cell kinetics of adriamycin (NSC-123127) on mammalian cells. *Cancer Chemother Rep Part 3.* **6**: 147-152.

Bartek J., Bartkova J. and Lukas J. (1997). The retinoblastoma protein pathway in cell cycle control and cancer. *Exp. Cell Res.* **237**: 1-6.

Bates S.E., Wilson W.H., Fojo A.T., Alvarez M., Zhan Z., Regis J., Robey R., Hose C., Monks A., Kang Y.K. and Chabner B. (1996). Clinical Reversal of Multidrug Resistance.*Oncologist.* **1**: 269-275.

Bauer, E., Recknagel, R.D., Fiedler, U., Wollweber, L., Bock, C., Greulich, K.O. (1998). The distribution of the tail moments in single cell gel electrophoresis (comet assay) obeys a chi-square (chi2) not a gaussian distribution. *Mutat. Res.* **398**: 101-10.

Bellamy, C.O.C. (1996). P53 and apoptosis. *Brit. Med. Bulletin.* **53**: 3, 522-538

Bennet M.R. (1999). Mechanism of p53-induced apoptosis. *Biochem. Pharmacol.* **58**: 1089-1095.

Berquin, I.M., Sloane, B.F. (1996). Cathepsin B expression in human tumors. *Adv. Exp. Med. Biol.* **389**: 281-94.

Bielack, S.S. (1989). Doxorubicin: effect of different schedules on toxicity and anti-tumour efficacy. *Eur J Cancer Clin Oncol.* **25**: 873-882.

Binaschi, M., Capranico, G., Bo, L.D., & Zunino, F. (1997). Relationship between lethal effects and topoisomerase II-mediated double-stranded DNA breaks produced by anthracyclines with different sequence specificity. *Mol. Pharmacol.* **51**: 1053-1059

Bird, S.J., Lloyd J.B. (1995). Mechanism of lysosome rupture by dipeptides. *Cell Biochem. Funct.* **132**: 79-83.

Bodey G.P., Coltman C.A., Hewlett J.S. and Freireich E.J. (1976). Progress in the treatment of adults with acute leukemia: review of regimens containing cytarabine studied by the Southwest Oncology Group. *Arch. Intern. Med.* **136**: 1383-8.

Broder L.E. and Carbone P.P. (1976). Pharmacokinetic considerations in the design of optimal chemotherapeutic regimens for the treatment of breast carcinoma: a comceptual approach. *Med. Pediatr. Oncol.* **2**: 11-27.

Brown, J.M, and Giaccia A.J. (1998). The unique physiology of solid tumours: opportunities (and problems) for cancer therapy. *Cancer Res.* **58**: 1408-1416.

Brown, W.J., Goodhouse, J., & Farquhar, M.G. (1986). Mannose-6-phosphate receptors for lysosomal enzymes cycle between the golgi complex and endosomes. *J. Cell Biol.* **103**, 1235-1247.

Buck, M.R., Karustis, D.G., Day, N.A., Honn, K.V., Sloane, B.F. (1992). Degradation of extracellular-matrix proteins by human cathepsin B from normal and tumour tissues. *Biochem. J.* **282**: 273-8.

Calabro-Jones P.M., Byfield J.E., Ward J.F. and Sharp T.R. (1982). Time-dose relationships for 5-fluorouracil cytotoxicity against human epithelial cancer cells in vitro. *Cancer Res.* **42**: 4413-20.

Campo E., Munoz J., Miquel R., Palacin A., Cardesa A., Sloane B.F., and Emmert-Buck M.R. (1994). Cathepsin B expression in colorectal carcinomas correlates with tumor progression and shortened patient survival. *Amer. J. Path.* **145**: 301-309.

Cera, C., Palumbo, M., Stefanelli, S., Rassu, M., Palu, G. (1992). Water-soluble polysaccharide-anthracycline conjugates: biological activity. *Anticancer Drug Des.* **7**: 143-51.

Chresta, C.M. & Hickman, J.A. (1996). Oddball p53 in testicular tumours. *Nature Med.* **2**: 745-746

Collins, A.R., Dobson, V.L., Dusinska, M., Kennedy, G., and Stetina, R. (1997). The comet assay: what can it really tell us?. *Mutat. Res.* **375**: 183-193

Collins, A.R., Horvathova, (2001). E. Oxidative DNA damage, antioxidants and DNA repair: applications of the comet assay. *Biochem. Soc. Trans.* **29**: 337-41.

Cotelle, S., Ferard, J.F. (1999). Comet assay in genetic ecotoxicology: a review. *Environ. Mol. Mutagen.***34**(4): 246-55.

Davies K.J. and Doroshow J.H. (1986) Redox cycling of anthracyclines by cardiac mitochondria. I. Anthracycline radical formation by NADH dehydrogenase. *J Biol. Chem.* **261**: 3060-7.

Demoy, M., Minko, T., Kopeckova, P., Kopecek, J. (2000). Time- and concentration-dependent apoptosis and necrosis induced by free and HPMA copolymer-bound doxorubicin in human ovarian carcinoma cells. *J. Control Release.* **69**: 185-96.

Despois R., Dubost M., Mancy D., Maral R., Ninet L., Pinnert S., Preud'homme J., Charpentie Y., Belloc A., Chezelles N.D.E., Chezelles N., Lunel J. and Renaut J.. (1967) [Isolation of a new antibiotic with antitumor activity: rubidomycin (l3,057 R.P.). Identity of rubidomycin and daunomycin]
Pathol Biol. **15**:887-91.

Doroshow J.H. and Davies K.J. (1986) Redox cycling of anthracyclines by cardiac mitochondria. II. Formation of superoxide anion, hydrogen peroxide, and hydroxyl radical. *J. Biol. Chem.* **261**:3068-74.

Doroshow, J.H., Locker, G. Y. and Myers, C.E. (1980). Enzymatic defences of mouse heart against reactive oxygen metabolite alterations produced by doxorubicin. J. Clin. Invest. **65**: (1): 128-135.

Duncan, R. (1992). Drug-polymer conjugates: potential for improved chemotherapy. *Anti-Cancer Drugs.* **3**: 175-210

Duncan, R. (1997). Drug Targeting: Where Are We Now and Where Are We Going? *J. Drug Targeting.* **5**: 1-4

Duncan, R. (1999). Polymer conjugates for tumour targeting and intracytoplasmic delivery. The EPR effect as a common gateway? *Pharm. Sci. Technol. Today.* **2**: 441-449.

Duncan R., Cable H.C., and Lloyd J.B. (1982). Degradation of side-chains of N-(2-hydroxypropyl)methacrylamide copolymers by lysosomal thiol-proteinases. *Biosci. Rep. 2*: 1041-1046.

Duncan, R., Coatsworth, J.K. & Burtles, S. (1998). Preclinical toxicology of a novel polymeric antitumour agent: HPMA copolymer-bound doxorubicin (PK1). *Hum. & Exp. Toxicol.* **17**: 93-104.

Duncan, R., Gac-Breton, S., Keane, R., Musila, R., Sat, Y.N., Satchi, R., Searle, F. (2001). Polymer-drug conjugates, PDEPT and PELT: basic principles for design and transfer from the laboratory to clinic. *J. Control Release.* **74**: 135-46.

Duncan, R., Kopecek, J., Lloyd, J.B. (1984). Drug targeting to lysosomes. *Biochem. Soc. Trans.* **12**: 913-5.

Duncan, R., Kopeckova, P., Strohalm, J., Hume, I.C., Lloyd, J.B., Kopecek, J. (1988). Anticancer agents coupled to N-(2-hydroxypropyl)methacrylamide copolymers. II. Evaluation of daunomycin conjugates in vivo against L1210 leukaemia. *Brit. J. Cancer.* **57**: 147-56.

Duncan, R., Kopeckova-Rejmanova, P., Strohalm, J., Hume, I., Cable, H.C., Pohl, J., Lloyd, J.B., & Kopecek, J. (1987). Anticancer agents coupled to N-(2-hydroxypropyl)methacrylamide copolymers. I. Evaluation of daunomycin and puromycin conjugates in vitro. *Brit. J. Cancer.* **55**: 165-174

Duncan, R., Rejmanova, P., Kopecek, J., Lloyd, J.B. (1981). Pinocytic uptake and intracellular degradation of N-(2-hydroxypropyl)methacrylamide copolymers. A potential drug delivery system. *Biochim. Biophys. Acta* **678**: 143-50.

Duncan, R., Seymour, L.W., O'Hare, K.B., Flanagan, P.A., Wedge, S., Hume, I.C., Ulbrich, K., Strohalm, J., Subr, V., Spreafico, F., Grandi, M., Ripamonti, M., Farao, M., & Suarato, A. (1992). Preclinical evaluation of polymer-bound doxorubicin. *J. Controlled Release*, **19**, 331-346.

Duncan, R. and Spreafico. (1994). Polymer conjugates. Pharmacokinetic considerations for design and development. *Clin. Pharmacokin.* 27: 290-306

Dvorak, M., Kopeckova, P., Kopecek, J. (1999). High-molecular weight HPMA copolymer-adriamycin conjugates. *J. Control Release.***60**: 321-32.

Eguchi, Y., Srinivasan, A., Tomaselli, K.J., Shigeomi, S. and Tsujimoto, Y. (1999). ATP-dependent Steps in Apoptotic Signal Transduction. *Cancer Res.* **59**: 2174-2181

Eichholtz-Wirth H. (1980). Dependence of the cytostatic effect of adriamycin on drug concenration and exposure time in vitro. *Br. J. Cancer.* **41**: 886-91.

Etrych, T., Jelinkova, M., Rihova, B., Ulbrich, K. (2001). New HPMA copolymers containing doxorubicin bound via pH-sensitive linkage: synthesis and preliminary in vitro and in vivo biological properties. *J. Control Release.* **73**: 89-102.

Evans, E.E. (1988). Clinical pharmacodynamic of anticancer drugs: a basis for extending the concept of dose-intensity. *Blut.* **56**: 241-248.

Fairbairn, D.W., Olive, P.L., O'Neill, K.L. (1995). The comet assay: a comprehensive review. *Mutat. Res.* **339**: 37-59.

Foglesong P.D., Reckord C. and Swink S. (1992). Doxorubicin inhibits human DNA topoisomerase I. *Cancer Chemother. Pharmacol.* **30**: 123-5.

Folkman J. (2002) Role of angiogenesis in tumor growth and metastasis. Semin Oncol. **29**(6 Suppl 16):15-8.

Fong, W.F., Lam, W., Yang, M. and Wong, J.T.F. (1996). Partial Synergism Between Dextran-Conjugated Doxorubicin and *Cancer* Drugs on the Killing of Multidrug resistant KB-V1 Cells. *Anticancer Res.* **16**: 3773-3778

Fornari, F.A., Jarvis, W.D., Grant, S., Orr, M.S., Randolph, J.K., White, F.K.H., and Gewirtz, D.A. (1996). Growth arrest and non-apoptotic cell death associated with the suppression of c-myc expression in MCF-7 breast tumor cells following acute exposure to doxorubicin. *Biochem. Pharmacol.* **51**: 931-940

Fornari, F.A., Randolph, J.K., Yalowich, J.C., Ritke, M.K. and Gewirtz, D.A. (1994). Interference by doxorubicin with DNA unwinding in MCF-7 breast tumor cells. *Mol. Pharmacol.* **45**: 649-656

Friesen, C., Herr, I., Krammer, P.H., and Debatin, K.M. (1996). Involvement of the CD95 (APO-1/Fas) receptor/ligand system in drug-induced apoptosis in leukemia cells. *Nature Med.* **2**: 574-577

Fukumura D. and Jain R.K. (1998). Role of nitric oxide in angiogenesis and microcirculation in tumors. *Cancer Metastasis Rev.* **17**: 77-89.

Garner, A.P., Paine, M.J.I., Rodriguez-Crespo, I., Chinje, E.C., Montellano, P.O.D., Stratford, I.J., Tew, D.G., and Wolf, C.R. (1999). Nitric oxide synthases catalyze the activation of redox cycling and bioreductive anticancer agents. *Cancer Res.* **59**: 1929-1934.

Gewirtz, D.A. (1999). A critical evaluation of the mechanisms of action proposed for the antitumour effects of the anthracycline antibiotics adriamycin and daunomycin. *Biochem Pharmacol.* **57**(7): 727-741.

Gianasi, E., Wasil, M., Evagorou, E.G., Keddle, A., Wilson, G., Duncan, R. (1999). HPMA copolymer platinates as novel antitumour agents: in vitro properties, pharmacokinetics and antitumour activity in vivo. *Eur. J. Cancer.* **35**: 994-1002.

Gieseler, F., Nubler, V., Brieden, T., Kunze, J., and Valsamas, S. (1998). Intracellular pharmacokinetics of anthracyclines in human leukemia cells: correlation of DNA-binding with apoptotic cell death. *Int. J. Clin. Pharmacol. & Therap.* **36**: 25-28.

Gillette J.R. (1974). A perspective on the role of chemically reactive metabolites of foreign compounds in toxicity. II. Alterations in the kinetics of covalent binding. *Biochem. Pharmacol.* **23**: 2927-38.

Gillette J.R. (1974). A perspective on the role of chemically reactive metabolites of foreign compounds in toxicity. I. Correlation of changes in covalent binding of reactivity metabolites with changes in the incidence and severity of toxicity. *Biochem. Pharmacol.* **23**: 2785-94.

Green, D.R. (1998). Apoptotic Pathways: The Roads to Ruin. *Cell.* 94: 695-698.

Green, D.R., and Reed, J.C. (1998). Mitochondria and apoptosis. *Science* **281**: 1309-1312.

Greene R.F., Collins J.M., Jenkins J.F., Speyer J.L. and Myers C.E. (1983) Plasma pharmacokinetics of adriamycin and adriamycinol: implications for the design of in vitro experiments and treatment protocols. *Cancer Res.* **43**: 3417-3421.

Halder, S., Negrini, M., Monne, M., Sabbioni, S. and Croce, C.M. (1994). Down-Regulation of bcl-2 by p53 in Breast Cancer Cells. *Cancer Res.* **54**: 2095-2097.

Hanauske, A.R., Osborne, C.K., Chamness, G.C., Clark, G.M., Forseth, B.J., Buchok, J.B., Arteaga, C.L., and Von Hoff, D.D. (1987). Alteration of EGF-Receptor Binding in Human Breast *Cancer* Cells by Antineoplastic Agents. *Eur. J. Cancer and Clin.* Oncol. **23**: 545-551.

Hayes, W.J. (1991). Dosage and other factors influencing toxicity. *Handbook of Pesticide Toxicology*, **1**: Chapter 2: 47-54.

Hartwell, L.H. and Kastan, M.B. (1994). Cell Cycle Control and Cancer. *Science* **266**: 1821-1821.

Hengartner, M. (1998). Death by Crowd Control. *Science* **281**: 1298-1299.

Hickman, J.A. and Boyle, C.C. (1997). Apoptosis and cytotoxins. *Brit. Med. Bulletin.* **53**: 632-643.

Hopewel, J.W., Duncan, R., Wilding, D., Chakrabarti, K. (2001). Preclinical evaluation of the cardiotoxicity of PK2: a novel HPMA copolymer-doxorubicin-galactosamine conjugate antitumour agent. *Hum. Exp. Toxicol.* **20**: 461-470.

Hortobagyi, G.N. (1997). Anthracyclines in the Treatment of Cancer. An Overview. *Drugs.* **54** Suppl. 4: 1-7.

Hovorka, O., St'astny, M., Etrych, T., Subr, V., Strohalm, J., Ulbrich, K., Rihova, B. (2002). Differences in the intracellular fate of free and polymer-bound doxorubicin.*J. Control Release.* **80**: 101-117.

Hryniuk W. and Bush H. (1984). The importance of dose intensity in chemotherapy of metastatic breast cancer. *J. Clin. Oncol.* **2**: 1281-8.

Jain, R.K. (1994). Barriers to drug delivery in solid tumours. *Sci. American.* July: 42-49.

Jain, R.K. (2001). Delivery of molecular medicine to solid tumours. *Adv. Drug Delivery Rev*: **46**: 149-168.

Janicke, R.U., Ng, P., Sprengart, M.L., and Porter, A.G. (1998). Caspase-3 Is Required for α-Fodrin Cleavage but Dispensable foe Cleavage of Other Substrates in Apoptosis. *J. Biol. Chem.* **273**: 15540-15545.

Janicke, R.U., Sprengart, M.l., Wati, M.R. and Porter, A.G. (1998). Caspase-3 Required for DNA Fragmentation and Morphological Changes Associated with Apoptosis. *J. Biol. Chem.* **273**: 9375-9360.

Jensen, K.D., Kopeckova, P., Bridge, J.H., Kopecek, J. (2001). The cytoplasmic escape and nuclear accumulation of endocytosed and microinjected HPMA copolymers and a basic kinetic study in Hep G2 cells. *AAPS Pharm.Sci.* **3**: E32.

Julyan, P.J., Seymour, L.W., Ferry, D.R., Daryani, S., Boivin, C.M., Doran, J., David, M., Anderson, D., Christodoulou, C., Young, A.M., Hesslewood, S., Kerr, D.J. (1999). Preliminary clinical study of the distribution of HPMA copolymers bearing doxorubicin and galactosamine. *J. Control Release.* **57**: 281-290.

Kasuya, Y., Lu, Z.R., Kopeckova, P., Tabibi, S.E., Kopecek, J. (2002). Influence of the structure of drug moieties on the in vitro efficacy of HPMA copolymer-geldanamycin derivative conjugates. *Pharm. Res.* **19**: 115-123.

Keizer H.G., Pinedo H.M., Schuurhuis G.J., and Joenje H. (1990) Doxorubicin (adriamycin): a critical review of free radical-dependent mechanisms of cytotoxicity. *Pharmac.Ther.* **47**: 219-231.

Keppler, D., Sameni, M., Moin, K., Mikkelsen, T., Diglio, C.A., Sloane, B.F. (1996). Tumor progression and angiogenesis: cathepsin B and Co. *Biochem. Cell Biol.* **74**: 799-810.

Keppler, D., Sloane, B.F. (1996). Cathepsin B: Multiple enzyme forms from a single gene and their relation to cancer. *Enz. Prot.* 49: 94-105.

Kirschke H and Barrett A.J. (1985). Cathepsin L - a lysosomal cysteine proteinase. *Prog Clin Biol Res.***180**: 61-9.

Klemm, A.R., Pell, K.L., Anderson, L.M., Andrew, C.L., Lloyd, J.B. (1998). Lysosome membrane permeability to anions. *Biochim. Biophys. Acta* **1373**: 17-26.

Koblinski, J,E., Ahram, M., Sloane, B.F. (2000). Unraveling the role of proteases in cancer. *Clin. Chim Acta* **291**: 113-35.

Kohn K.W. (1996) Beyond DNA cross-linking: history and prospects of DNA-targeted cancer treatment-fifteenth Bruce F. Cain memorial ward lecture. *Cancer Res.* **56**: 5533-5546.

Kohn, K.W. (1996). Beyond DNA Cross-Linking: History and Prospects of DNA-targeted Cancer Treatment-Fifteenth Bruce F. Cain Memorial Award Lecture. *Cancer Res.* **56**: 5533-5546.

Koli, K.M. and Arteaga, C.L. (1997). Predominant Cytosolic Localization of Type II *Trans.*forming Growth Factor β receptors in Human Breast Carcinoma Cells. *Cancer Res.* **57**: 970-977.

Kooistra, T., Pratten, M.K., Lloyd, J.B. (1981). Serum-dependence of fluid-phase pinocytosis and specificity in adsorptive pinocytosis of simple proteins in rat peritoneal macrophages. *Biosci. Rep.* **1**: 587-594.

Kopecek, J., Kopeckova, P., Minko, T., Lu, Z. (2000). HPMA copolymer-anticancer drug conjugates: design, activity, and mechanism of action. *Eur. J. Pharm. Biopharm.* **50**: 61-81.

Kovar, M., Strohalm, J., Ulbrich, K., Rihova, B. (2002). In vitro and in vivo effect of HPMA copolymer-bound doxorubicin targeted to transferrin receptor of B-cell lymphoma 38C13. *J.* Drug *Target.* **10**: 23-30.

Kwon, G.S., Yokoyama. M., Okano, T., Sakurai, Y., Kataoka, K. (1993). Biodistribution of micelle-forming polymer-drug conjugates. *Pharm. Res.* **10**(7): 970-974.

Langer, R. (1998). Drug delivery and targeting. *Nature* **392**: 5-10.

Larsen A.K., Skladanowski A. and Bojanowski K. (1996) The roles of DNA topoisomerase II during the cell cycle. *Prog. Cell Cycle Res.* **2**: 229-239.

Li, H. and Yuan, J. (1999). Deciphering the pathways of life and death. *Curr. Opin. Cell Biol.* **11**: 261-266.

Ling, Y., Priebe, W., and Perez-Soler, R. (1993). Apoptosis Induced by Anthracycline Antibiotics in P388 Parent and Multidrug-resistant Cells. *Cancer Res.* **53**: 1845-1852.

Liu, *et al.* (1997). Mechanism of cellular 3- (4,5-dimethylthiazol-2-yl)-2,5-diphenyltetrazolium bromide (MTT) reduction. *J. Neurochem.* **69**: 581-593.

Lloyd, J.B. (1984). Penetration of small molecules across the lysosome membrane: the 'classical' view. *Biochem. Soc. Trans.* **12**: 906.

Lloyd, J.B. (1996). Metabolite efflux and influx across the lysosome membrane. *Subcell. Biochem.* **27**: 361-386.

Lloyd, J.B. (2000). Lysosome membrane permeability: implications for drug delivery. *Adv. Drug Deliv. Rev.* **41**: 189-200.

Lloyd, J.B., Duncan, R., Kopecek, J. (1986). Synthetic polymers as carriers for chemotherapeutic agents. *Biochem. Soc. Trans.* **14**: 391-392.

Lloyd, J.B., Pratten, M.K., Duncan, R., Kooistra, T., Cartlidge, S.A. (1984). Substrate selection and processing in endocytosis. *Biochem. Soc. Trans.* **12**: 977-978.

Loadman, P.M., Bibby, M.C., Double, J.A., Al-Shakhaa, W.M., Duncan, R. (1999). Pharmacokinetics of PK1 and doxorubicin in experimental colon tumor models with differing responses to PK1. *Clin. Cancer Res.* **5**: 3682-8.

Lovell, D.P., Thomas, G., Dubow, R. (1999). Issues related to the experimental design and subsequent statistical analysis of in vivo and in vitro comet studies. *Teratog. Carcinog. Mutagen.* **19**: 109-119.

Luo, Y., Bernshaw, N.J., Lu, Z.R., Kopecek, J., Prestwich, G.D. (2002). Targeted delivery of doxorubicin by HPMA copolymer-hyaluronan bioconjugates. *Pharm. Res.* **19**: 396-402.

McKelvey-Martin, V.J., Green, M.H., Schmezer, P., Pool-Zobel, B.L., De Meo, M.P., Collins, A. (1993). The single cell gel electrophoresis assay (comet assay): a European review. *Mutat. Res.* **288**: 47-63.

Maeda H., Wu J., Sawa T., Matsumura Y. and Hori K. (2000). Tumour vascular permeability and the EPR effect in macromolecular therapeutics: a review. *J. Control. Rel.* **65**: 271-84.

Milano, G., Cassuto-Viguier, E., Fischel, J.L., Formento, P., Renee, N., Frenay, M., Thyss, A. and Namer, M. (1992). Doxorubicin weekly low doses administration: in vitro cytotoxicity generated by the typical pharmacokinetic profile. *Eur. J. Cancer.* **28A**: 1881-1885.

Mimnaugh, E.G., Dusre, L., Atwell, J., and Myers, C.E. (1989). Differential Oxygen radical Susceptibility of Adriamycin-sensitive and –resistant MCF-7 Human Breast tumor Cells. *Cancer Res.* **49**: 8-15.

Minderman H., Linssen P., Wessels J. and Haanen C. (1993). Cell cycle related uptake, retention and toxicity of idarubicin, daunorubicin and doxorubicin. *Anticancer Res.* **13**: 1161-5.

Minko, T., Kopeckova, P., Kopecek, J. (1999). Chronic exposure to HPMA copolymer-bound adriamycin does not induce multidrug resistance in a human ovarian carcinoma cell line. *J. Control Release.* **59**: 133-48.

Minko, T., Kopeckova, P., Kopecek, J. (1999). Comparison of the anticancer effect of free and HPMA copolymer-bound adriamycin in human ovarian carcinoma cells. *Pharm. Res.* 16: 986-96.

Minko, T., Kopeckova, P., Kopecek, J. (2000). Efficacy of the chemotherapeutic action of HPMA copolymer-bound doxorubicin in a solid tumor model of ovarian carcinoma. *Int. J. Cancer.* **86**: 108-17.

Minko, T., Kopeckova, P., Kopecek, J. (2001). Preliminary evaluation of caspases-dependent apoptosis signaling pathways of free and HPMA copolymer-bound doxorubicin in human ovarian carcinoma cells. *J. Control Release.* **71**: 227-37.

Minko, T., Kopeckova, P., Pozharov, V., Jensen, K.D., Kopecek, J. (2000). The influence of cytotoxicity of macromolecules and of VEGF gene modulated vascular permeability on the enhanced permeability and retention effect in resistant solid tumors. *Pharm. Res.* **17**: 505-14.

Minko, T., Kopeckova, P., Pozharov, V., Kopecek, J. (1998). HPMA copolymer bound adriamycin overcomes MDR1 gene encoded resistance in a human ovarian carcinoma cell line. *J. Control Release.* **54**: 223-33.

Minotti G., Cairo G. and Monti E. (1999) Role of iron in anthracycline cardiotoxicity: new tunes for an old song? *Faseb J.* **13**: 199-212.

Moin, K., Cao, L., Day, N.A., Koblinski, J.E., Sloane, B.F. (1998). Tumor cell membrane cathepsin B. *Biol. Chem.* **379**(8-9): 1093-9.

Moin, K., Day, N.A., Sameni, M., Hasnain, S., Hirama, T., Sloane, B.F. (1992). Human tumour cathepsin B. Comparison with normal liver cathepsin B. *Biochem. J.* **285**: 427-34.

Moin, K., Rozhin, J., McKernan, T.B., Sanders, V.J., Fong, D., Honn, K.V., Sloane, B.F. (1989). Enhanced levels of cathepsin B mRNA in murine tumors. *FEBS Lett.* **244**: 61-4.

Mosmann, T. (1983). Rapid colorimetric assay for cellular growth and survival: Application to proliferation and cytotoxicity assays. *J. Immunol. Methods.* **65**: 55-63.

Muggia, F.M. (1999). Doxorubicin-polymer conjugates: further demonstration of the concept of enhanced permeability and retention. *Clin. Cancer Res.***5**: 7-8.

Muller I., Jenner A., Bruchelt G., Niethammer D. and Halliwell B. (1997). Effect of concentration on the cytotoxic mechanism of doxorubicin--apoptosis and oxidative DNA damage.*Biochem. Biophys. Res. Comm.* **230**: 254-7.

Muller I., Niethammer D. and Bruchelt G. (1998) Anthracycline-derived chemotherapeutics in apoptosis and free radical cytotoxicity. *Int. J. Mol. Med.* **1**: 491-4.

Muller M., Wilder S., Bannasch D., Israeli D., Lehlbach K., Li-Weber M., Friedman S.L., Galle P.R., Stremmel W., Oren M. and Krammer P.H. (1998). p53 activates the CD95 (APO-1/Fas) gene in response to DNA damage by anticancer drugs. *J. Exp. Med.* **188**: 2033-45.

Negrini, M., Sabbioni, S., Halder, S., Possati, L., Castagnoli, A., Corallini, A., Barbanti-Brodano, G. and Croce, C.M. (1994). Tumor and growth suppression of breast cancer cells by chromosome 17-associated functions. *Cancer Res.* **54**: 1818-1824

Noguchi, Y., Wu, J., Duncan, R., Strohalm, J., Ulbrich, K., Akaike, T., Maeda, H. (1998). Early phase tumor accumulation of macromolecules: a great difference in clearance rate between tumor and normal tissues. *Jpn. J. Cancer Res.* **89**: 307-14.

O'Hare, K.B., Duncan, R., Strohalm, J., Ulbrich, K., Kopeckova, P. (1993). Polymeric drug-carriers containing doxorubicin and melanocyte-stimulating hormone: in vitro and in vivo evaluation against murine melanoma. *J. Drug Target.* **1**: 217-29.

Ogretmen, B. and Safa, A. (1996). Down-regulation of apoptosis-related bcl-2 but not bcl-x1 or bax proteins in Multidrug-resistant MCF-7/Adr human breast cancer cells. *Int. J. Cancer.* **67**: 608-614

Olive, P.L. (1999). DNA damage and repair in individual cells: applications of the comet assay in radiobiology. *Int. J. Radiat. Biol.* **75**: 395-405.

Omelyanenko V, Gentry, C., Kopeckova, P., Kopecek, J. (1998). HPMA copolymer-anticancer drug-OV-TL16 antibody conjugates. II. Processing in epithelial ovarian carcinoma cells in vitro. *Int. J. Cancer.* **75**: 600-8.

Omelyanenko, V., Kopeckova, P., Gentry, C., Kopecek, J. (1998). Targetable HPMA copolymer-adriamycin conjugates. Recognition, internalization, and subcellular fate. *J. Control Release.* **53**: 25-37.

Phillips, R.M., Loadman, P.M., Cronin, B.P. (1998). Evaluation of a novel in vitro assay for assessing drug penetration into avascular regions of tumours. *Brit. J. Cancer.* **77**: 2112-9.

Phillips, R.M., Pearce, J., Loadman, P.M., Bibby, M.C., Cooper, P.A., Swaine, D.J., Double, J.A. (1998). Angiogenesis in the hollow fiber tumor model influences drug delivery to tumor cells: implications for anticancer drug screening programs. *Cancer Res.* **58**: 5263-6.

Pimm, M.V., Perkins, A.C., Strohalm, J., Ulbrich, K., Duncan, R. (1996). Gamma scintigraphy of a 123I-labelled N-(2-hydroxypropyl)methacrylamide copolymer-doxorubicin conjugate containing galactosamine following intravenous administration to nude mice bearing hepatic human colon carcinoma. *J.* Drug *Target.* **3**: 385-90.

Platt, J.L. and Nath, K.A. (1998). Heme oxygenase: protective gene or Trojan horse. *Nature Med.* **4**: 1364-1365

Poole, A,R., Tiltman, K.J., Recklies, A.D., and Stoker, T.A.M. (1978). Differences in secretion of the proteinase cathepsin B at the edges of human breast carcinomas and fibroadenomas. *Nature (London).* **273**, 545-547.

Pourquier, P., Montaudon, D., Huet, S., Larrue, A., Clary, A. and Robert, J. (1998). doxorubicin-Induced Alterations of c-myc and c-jun gene expression in rat glioblastoma cells: role of c-jun in drug resistance and cell death. *Biochem. Pharmacol.* **55**: 1963-1971

Ranade, V.V. (1990). Drug delivery systems: 3A. Role of polymers in drug delivery. *J. Clin Pharmacol.* 30: 10-23

Rasbridge, S.A., Gillett, C.E., Seymour, A.M., Patel, K., Richards, M.A., Rubens, R.D., Millis, R.R. (1994). The effects of chemotherapy on morphology, cellular proliferation, apoptosis and oncoprotein expression in primary breast carcinoma. *Brit. J. Cancer.* **70**: 335-41.

Reddy V.Y., Zhang Q.Y. and Weiss S.J. (1995). Pericellular mobilization of the tissue-destructive cysteine proteinases, cathepsins B, L, and S, by human monocyte-derived macrophages. *Proc. Natl. Acad. Sci. U S A.* **92**: 3849-53.

Ren, W.P., Sloane, B.F. (1996). Cathepsins D and B in breast cancer. *Cancer* Treat *Res.* **83**: 325-52. .

Richardson, D.S. and Johnson, S.A. (1997). Anthracyclines in haematology: preclinical studies, toxicity and delivery systems. *Blood Revs.* **11**: 201-223

Rifkin B.R., Vernillo A.T., Kleckner A.P., Auszmann J.M., Rosenberg L.R. and Zimmerman M. (1991). Cathepsin B and L activities in isolated osteoclasts. *Biochem. Biophys. Res. Comm.* **30**: 63-9.

Rihova, B., Etrych, T., Pechar, M., Jelinkova, M., Stastny, M., Hovorka, O., Kovar, M., Ulbrich, K. (2001). Doxorubicin bound to a HPMA copolymer carrier through hydrazone bond is effective also in a cancer cell line with a limited content of lysosomes. *J. Control Release.* **74**: 225-32.

Rihova, B., Jelinkova, M., Strohalm, J., Subr, V., Plocova, D., Hovorka, O., Novak, M., Plundrova, D., Germano, Y., Ulbrich, K. (2000). Polymeric drugs based on conjugates of synthetic and natural macromolecules. II. Anti-cancer activity of antibody or (Fab')(2)-targeted conjugates and combined therapy with immunomodulators. *J. Control Release.* **64**: 241-61.

Batz H.G., Franzmann G., Ringsdorf H. (1972). Model reactions for synthesis of pharmacologically active polymers by way of monomeric and polymeric reactive esters. *Angew Chem Int Ed Engl.* **11**(12): 1103-4.

Rojas, E., Lopez, M.C., Valverde, M. (1999). Single cell gel electrophoresis assay: methodology and applications. *J. Chromatogr. B Biomed. Sci.* Appl. **722**: 225-54.

Rozhin, J., Sameni, M., Ziegler, G., Sloane, B.F. (1994). Pericellular pH affects distribution and secretion of cathepsin B in malignant cells. *Cancer Res.* **54**: 6517-25.

Salti, G.I., Das Gupta, T.K., Constantinou, A.I. (2000). A novel use for the comet assay: detection of topoisomerase II inhibitors. *Anticancer Res.* **20**: 3189-93.

Satchi, R., Connors, T.A., Duncan, R. (2001). PDEPT: polymer-directed enzyme prodrug therapy. I. HPMA copolymer-cathepsin B and PK1 as a model combination. *Brit. J. Cancer.* **85**: 1070-6.

Seymour, L.W. (1992). Passive tumor targeting of soluble macromolecules and drug conjugates. *Crit Rev. Ther Drug Carrier Syst.* **9**: 135-87.

Seymour, L.W., Ferry, D.R., Anderson, D., Hesslewood, S., Julyan, P.J., Poyner, R., Doran, J., Young, A.M., Burtles, S., Kerr, D.J. (2002). Hepatic drug targeting: phase I evaluation of polymer-bound doxorubicin. *J. Clin. Oncol.* **20**: 1668-76.

Seymour, L.W., Miyamoto, Y., Maeda, H., Brereton, M., Strohalm, J., Ulbrich, K., Duncan, R. (1995). Influence of molecular weight on passive tumour accumulation of a soluble macromolecular drug carrier. *Eur. J. Cancer.* **31A**: 766-70.

Seymour, L.W., Ulbrich, K., Steyger, P.S., Brereton, M., Subr, V., Strohalm, J., Duncan, R. (1994). Tumour tropism and anti-cancer efficacy of polymer-based doxorubicin prodrugs in the treatment of subcutaneous murine B16F10 melanoma. *Brit. J. Cancer.* **70**: 636-41.

Seymour, L.W., Ulbrich, K., Strohalm, J., Kopecek, J., Duncan, R. (1990). The pharmacokinetics of polymer-bound adriamycin. *Biochem. Pharmacol.* **39**: 1125-31.

Seymour, L.W., Ulbrich, K., Wedge, S.R., Hume, I.C., Strohalm, J., Duncan, R. (1991). N-(2-hydroxypropyl)methacrylamide copolymers targeted to the hepatocyte galactose-receptor: pharmacokinetics in DBA2 mice. *Brit. J. Cancer.* **63**: 859-66.

Shapiro G.I., Edwards C.D., Ewen M.E. and Rollins B.J. (1998). p16INK4A participates in a G1 arrest checkpoint in response to DNA damage. *Mol. Cell. Biol.* **18**: 378-87.

Shiah, J.G., Dvorak, M., Kopeckova, P., Sun, Y., Peterson, C.M., Kopecek, J. (2001). Biodistribution and antitumour efficacy of long-circulating N-(2-hydroxypropyl)methacrylamide copolymer-doxorubicin conjugates in nude mice. *Eur. J. Cancer.* **37**: 131-9.

Sinha A.A., Wilson M.J., Gleason D.F., Reddy P.K., Sameni M. and Sloane B.F. (1995). Immunohistochemical localization of cathepsin B in neoplastic human prostate. *Prostate.* **26**: 171-8.

Sinha, B.K., Katki, A.G., Batist, G., Cowan, K.H., and Myers, C.E. (1987). Differential formation of hydroxyl radicals by adriamycin in sensitive and resistant mcf-7 human breast tumor cells: implications for the mechanism of action. *Biochem.* **27**: 3776-3781.

Sinha B.K. and Politi P.M. (1990). Anthracyclines. *Cancer Chemother. Biol. Response Modif.* **11**: 45-57.

Sinha B.K., Trush M.A., Kennedy K.A. and Mimnaugh E.G. (1984). Enzymatic activation of adriamycin to nuclear DNA. *Cancer Res.* **44**: 2892-2896.

Sinha B.K., Mimnaugh E.G., Rajagopalan S. and Myers C.E. (1989). Adriamycin activation and oxygen free radical formation in human breast cancer cells: protective role of glutathione peroxidase in adriamycin resistance. *Cancer Res.* **49**: 3844-3848.

Skipper H.E. (1965). The effects of chemotherapy on the kinetics of leukemic cell behavior. *Cancer Res.* **25**: 1544-50.

Skladanowski A. and Konopa J. (1993). Adriamycin and daunorubicin induce programmed cell death (apoptosis) in tumour cells. *Biochem. Pharmacol.* **46**: 375-382.

Skladanowski A. and Konopa J. (1994). Interstrand DNA crosslinking induced by anthracyclines in tumour cells. *Biochem. Pharmacol.* **47**: 2269-2278.

Skladanowski A. and Konopa J. (1994). Relevance of interstrand DNA crosslinking induced by anthracyclines for their biological activity. *Biochem. Pharmacol.* **47**: 2279-2287.

Sloane, B.F., Dunn, J.R., Honn, K.V. (1981). Lysosomal cathepsin B: correlation with metastatic potential. *Science.* **212**: 1151-1153.

Sloane, B.F., Honn, K.V., Sadler, J.G., Turner, W.A., Kimpson, J.J., Taylor, J.D. (1982). Cathepsin B activity in B16 melanoma cells: a possible marker for metastatic potential. *Cancer Res.* **42**: 980-6.

Sloane, B.F., Moin, K., Krepela, E., Rozhin, J. (1990). Cathepsin B and its endogenous inhibitors: the role in tumor malignancy. *Cancer Metastasis Rev.* **9**: 333-52.

Sloane, B.F., Moin, K., Sameni, M., Tait, L.R., Rozhin, J., Ziegler, G. (1994). Membrane association of cathepsin B can be induced by transfection of human breast epithelial cells with c-Ha-ras oncogene. *J. Cell Sci.* **107**: 373-84.

Sloane, B.F., Rozhin, J., Johnson, K., Taylor, H., Crissman, J.D., Honn, K.V. (1986). Cathepsin B: association with plasma membrane in metastatic tumors. *Proc. Natl. Acad. Sci. USA.* **838**: 2483-7.

Sloane B.F., Sadler J.G., and Evens C. (1984). Cathepsin B-like cysteine proteinases and tumor metastasis. *Cancer Bull.* **36**: 196-200

Smith I.E. (1985). Optimal schedule for anthracyclines. *Eur. J. Cancer Clin. Oncol.* 21: 159-61.

Subr V., Kopecek J., Pohl J., Baudys M., and Kostka V. (1988). Cleavage of oligopeptide side-chains in N-(2-hydroxypropyl)methacrylamide copolymers by mixtures of lysosomal enzymes. *J. Control. Release.* **8**: 133-140.

Subr V., Strohalm J., Ulbrich K., Duncan R., and Hume I.C. (1992). Polymers containing enzymatically degradable bonds, XII. Effect of spacer structure on the rate of release of daunomycin and adriamycin from poly[N-(2-hydroxypropyl)-methacrylamide] copolymer drug carriers in vitro and antitumour activity measured in vivo. *J. Control. Rel.* **18**: 123-132.

Taatjes, D.J., Koch, T.H. (2001). Nuclear targeting and retention of anthracycline antitumor drugs in sensitive and resistant tumor cells. *Curr. Med. Chem.* **8**: 15-29.

Teixeria, C., Reed, J.C., and Pratt, M.A.C. (1995). Estrogen promotes chemotherapeutic drug resistance by a mechanism involving BCl-2 proto-oncogene expression in human breast cancer cells. *Cancer Res.* **55**: 3902-3907

Tewey K.M., Rowe T.C., Yang L., Halligan B.D. and Liu L.F. (1984) Adriamycin-induced DNA damage mediated by mammalian DNA topoisomerase II. *Science.* **226**: 466-468.

Tewey K.M., Chen G.L., Nelson E.M. and Liu L.F. (1984) Intercalative antitumour drugs interfere with the breakage-reunion reaction of mammalian DNA topoisomerase II. *J. Biol. Chem.* **259**: 9182-9127.

Thomson, A.H., Vasey, P.A., Murray, L.S., Cassidy, J., Fraier, D., Frigerio, E., Twelves, C. (1999). Population pharmacokinetics in phase I drug development: a phase I study of PK1 in patients with solid tumours. *Brit. J. Cancer.* **81**: 99-107.

Thornberry, N.A. and Lazebnik, Y. (1988). Caspases enemies within. *Science.* **281**: 1312-1316.

Tice, R.R., Agurell, E., Anderson, D., Burlinson, B., Hartman, A., Kabayashi, H., Miyamae, Y., Rojas, E., Ryu, J.C. and Sasaki, Y.F. (2000). Single Cell Gel/Comet Assay: Guidelines for In Vitro and In Vivo Genetic Toxicology Testing. *Environ. and Mol. Mutagenesis.* **35**: 206-221.

Tijerina, M., Fowers, K.D., Kopeckova, P., Kopecek, J. (2000). Chronic exposure of human ovarian carcinoma cells to free or HPMA copolymer-bound mesochlorin e6 does not induce P-glycoprotein-mediated multidrug resistance. *Biomaterials.* **21**: 2203-10.

Tritton, T.R. and Hickman, J.A. (1990). How to kill cancer cells: membranes and cell signalling as targets in cancer chemotherapy. *Cancer Cells.* **2**: 95-105

Tritton T.R., Yee G. and Wingard L.B. Jr. (1983). Immobilised adriamycin: a tool for separating cell surface from intracellular mechanisms. *Fed. Proc.* **42**: 284-287.

Tsujimoto Y. and Shimizu S. (2000). Bcl-2 family: Life-or-death switch. *FEBS Lett.* **466**: 6-10.

Ulbrich, K., Subr, V., Strohalm, J., Plocova, D., Jelinkova, M., Rihova, B. (2000). Polymeric drugs based on conjugates of synthetic and natural macromolecules. I. Synthesis and physico-chemical characterisation. *J. Control Release.* **64**: 63-79.

Vasey, P.A., Kaye, S.B., Morrison, R., Twelves, C., Wilson, P., Duncan, R., Thomson, A.H., Murray, L.S., Hilditch, T.E., Murray, T., Burtles, S., Fraier, D., Frigerio, E. and Cassidy, J. (1999). Phase I clinical and pharmacokinetic study of PK1 [N-(2-hydroxypropyl)methacrylamide copolymer doxorubicin]: first member of a new class of chemotherapeutic agents-drug-polymer conjugates. *Clin. Cancer Res.* **5**: 83-94.

Vichi, P. and Tritton, T.R. (1989). Stimulation of growth in human and murine cells by adriamycin. *Cancer Res.* **49**: 2679-2682

Vichi, P. and Tritton, T.R. (1992). Adriamycin: protection from cell death by removal of extracellular drug. *Cancer Res.* **52**: 4135-4138

Wang, T.T.Y. and Phang, J.M. (1995). Effects of estrogen on apoptotic pathways in human breast cancer cell line MCF-7. *Cancer Res.* **55**: 2487-2489

Wani, M.A., Zhu, Q.Z., El-Mahdy, M., and Wani, A.A. (1999). Influence of p53 tumor suppressor protein on bias of DNA repair and apoptotic response in human cells. *Carcinogenesis.* **20**: 765-772

Winterbourn C.C. (1985). Free-radical production and oxidative reactions of hemoglobin.*Environ. Health Perspect.* 64: 321-30.

Yan, M., Lee, J., Schibach, S., Goddard, A., and Dixit, V. (1999). mE10, a novel caspase recruitment domain-containing proapoptotic molecule. *J. Biol. Chem.* **274**: 10287-10292

Yan, S., Sameni, M., Sloane, B.F. (1998). Cathepsin B and human tumor progression. *Biol. Chem.* **379**: 113-23.

Yang, M., Chan, H.L., Lam, W., Fong, W.F. (1998). Cytotoxicity and DNA binding characteristics of dextran-conjugated doxorubicins. *Biochimica et Biophysica Acta* **1380**: 329-335

Yeung, T.K., Hopewell, J.W., Simmonds, R.H., Seymour, L.W., Duncan, R., Bellini, O., Grandi, M., Spreafico, F., Strohalm, J., Ulbrich, K. (1991). Reduced cardiotoxicity of doxorubicin given in the form of N-(2-hydroxypropyl)methacrylamide conjugates: and experimental study in the rat. *Cancer Chemother. Pharmacol.* **29**: 105-11.

Zaleskis G., Berleth E., Verstovsek S., Ehrke M.J. and Mihich E. (1994). Doxorubicin-induced DNA degradation in murine thymocytes. *Mol. Pharmacol.* **46**: 901-908.

Appendix 1.1 *– Log C versus log T plots expressed on a linear scale for* ***doxorubicin*** *at various percentage of cell kill.*

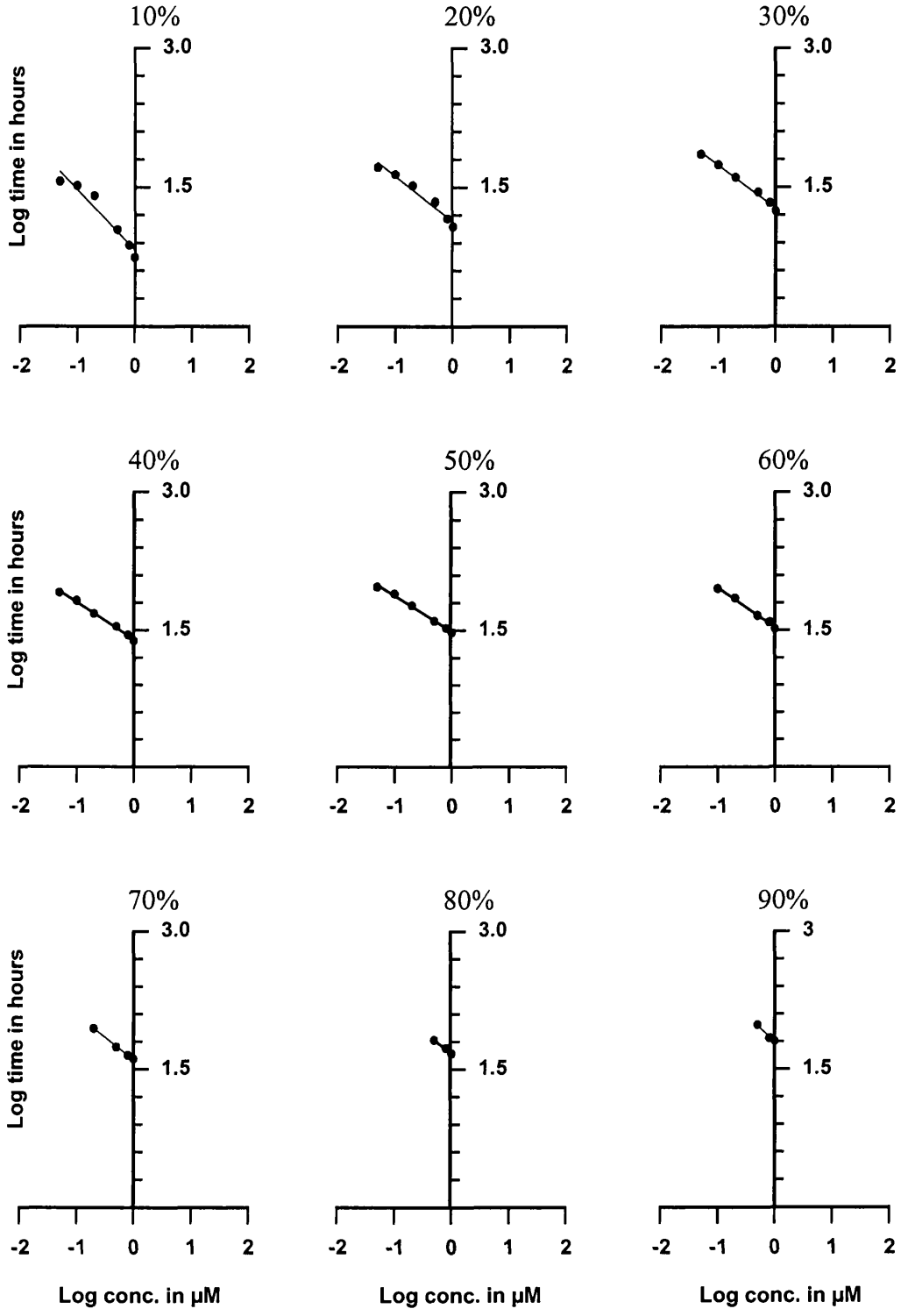

Appendix 1.2 *– Log C versus log T plots expressed on a linear scale for doxorubicin with 72 hours post incubation at various percentage of cell kill.*

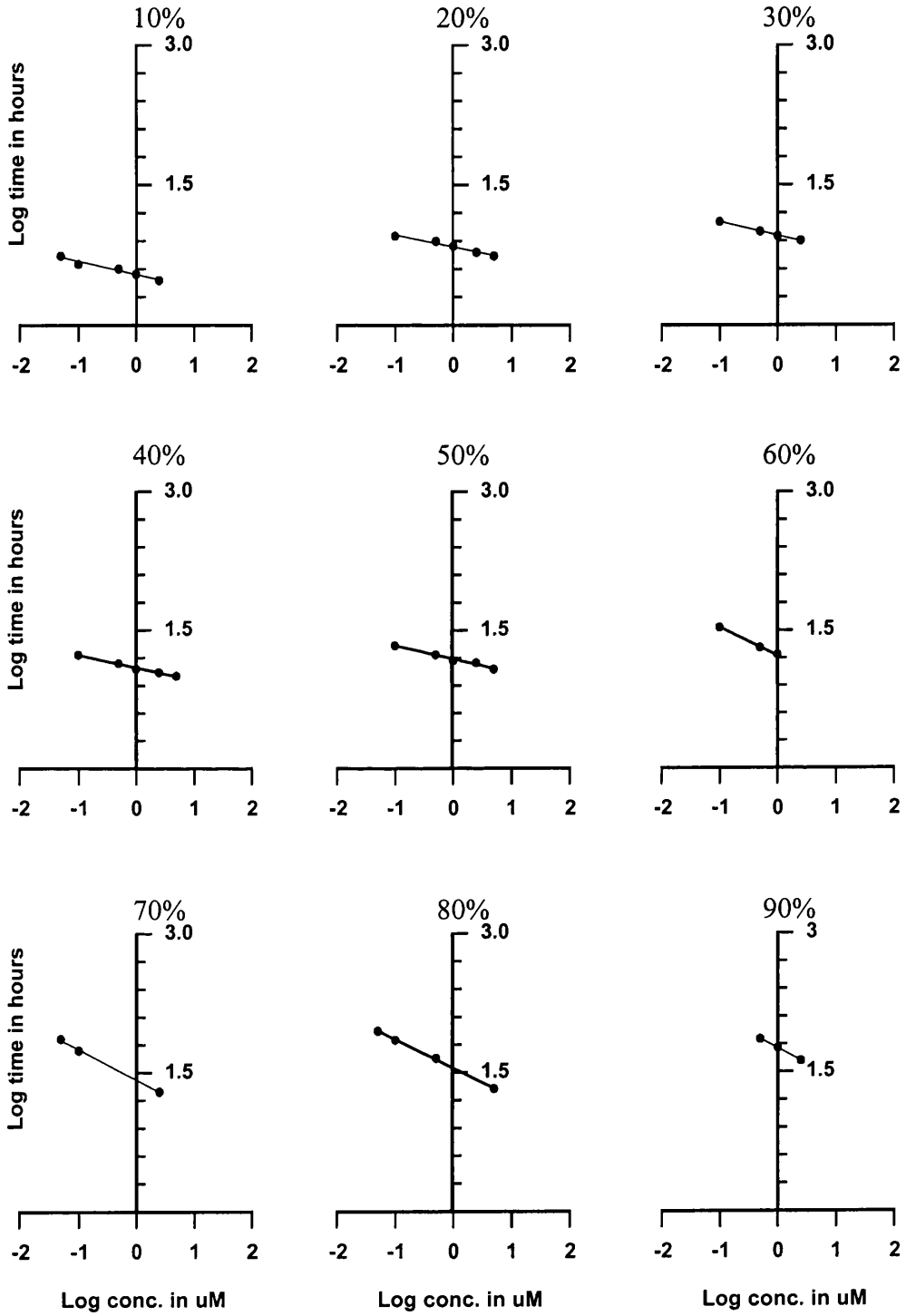

Appendix 1.3 *– Log C versus log T plots expressed on a linear scale for PK1at various percentage of cell kill.*

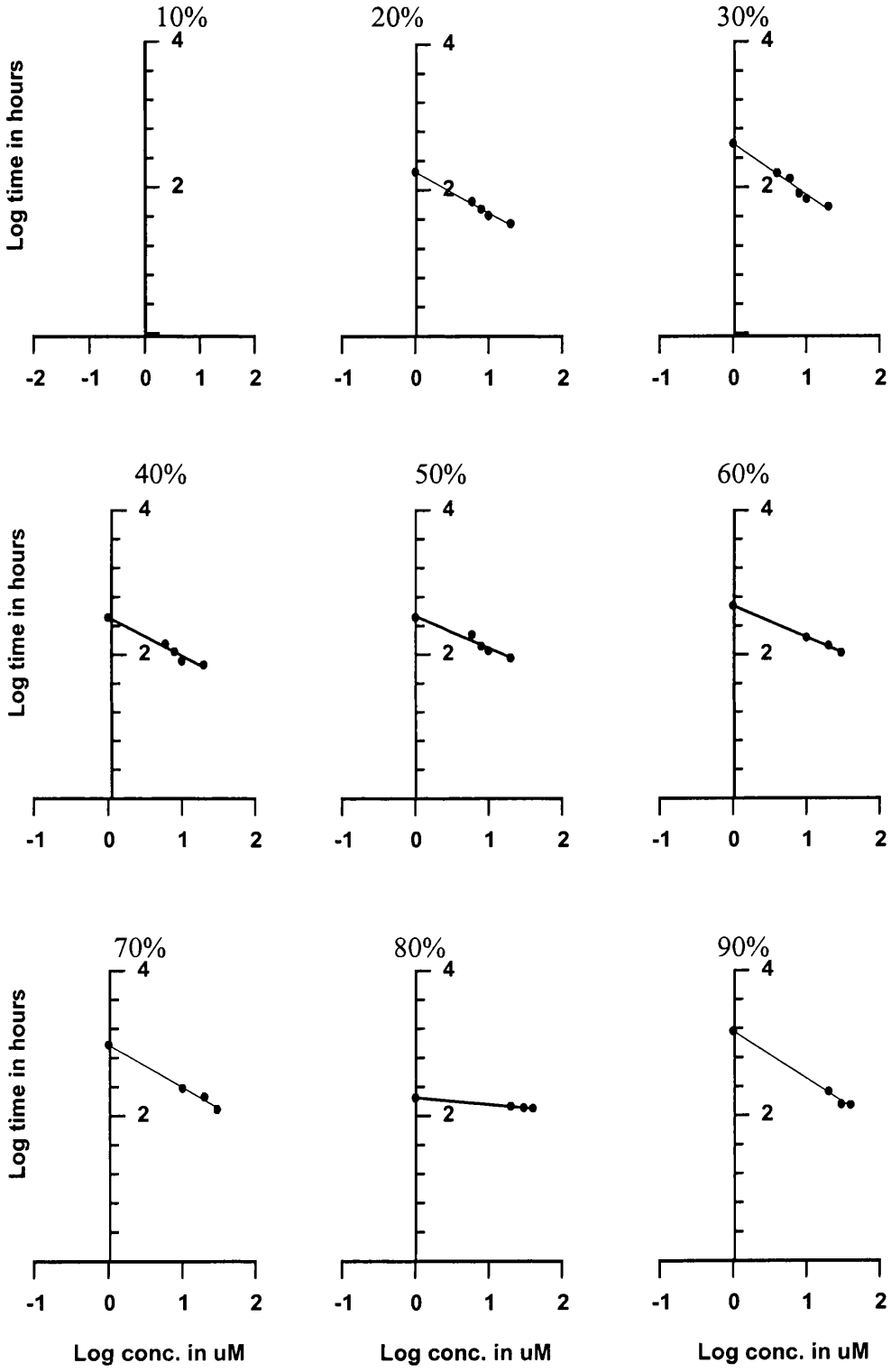

Appendix 1.4 *– Log C versus log T plots expressed on a linear scale for free unbound doxorubicin present on PK1 at various percentages of cell kill.*

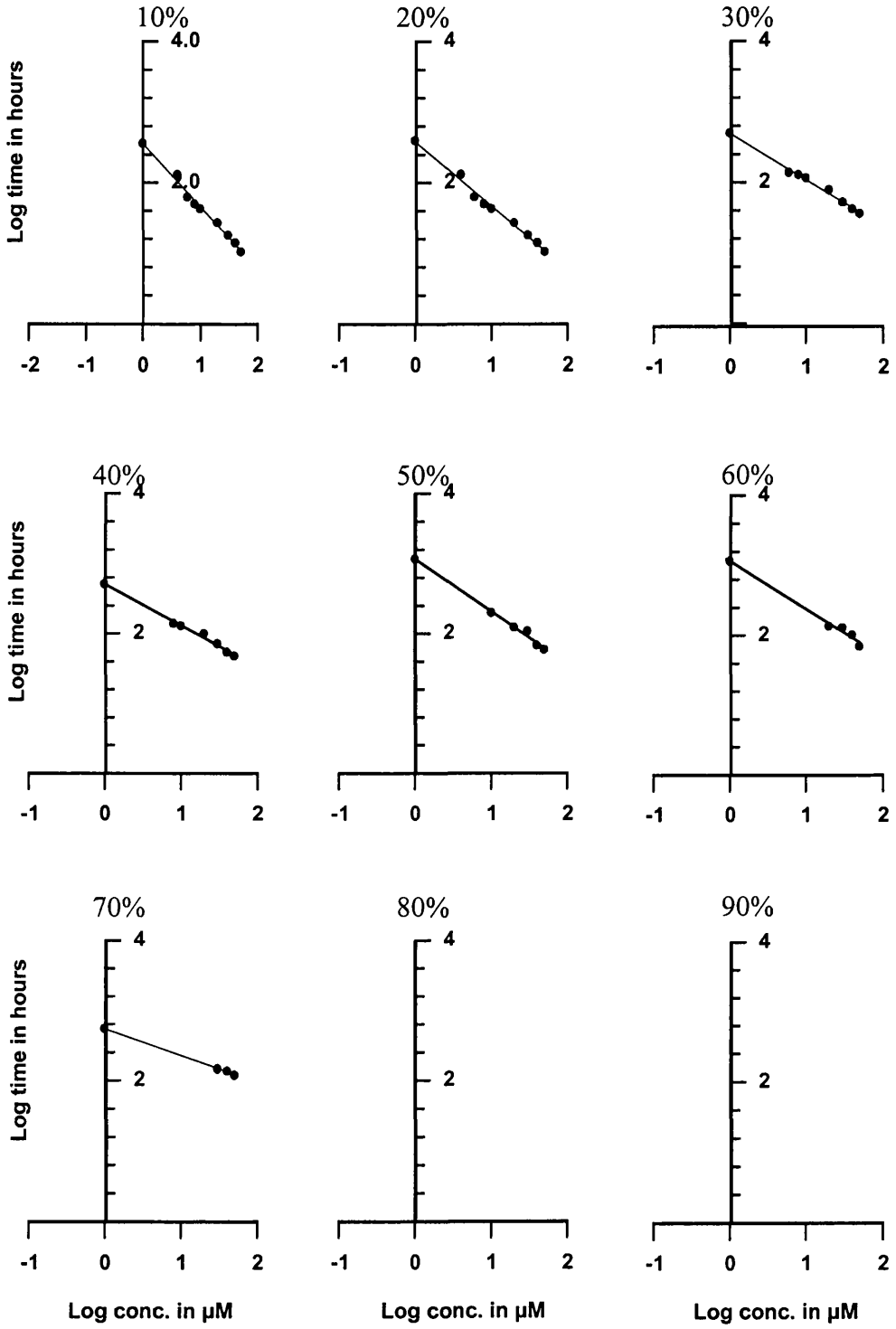

Appendix 1.5 *– Minimum concentration versus time plots for* ***doxorubicin*** *expressed on a linear scale at various percentages of cell kill. The minimum C x T is found at the intersection of the curve,* $C = (K/T)^{1/n}$*, with the red line C = nT.*

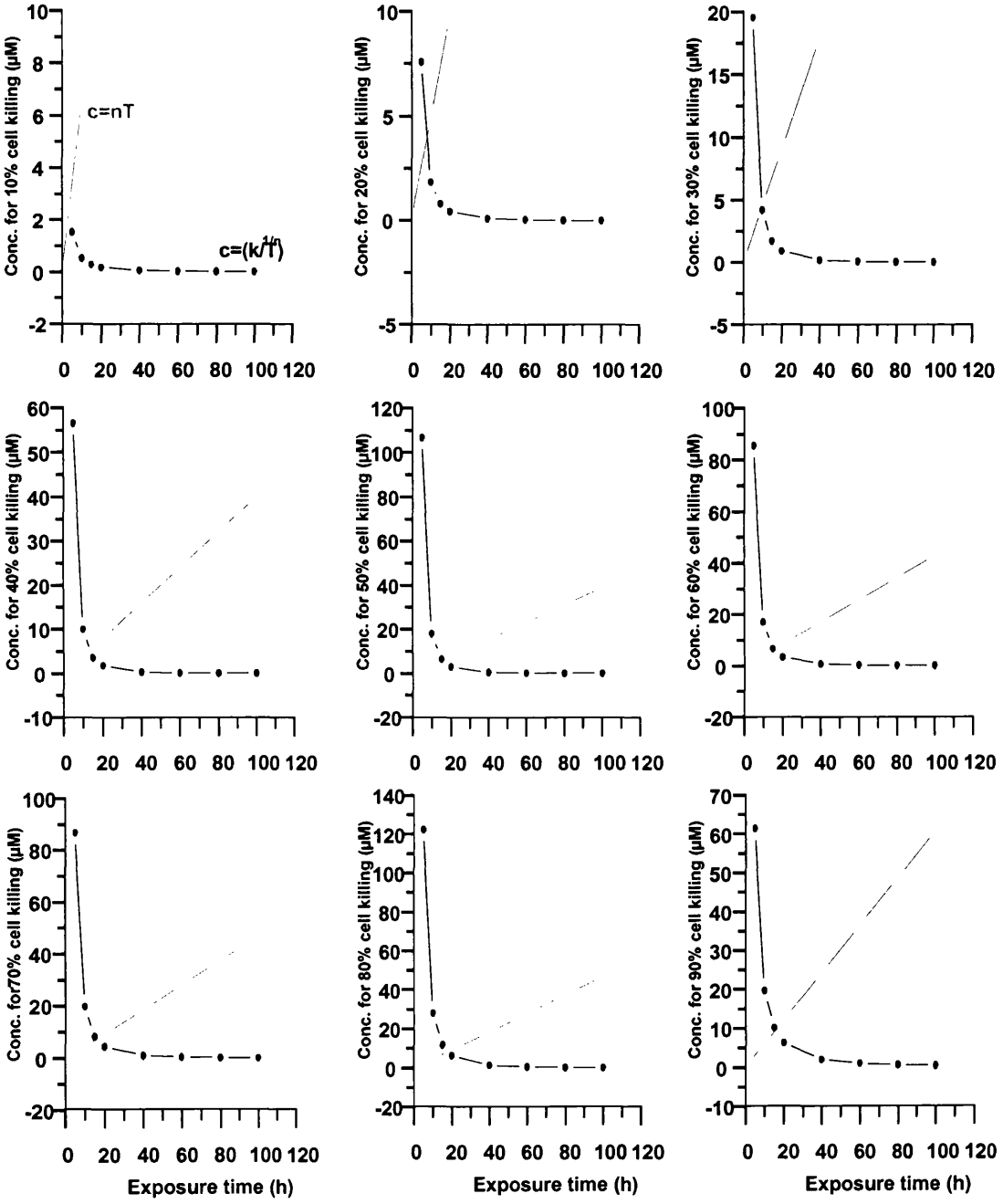

Appendix 1.6 *– Minimum concentration versus time plots for* ***doxorubicin with 72 hours post incubation*** *expressed on a linear scale at various percentages of cell kill. The minimum C x T is found at the intersection of the curve, $C = (K/T)^{1/n}$, with the red line C = nT.*

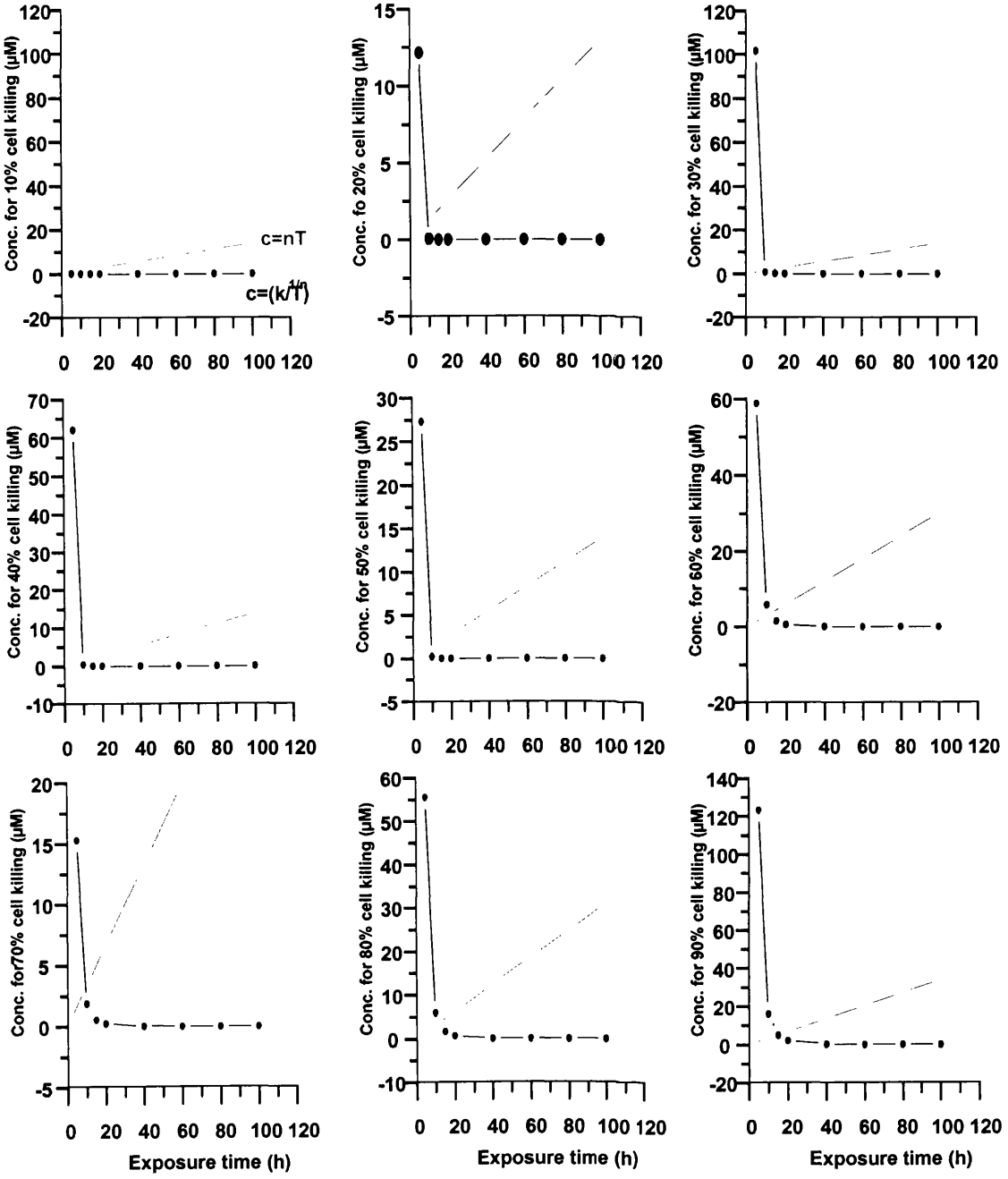

Appendix 1.7 *– Minimum concentration versus time plots for* ***PK1*** *expressed on a linear scale at various percentages of cell kill. The minimum C x T is found at the intersection of the curve,* $C = (K/T)^{1/n}$*, with the red line* $C = nT$*.*

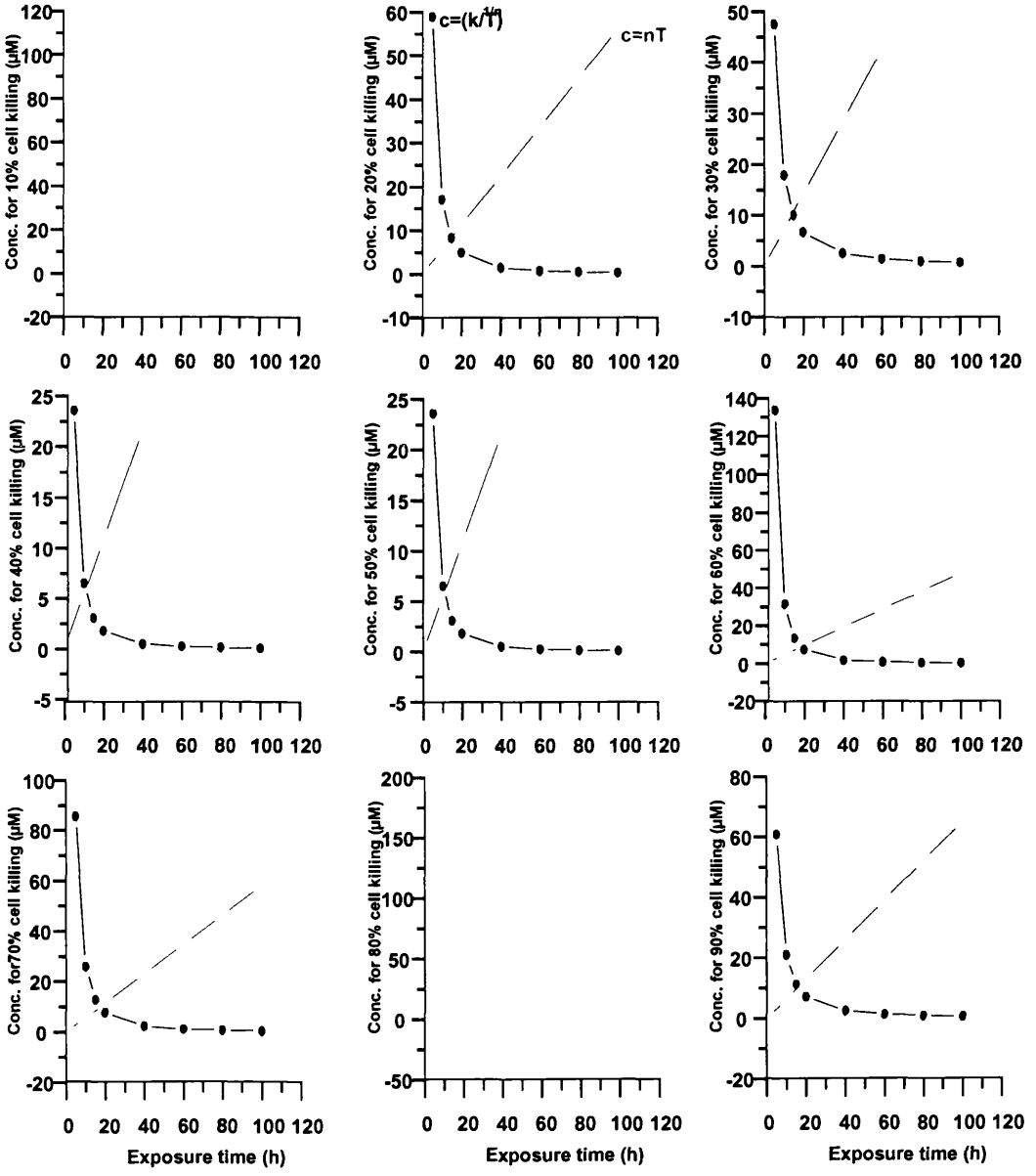

Appendix 1.8 *– Minimum concentration versus time plots for* ***free doxorubicin*** *on PK1 expressed on a linear scale at various percentages of cell kill. The minimum C x T is found at the intersection of the curve, $C = (K/T)^{1/n}$, with the red line C = nT.*

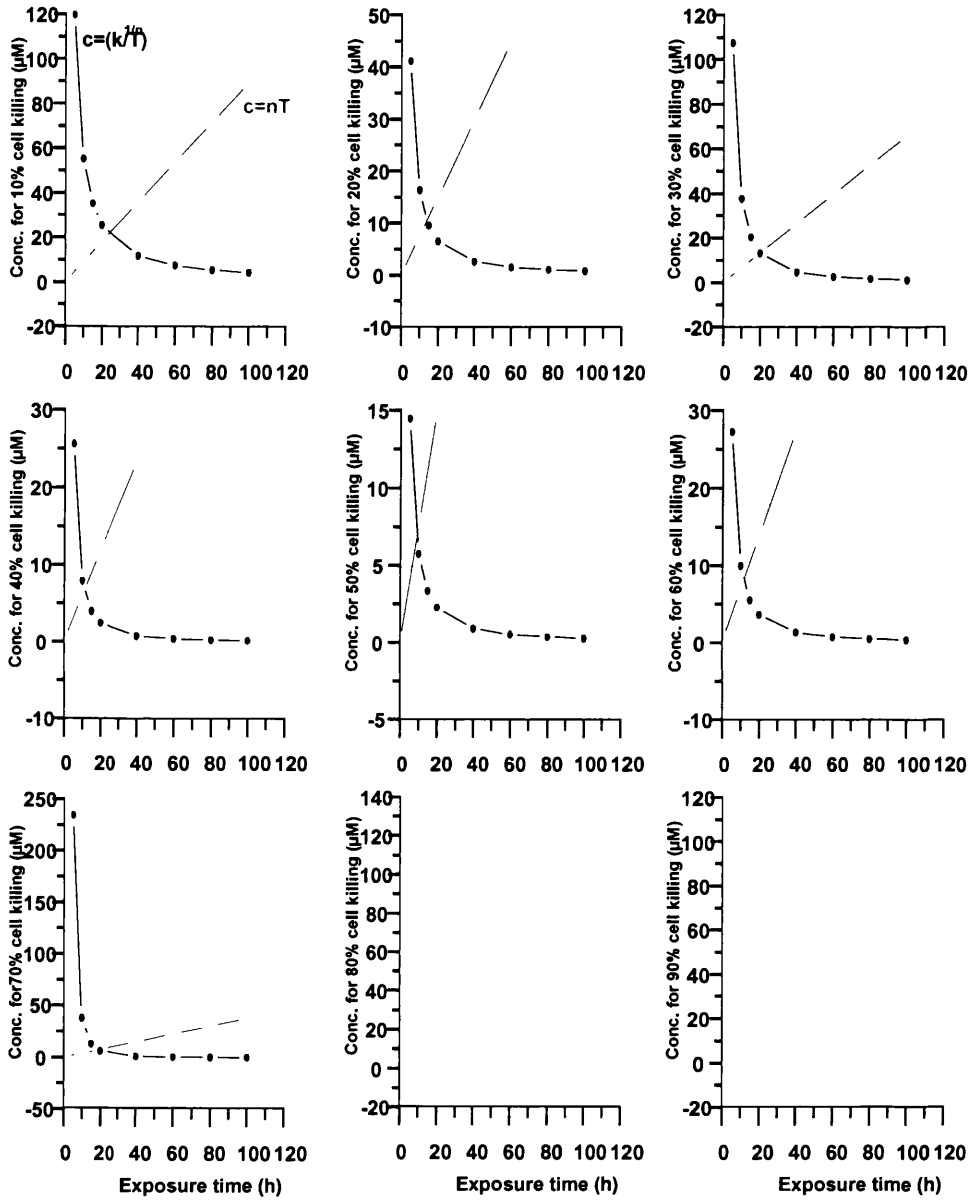

Appendix 1.9 *- Individual C57 mice total body and tumour weights obtained from first comet assay experiment for each time period. 100 cells were randomly selected and analysed from samples of each animal per group.*

5 hours

Animal No.	*Treatment*	*Dose (mg/kg*)*	*Animal Weight (g)*	*Tumour weight (g)*
1	0.9% Saline	-	26.4	0.3
2	0.9% Saline	-	27.4	0.4
3	0.9% Saline	-	29.2	0.8
1	DOX	7.5	26.4	0.4
2	DOX	7.5	26.1	0.7
3	DOX	7.5	26.1	1.5
1	PK1	15.0	25.2	0.1
2	PK1	15.0	30.0	0.2
3	PK1	15.0	28.8	1.1

24 hours

Animal No.	*Treatment*	*Dose (mg/kg*)*	*Animal Weight (g)*	*Tumour weight (g)*
1	0.9% Saline	-	28.3	0.3
2	0.9% Saline	-	26.3	0.4
3	0.9% Saline	-	26.4	0.5
1	DOX	7.5	27.0	0.4
2	DOX	7.5	27.3	0.5
3	DOX	7.5	27.7	0.7
1	PK1	15.0	29.5	0.3
2	PK1	15.0	26.3	0.5
3	PK1	15.0	28.1	0.7

48 hours

Animal No.	*Treatment*	*Dose (mg/kg*)*	*Animal Weight (g)*	*Tumour weight (g)*
1	0.9% Saline	-	25.4	0.2
2	0.9% Saline	-	30.5	1.0
3	0.9% Saline	-	27.4	0.3
1	DOX	7.5	27.3	0.8
2	DOX	7.5	27.2	0.7
3	DOX	7.5	30.3	1.1
1	PK1	15.0	28.3	0.8
2	PK1	15.0	26.8	0.4
3	PK1	15.0	27.6	0.5

72 hours

Animal No.	*Treatment*	*Dose (mg/kg*)*	*Animal Weight (g)*	*Tumour weight (g)*
1	0.9% Saline	-	27.3	1.7
2	0.9% Saline	-	27.0	1.5
3	0.9% Saline	-	26.4	1.3
1	DOX	7.5	28.3	1.6
2	DOX	7.5	30.0	1.3
3	DOX	7.5	24.6	0.6
1	PK1	15.0	27.1	1.8
2	PK1	15.0	28.9	1.7
3	PK1	15.0	26.9	1.3

**Doxorubcin-equivalent*

Appendix 1.10 *- Individual C57 mice total body and tumour weights obtained from second comet assay experiment for each time period. 100 cells were randomly selected and analysed from samples of each animal per group.*

5 hours

Animal No.	*Treatment*	*Dose (mg/kg*)*	*Animal Weight (g)*	*Tumour weight (g)*
1	0.9% Saline	-	31.2	0.2
2	0.9% Saline	-	27.3	0.3
3	0.9% Saline	-	27.9	0.6
1	DOX	7.5	29.8	0.5
2	DOX	7.5	25.6	0.3
3	DOX	7.5	26.6	1.1
1	PK1	15.0	26.1	0.2
2	PK1	15.0	30.3	0.5
3	PK1	15.0	28.2	0.6

24 hours

Animal No.	*Treatment*	*Dose (mg/kg*)*	*Animal Weight (g)*	*Tumour weight (g)*
1	0.9% Saline	-	30.8	1.8
2	0.9% Saline	-	30.8	0.8
3	0.9% Saline	-	27.1	0.3
1	DOX	7.5	30.0	1.3
2	DOX	7.5	26.0	0.4
3	DOX	7.5	31.1	0.1
1	PK1	15.0	27.0	1.3
2	PK1	15.0	25.8	1.2
3	PK1	15.0	30.1	0.2

48 hours

Animal No.	*Treatment*	*Dose (mg/kg*)*	*Animal Weight (g)*	*Tumour weight (g)*
1	0.9% Saline	-	28.0	1.9
2	0.9% Saline	-	27.0	0.9
3	0.9% Saline	-	25.6	0.6
1	DOX	7.5	28.9	1.5
2	DOX	7.5	27.9	0.8
3	DOX	7.5	26.4	1.2
1	PK1	15.0	27.9	1.1
2	PK1	15.0	26.5	1.1
3	PK1	15.0	28.8	0.6

72 hours

Animal No.	*Treatment*	*Dose (mg/kg*)*	*Animal Weight (g)*	*Tumour weight (g)*
1	0.9% Saline	-	27.3	2.8
2	0.9% Saline	-	28.1	1.4
3	0.9% Saline	-	29.7	1.2
1	DOX	7.5	28.4	0.2
2	DOX	7.5	25.8	0.3
3	DOX	7.5	30.3	1.3
1	PK1	15.0	28.8	1.0
2	PK1	15.0	26.1	0.9
3	PK1	15.0	30.3	1.4

**Doxorubicin-equivalent*

Appendix 1.11 – Statistical significance of PK1 and Dox induced DNA damage in tumour and bone marrow cells relative to 0.9% saline treatment.

Tumour

Wilcoxon-Mann-Whitney U test (P values)

Treatment	5 h	24 h	48 h	72 h
Doxorubicin	0.0055**	0.0035**	<0.0001***	0.001***
PK1	0.0035**	0.0212*	<0.0001***	0.0024**
Dox vs. PK1	0.435ns	0.205ns	<0.0001***	0.3848*

ns = not significant

Bone marrow

Wilcoxon-Mann-Whitney U test (P values)

Treatment	5 h	24 h	48 h	72 h
Doxorubicin	0.0026**	<0.0001***	<0.0001***	0.0102*
PK1	<0.0001***	<0.0001***	<0.0001***	0.0006***
Dox vs. PK1	0.0701^{ns}	0.2478^{ns}	<0.0001***	0.224^{ns}

ns = not significant

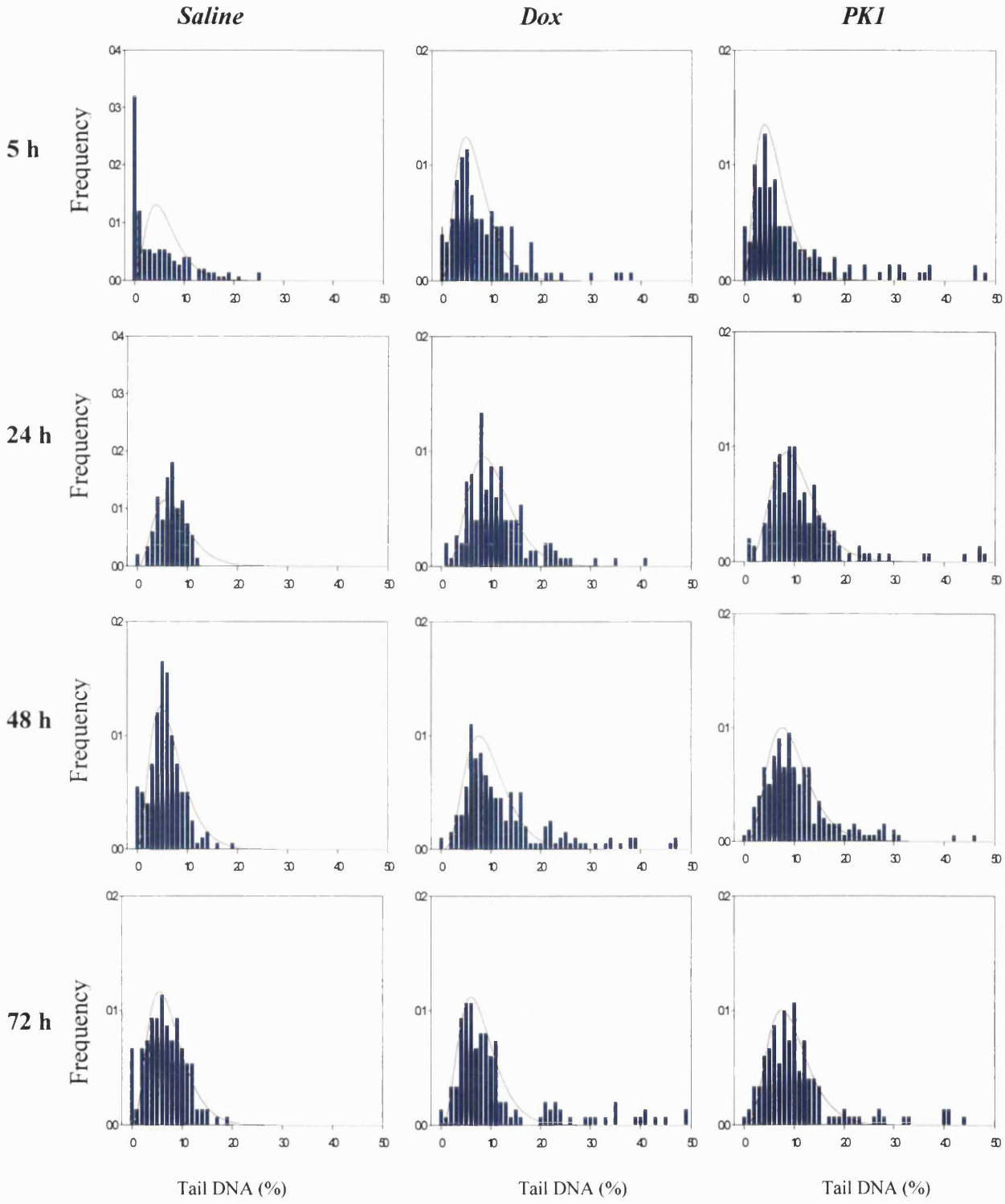

Appendix 1.12 – Distribution of DNA strand breaks with time in bone marrow isolated cells from C57 mice given a single intravenous injection of doxorubicin (7.5 mg/kg), PK1 (15 mg/kg, doxorubicin equivalent) or 0.9% saline. Data represents quantitative frequency distributions superimposed with curve fit calculated with χ^2-function (red line). Each histogram contains 300 analysed cells from two independent experiments.

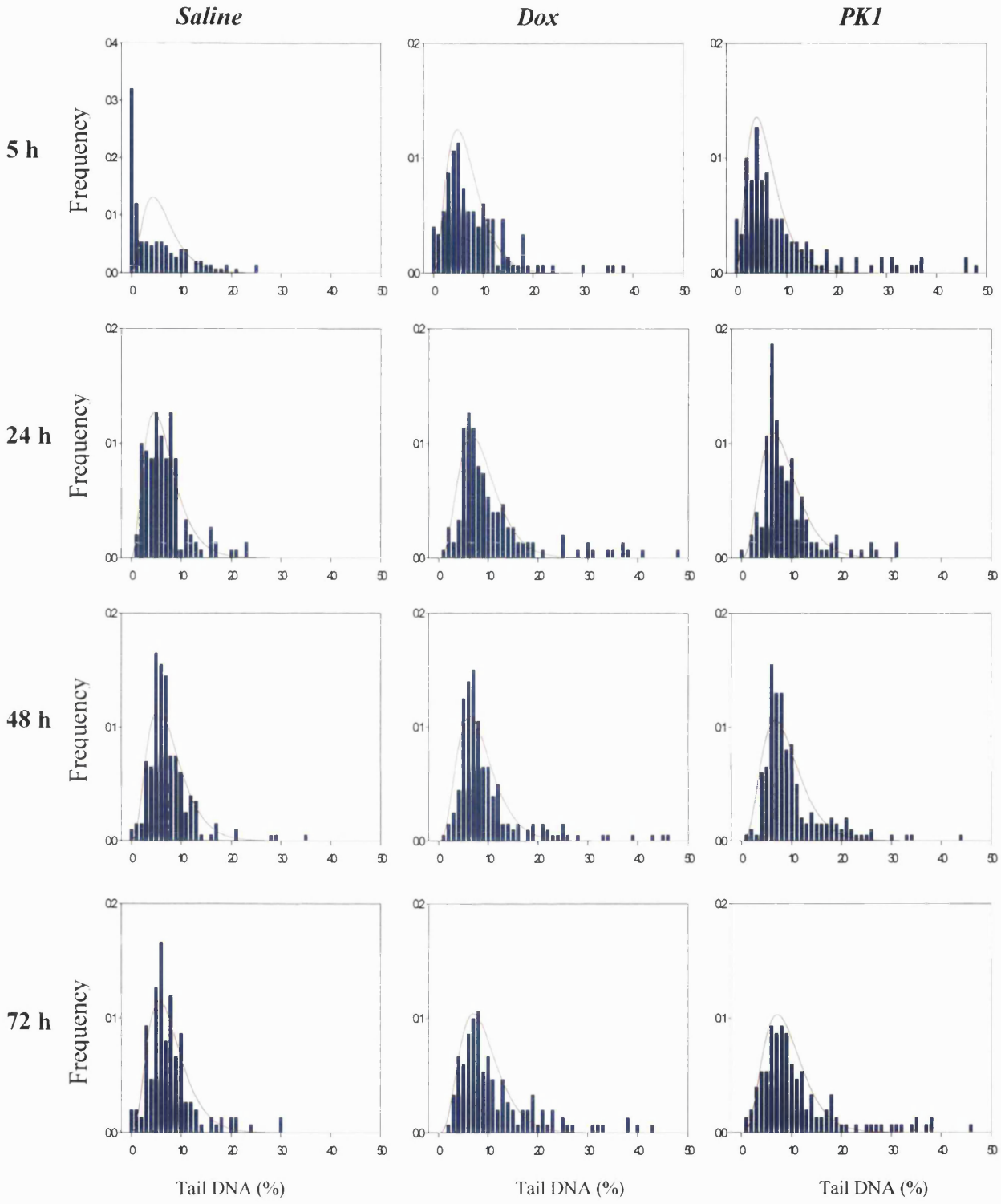

Appendix 1.13 – Histograms showing the distributions of % tail DNA in tumour cells isolated from C57 mice given a single intravenous injection of doxorubicin (7.5 mg/kg), PK1 (15 mg/kg, doxorubicin equivalent) or 0.9% saline. Data represents quantitative frequency distributions superimposed with curve fit calculated with χ2-function (red line). Each histogram contains 300 analysed cells from two independent experiments. (Animal and tumour weights per treatment group are listed in Appendix 4.1 and 4.2).

Pharmacia
Farmitalia Carlo Erba

Appendix 1.14

RD/Analytical Chemistry
December, 1994

CERTIFICATE OF ANALYSIS Nr: 7206

Product name : FCE 28068 (PK1)
Produced by : Polymer Laboratories Ltd, Church Stretton, UK
Batch : 0187 Batch size : 248.4 g
Product code : 7480 Prep. date : November, 1994

Appearance	: red powder	
Identity	: confirmed by ^{1}H-NMR (DMSO-d6)	
Residue on ignition (R.O.I.)	:	≤ 0.1%
Water (K. Fischer)	:	2.2%
Residual solvents (GLC)	: acetone	≤ 0.1%
	: ethanol	3.9%
Heavy metals	:	≤ 10 ppm
Total doxorubicin (HPLC assay)		: 6.2%
Free doxorubicin (HPLC assay)		: 0.02%
Doxorubicin related contaminants (HPLC assay)		: 0.3%
p-Nitrophenol (HPLC assay)		: < 0.01%
Mw (weight-average molecular weight, SEC)[1]		: 29700
Mw/Mn (polydispersity, SEC)[1]		: 1.48

1) Analysis performed by the Institute of Macromolecular Chemistry of the Czech. Acad. Sci. - Prague

Storage: +4°C
Provisional retest date: December 1997

The value of total doxorubicin is below the lower limit in the specifications (7%). This batch cannot be used for clinical or toxicologic studies.

A. Vigevani